Mathematical Biosciences and Engineering

http://www.aimspress.com/journal/MBE

MBE, 18(5): 5865–5920.
DOI: 10.3934/mbe.2021295
Received: 29 April 2021
Accepted: 08 June 2021
Published: 30 June 2021

Research article

Mathematical modeling of intervention and low medical resource availability with delays: Applications to COVID-19 outbreaks in Spain and Italy

Sarita Bugalia[1], **Jai Prakash Tripathi**[1,*] **and Hao Wang**[2]

[1] Department of Mathematics, Central University of Rajasthan, Bandar Sindri, Kishangarh-305817, Ajmer, Rajasthan, India

[2] Department of Mathematical and Statistical Sciences,University of Alberta, Edmonton AB T6G 2G1, Canada

* **Correspondence:** Email: jtripathi85@gmail.com.

Abstract: Infectious diseases have been one of the major causes of human mortality, and mathematical models have been playing significant roles in understanding the spread mechanism and controlling contagious diseases. In this paper, we propose a delayed SEIR epidemic model with intervention strategies and recovery under the low availability of resources. Non-delayed and delayed models both possess two equilibria: the disease-free equilibrium and the endemic equilibrium. When the basic reproduction number $R_0 = 1$, the non-delayed system undergoes a transcritical bifurcation. For the delayed system, we incorporate two important time delays: τ_1 represents the latent period of the intervention strategies, and τ_2 represents the period for curing the infected individuals. Time delays change the system dynamics via Hopf-bifurcation and oscillations. The direction and stability of delay induced Hopf-bifurcation are established using normal form theory and center manifold theorem. Furthermore, we rigorously prove that local Hopf bifurcation implies global Hopf bifurcation. Stability switching curves and crossing directions are analyzed on the two delay parameter plane, which allows both delays varying simultaneously. Numerical results demonstrate that by increasing the intervention strength, the infection level decays; by increasing the limitation of treatment, the infection level increases. Our quantitative observations can be useful for exploring the relative importance of intervention and medical resources. As a timing application, we parameterize the model for COVID-19 in Spain and Italy. With strict intervention policies, the infection numbers would have been greatly reduced in the early phase of COVID-19 in Spain and Italy. We also show that reducing the time delays in intervention and recovery would have decreased the total number of cases in the early phase of COVID-19 in Spain and Italy. Our work highlights the necessity to consider the time delays in intervention and recovery in an epidemic model.

Keywords: basic reproduction number; stability; local Hopf bifurcation; global Hopf bifurcation;

Nyquist criterion; stability switching curves

1. Introduction

In the past decade, infectious diseases have been frequently threatening human lives on a large scale. After the first epidemic model of *smallpox* was proposed by a pioneering mathematician Daniel Bernoulli in the eighteenth century [1, 2], a huge number of epidemic models have been proposed and studied to uncover the underlying spread mechanisms and to control the spread of infectious diseases. Kermack and Mckendrick [3] introduced a seminal SIR compartmental model in 1927 to study the *plague* disease in Mumbai and succeeded in revealing its epidemiological transition. Since then, mathematical modeling has been growing as a vital tool to suggest public health responses against the spread and transmission of infectious diseases. The SIR and SEIR type models have been performed a crucial role in modern mathematical epidemiology [4, 5].

Numerous factors significantly affect the dynamical behavior of a particular epidemic model, such as the demographics, recovery or treatment rates, and incidence rates [6,7]. In particular, different types of incidence functions can ensure appropriate dynamical characteristics of the associated infectious diseases [8, 9]. In classical SIR/SEIR models, the general incidence rate $\frac{\beta SI}{N}$, bilinear incidence rate βSI and linear recovery rate γI are commonly used. The constant β represents the average number of adequate contacts between susceptible and an infected individual per unit time, and γ represents the per capita recovery rate of infected individuals. Since the infection risk increases with the increase in the number of infective individuals, therefore, the mobility of individuals probably influences these numbers. When a particular infectious disease appears and spreads in a region/community, intervention strategies play a crucial role in controlling the disease [10, 11].

The impacts of intervention strategies, such as *mask-wearing, border screening, isolation, quarantine, or communications through the mass media* (to convey the information to the public about the epidemic/outbreak and probably risk-reducing behavior), play their significant roles in managing effectual interventions to control the spread of disease and expectantly remove epidemic diseases [12–15]. For instance, during the outbreak of the H1N1 influenza pandemic in 2009 [16, 17] and the outbreak of SARS in 2003 [18, 19], the intervention strategies (such as *postponing conferences, closing restaurants/schools, isolating infectives*, etc.) were chosen by the Chinese government. Recently, a new pandemic COVID-19 appeared and affected more than 200 countries and territories worldwide. To control the spread of COVID-19, governments of different countries strictly implemented the lockdown [20]. Besides lockdown, various governments are also adopting numerous steps and implementing different intervention strategies, such as *social distancing, tracing close contacts, washing hands for 30 seconds*, etc [21]. In many countries, these strategies impressively worked so that the contacts between susceptible and infected individuals per unit time are being decreased sufficiently, and therefore, the reduced incidence rate [22–25]. This showed the importance of considering the infection forces that comprises the adaptation of individuals to infection risks under intervention strategies.

In classical epidemic models, the recovery rate of infected individuals is commonly considered to be proportional to the number of infectives [26, 27]. However, in general, this is unacceptable because

the implicit assumption is that treatment resources are sufficient [28]. Every society should have a limited capacity of resources for treatment. If medical resources are available in large quantities, the community needs to pay unnecessary costs during non-epidemic periods, and if available resources are low, the community has the risk of a disease outbreak without needed treatment [26]. The recovery rate depends on the resources of the health system available to the community, particularly, the capacity of the hospital settings, efficiency, and effectiveness of treatment [29, 30]. The prime factor is the number of health employees, including nurses, physicians, pharmacists, and other health care workers (HCW). The amenities of the hospital, such as equipment and medical apparatus, medicines, and the number of hospital beds are other noteworthy factors that are important for effective and safe prevention, treatment, and diagnosis of patients [28].

Shan et al. [28] studied an SIR model with the impact of the number of beds in hospitals. The authors considered the standard incidence rate and nonlinear recovery rate. They studied the complex dynamics of the model including numerous bifurcations such as backward bifurcation, saddle-node bifurcation, Hopf bifurcation, Bogdanov-Takens bifurcation. The study recommends that maintaining an adequate number of beds in the hospital is crucial to control the disease. Li et al. [29] investigated the dynamics of an SIR model using nonlinear incidence rate and nonlinear recovery rate. The model exhibited complicated dynamics and suggested that a sufficient number of beds is critical to control the disease. Mu et al. [30] proposed an SI-SIR model for *avian influenza* with a nonlinear recovery rate under available hospital resources. Zhao et al. [31] investigated the complex dynamics of Zika virus transmission via mathematical modeling with limited medical resources. In [28–31], the authors considered a similar recovery rate that decreases with a decrease in the number of beds/resources in the hospitals. In the case of low availability of resources for treatment, the recovery rate primarily grows with an increase in the number of infected individuals and approaches the maximum and then starts decreasing. When deliveries of treatment (immunization, medicine, etc.) are depleted due to a large number of infected individuals, the available resources for treatment become very low.

Time delays are inevitable in almost all realistic systems. Introducing time delays in epidemic models can be important, and time delays include the latency period [32, 33], the delay in recovery [34], the delay in media broadcast [35], the delay in awareness programs [36] etc. Different types of delay differential equations (DDEs) have fruitfully been utilized to study infectious diseases [37–39]. Greenhalgh et al. [40] proposed a mathematical model with multiple time delays, one delay due to the memory disappearance of aware individuals, and the other delay between the rising awareness and the disease appearance. Zhou et al. [41] analyzed an SIR model with media coverage incorporating time delay and studied delay induced local and global Hopf-bifurcation. The authors found that the delay in media coverage does not influence the stability of the disease-free equilibrium. In [42], the authors proposed a mathematical model with media coverage incorporating time delay. Recently, Liu et al. [43] studied the delay induced local Hopf bifurcation of an SEIR model with multiple time delays caused by the latent period and the recovery period.

A common assumption about intervention strategies in mathematical models [10, 11] is that the impact of intervention strategies on the transmission dynamics is effective, i.e., the number of infected individuals instantly decrease. The recovery rate is assumed to be proportional to the number of infectives, but many researchers argued that this assumption is questionable in reality as we have discussed earlier. As an improvement, we propose an SEIR model with infection force under intervention strategies and a nonlinear recovery function (under low availability of treatment

resources), where treatment declines (due to resources limitation) after attaining its maximum value. Further, we incorporate two time delays, the first delay represents the latent period of interventions and the second delay represents the period for curing the infected individuals. The two main objectives of the study are (*i*) to investigate the impact of low availability of resources for treatment in the presence of intervention strategies, and (*ii*) to assess the role of time delays in the transmission dynamics. Furthermore, we validate our model and estimate the parameter values based on the available COVID-19 data in Spain and Italy.

The remaining paper is organized as follows. In Section 2, we formulate an SEIR model (both non-delayed and delayed) with infection force under intervention strategies and recovery rate (under low treatment resources). In Section 3, we analyze the non-delayed system (2.2). In Section 4, we analyze the delayed system (2.3). Persistence has been shown in Section 5. In Section 6, numerical simulations have been presented for both non-delayed system (2.2) and delayed system (2.3). In Section 7, a case study has been discussed for COVID-19 outbreaks in Spain and Italy. The paper ends with conclusion and future developments in Section 8.

2. Mathematical formulation of the model

We start with the classical SEIR model in which the total population is divided into four compartments: susceptible individuals (S), exposed individuals (E), infected individuals (I), and recovered individuals (R). Susceptible individuals are healthy but can be infected via contacting with infectives. Individuals who are exposed to disease pathogen and may be infected via contacts are called exposed individuals. Exposed individuals may or may not develop the disease, and these individuals are typically not infectious. Infected individuals are those who have been infected and are capable of transmitting the disease to susceptible individuals. Recovered individuals are those who were infected but have been healthy now, and they have immune protection for a long time. Under the above assumptions, the SEIR model with incidence rate under intervention strategies and recovery rate under low availability of medical resources is provided by

$$\begin{aligned} \frac{dS}{dt} &= A - \mu S - F(I)S, \\ \frac{dE}{dt} &= -(\mu + q)E + F(I)S, \\ \frac{dI}{dt} &= qE - (\mu + \delta)I - G(I), \\ \frac{dR}{dt} &= G(I) - \mu R, \end{aligned} \tag{2.1}$$

associated with the state space $\mathbb{R}^4_+ = \{(S, E, I, R) : S > 0, E > 0, I > 0, R > 0\}$. All parameters are assumed to be positive. Here A is the rate at which new individuals (including immigrants and newborns) enter into the susceptible population; μ is the natural mortality rate; q is the rate at which exposed individuals become infectious; δ is the disease induced death rate. The infection force $F(I)$ and recovery function $G(I)$ in system (2.1) are the functions of infective individuals. These two functions play important roles in governing the disease transmission dynamics. There are various nonlinear transmission rates and nonlinear recovery rates proposed by researchers, for instance, [10, 11, 13, 14, 28, 44, 45] and references therein.

System (2.1) comprises the adaptation of human behavior under intervention strategies. In fact, when a new infectious disease emerges, both the infection probability and contact rate increase since people have less knowledge about the disease. Further, when the number of infective individuals get larger and the disease becomes more serious, psychological factors lead people to modify their behavior and implement suitable measures/intervention to reduce the opportunities of contact and the probability of infection. For instance, $F(I)$ may decrease when the number of infectives increases since the government may tend to contain the infectious disease by intervention strategies. It has also been interpreted as the psychological effect [14]. Mathematically, this idea could be modeled as follows: the infection force $F(I)$ increases when I is small and decreases when I is large (shown in Figure 1). For notational convenience, we assume that the infection force $F(I)$ could be factorized into $\frac{\beta I}{f(I)}$, where $\frac{1}{f(I)}$ signifies the impact of intervention strategies on the decrease of effective contact coefficient β [27]. In the absence of intervention strategies, i.e., $f(I) = 1$, it is notable that the infection force takes the form of well-known bilinear transmission $\beta S I$. Here, we have the following assumptions for $f(I)$:

- $H(1)$: $f(0) > 0$ and $f'(I) > 0$ for $I > 0$,
- $H(2)$: There is a ξ such that $\left(\frac{I}{f(I)}\right)' > 0$ for $0 < I < \xi$ and $\left(\frac{I}{f(I)}\right)' < 0$ for $I > \xi$.

These assumptions explain the impacts of intervention strategies determined by a critical value ξ : if $0 < I < \xi$, the infection force increases, while if $I > \xi$, the infection force decreases.

In case of low availability of medical resources for a large number of infectives, the recovery function primarily grows with increase of the number of infectives and approaches the maximum and then declines (shown in Figure 1). We have the following assumptions for $g(I)$:

- $H(3)$: $g(0) > 0$ and $g'(I) > 0$ for $I > 0$,
- $H(4)$: There is a η such that $\left(\frac{I}{g(I)}\right)' > 0$ for $0 < I < \eta$ and $\left(\frac{I}{g(I)}\right)' < 0$ for $I > \eta$.

These assumptions explain the impacts of treatment policies determined by a critical value η : if $0 < I < \eta$, the recovery function increases, while if $I > \eta$, the recovery function decreases.

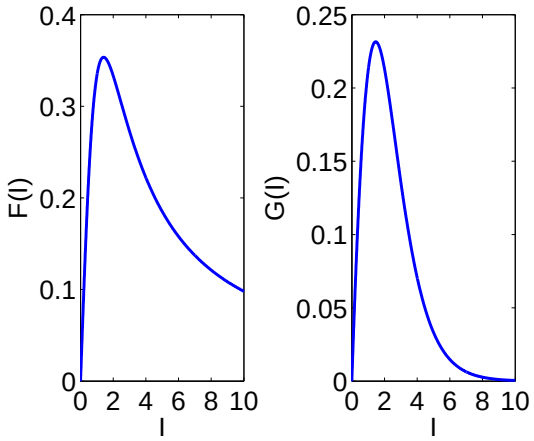

Figure 1. The graphs show that both infection force and recovery function first increase with respect to the number of infected individuals, and after a critical number of infected individuals, both functions decrease.

Under the above assumptions on the infection force and recovery function, the new SEIR model (2.1) takes the following form:

$$\begin{aligned}
\frac{dS}{dt} &= A - \mu S - \frac{\beta I}{f(I)}S,\\
\frac{dE}{dt} &= \frac{\beta I}{f(I)}S - (\mu + q)E,\\
\frac{dI}{dt} &= qE - (\mu + \delta)I - \frac{\gamma I}{g(I)},\\
\frac{dR}{dt} &= \frac{\gamma I}{g(I)} - \mu R.
\end{aligned} \tag{2.2}$$

Furthermore, the functions $f(I)$ and $g(I)$ could be chosen from a combination of any of the following formats:

1. $f(I)$ or $g(I) = 1 + \alpha I^p, \quad p > 1,$
2. $f(I)$ or $g(I) = \exp(\alpha I),$
3. $f(I)$ or $g(I) = 1 + I + \alpha I^p, \quad p > 1,$

where α and p are positive constants. For the case of intervention strategies, the parameter α could be understood as the strength of interventions, and for the case of treatment, the parameter α could be understood as limitation on the treatment availability. In particular, if we take $g(I) = 1$, then model (2.2) becomes same as the model discussed in [11].

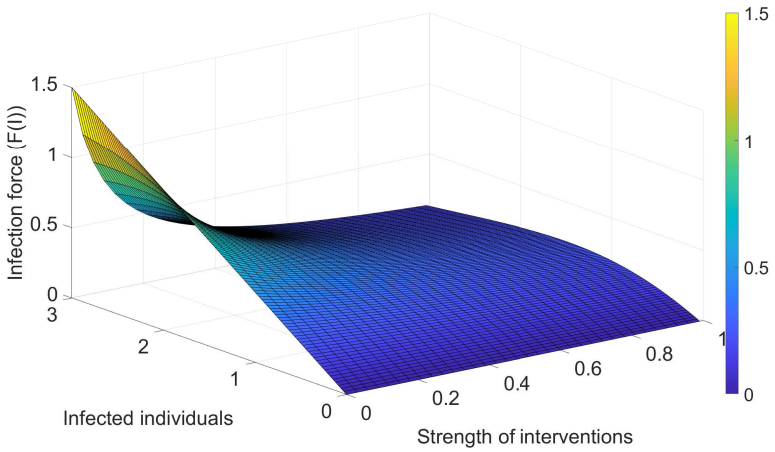

Figure 2. The graph shows the surface plot of the infection force with respect to infected individuals and strength of interventions.

In Figure 2, the infection force has been plotted with respect to infected individuals and the strength of interventions. It depicts that when the strength of interventions is zero, then incidence function always increases. However, in presence of interventions, the incidence function first increases and then decreases. Moreover, the maximum of $F(I)$ becomes smaller with an increase in the strength of interventions. Similarly in Figure 3, the recovery function has been plotted with respect to infected individuals and limitation on treatment resources. We see that when the resource limitation is zero, then

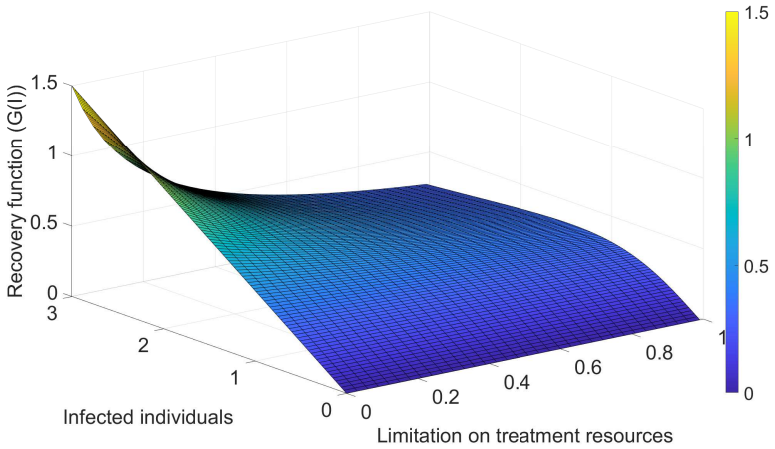

Figure 3. The graph shows the surface plot of the recovery function with respect to infected individuals and limitation on treatment resources.

the recovery function increases. However, in presence of resource limitations, the recovery function first increases and then decreases. In addition, the maximum of $G(I)$ becomes smaller with an increase in resource limitations.

Delays naturally exist and can play an important role in disease dynamics. We include two time delays in system (2.2), the first delay τ_1 represents the latent period of the intervention strategies and the second delay τ_2 represents the period for curing the patients. Delays in intervention and curing processes are significant in infectious disease modeling. For example, the delay in intervention strategies, including the time duration for individuals' responses to the reported infection and the reporting delay, have been observed in H1N1-2009 [35]. The model (2.2) with these time delays is provided by

$$\begin{aligned}
\frac{dS}{dt} &= A - \mu S - \frac{\beta I}{f(I(t-\tau_1))}S,\\
\frac{dE}{dt} &= \frac{\beta I}{f(I(t-\tau_1))}S - (\mu+q)E,\\
\frac{dI}{dt} &= qE - (\mu+\delta)I - \frac{\gamma I(t-\tau_2)}{g(I(t-\tau_2))},\\
\frac{dR}{dt} &= \frac{\gamma I(t-\tau_2)}{g(I(t-\tau_2))} - \mu R.
\end{aligned} \tag{2.3}$$

The initial conditions for the model (2.3) are defined as

$$S(\theta) = \phi_1(\theta), E(\theta) = \phi_2(\theta), I(\theta) = \phi_3(\theta), R(\theta) = \phi_4(\theta), \tag{2.4}$$

where $\theta \in [-\tau, 0]$, $\tau = \max\{\tau_1, \tau_2\}$, $(\phi_1, \phi_2, \phi_3, \phi_4) \in C([-\tau, 0], \mathbb{R}^4)$, $\phi_i(0) > 0, i = 1, 2, 3, 4$, and $C([-\tau, 0], \mathbb{R}^4)$ is the Banach space of continuous functions from $[-\tau, 0]$ to $\mathbb{R}^4$ equipped with the sup-norm. It could easily be established from the elementary theory of functional differential equations [49] that the system (2.3) possesses a unique solution with initial conditions (2.4).

3. Dynamics of non-delayed system (2.2)

3.1. Positivity and boundedness

It is essential to show that all the population variables are nonnegative for all $t \geq 0$, which indicates that any trajectory that begins with positive initial condition will stay positive for $t \geq 0$.

Theorem 3.1. *The closed region*

$$\mho = \left\{(S, E, I, R) \in \mathbb{R}^4_+ : 0 < S + E + I + R \leq \frac{A}{\mu} \subset \mathbb{R}^4_+\right\} \tag{3.1}$$

is positively invariant for system (2.2).

Proof. See Appendix A. □

3.2. Equilibrium analysis

The system (2.2) has the following two equilibria:

1. The disease-free equilibrium $D_0(\frac{A}{\mu}, 0, 0, 0)$, which always exists. Here we define the basic reproduction number R_0 for system (2.2) as

$$R_0 = \frac{\beta A q}{\mu f(0)(\mu + q)(\mu + \delta + \frac{\gamma}{g(0)})}, \tag{3.2}$$

   where $\frac{1}{\mu+\delta+\frac{\gamma}{g(0)}}$ is the life expectancy of infectious persons. $\frac{A}{\mu}$ signifies the number of susceptible persons at the starting of the infectious process and $\frac{\beta A}{\mu f(0)}$ represents the value when all the individuals are susceptible. $\frac{q}{\mu+q}$ represents the fraction of exposed individuals who survive in class E and become infected. Hence the basic reproduction number R_0 is biologically well interpreted.

2. The endemic equilibrium $D^*(S^*, E^*, I^*, R^*)$, where

$$S^* = \frac{A f(I^*)}{\beta I^* + \mu f(I^*)}, \quad E^* = \frac{\beta A I^*}{(\mu + q)(\beta I^* + \mu f(I^*))}, \quad R^* = \frac{\gamma}{\mu}\frac{I^*}{g(I^*)},$$

   and I^* is a unique positive root of the following equation

$$\frac{A\beta}{\beta I + \mu f(I)} - \frac{\gamma}{q}\frac{(\mu + q)}{g(I)} - \frac{(\mu + q)(\mu + \delta)}{q} = 0. \tag{3.3}$$

Let

$$Q(I) = \frac{A\beta}{\beta I + \mu f(I)} - \frac{\gamma}{q}\frac{(\mu + q)}{g(I)} - \frac{(\mu + q)(\mu + \delta)}{q},$$

then we can see that $Q(0) = \frac{A\beta}{\mu f(0)} - \frac{\gamma}{q}\frac{(\mu+q)}{g(0)} - \frac{(\mu+q)(\mu+\delta)}{q} > 0$, if $R_0 > 1$. Let $Q_1(I) = \frac{A\beta}{\beta I+\mu f(I)}$ and $Q_2(I) = \frac{(\mu+q)(\mu+\delta)}{q} + \frac{\gamma}{q}\frac{(\mu+q)}{g(I)}$, then we have $\lim_{I\to\infty} Q_1(I) = 0$, $\lim_{I\to\infty} Q_2(I) = \frac{(\mu+q)(\mu+\delta)}{q}$, $Q_1'(I) < 0$ and $Q_2'(I) < 0$. We also observe that $Q_1(0) > Q_2(0)$ when $R_0 > 1$. Hence $Q_1(I)$ and $Q_2(I)$ intersect each other only once when $R_0 > 1$, which proves the existence and uniqueness of D^*.

We observe that $Q_1(0) < Q_2(0)$ when $R_0 < 1$ and both $Q_1(I)$ and $Q_2(I)$ are monotonically decreasing. Thus, $Q_1(I)$ and $Q_2(I)$ do not intersect each other when $R_0 < 1$. Therefore, there is no endemic equilibrium when $R_0 < 1$.

On the other hand, by choosing $f(I) = 1 + \alpha_1 I^2$ and $g(I) = 1 + \alpha_2 I^2$, we see the existence of D^* by plotting the two nullclines in SI-plane.

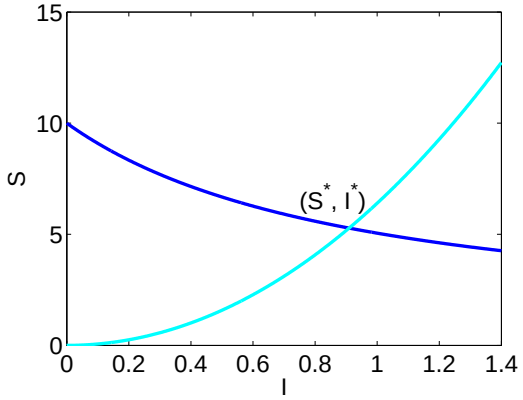

Figure 4. Figure shows the existence of a unique endemic equilibrium D^* when $R_0 > 1$.

3.3. Local stability behavior

Theorem 3.2. *1. The disease-free equilibrium D_0 is locally asymptotically stable when $R_0 < 1$ and unstable when $R_0 > 1$.*

2. System (2.2) undergoes a transcritical bifurcation when $R_0 = 1$ and the endemic equilibrium D^* is locally asymptotically stable when $R_0 > 1$.

Proof. For the proof of Theorem 3.2, interested readers may refer to Appendix A. □

The threshold quantity R_0 denotes the average number of new disease infection generated by a single infection introduced into a community of susceptible individuals. The result of Theorem 3.2 shows that the disease can be eliminated in the community when the basic reproduction number $R_0 < 1$ and the initial population sizes are within the attraction basin of D_0.

3.4. Global stability behavior

Theorem 3.3. *The disease-free equilibrium D_0 is globally asymptotically stable when $R_0 < 1$.*

Proof. For the proof of Theorem 3.3, one may refer to Appendix A. □

Theorem 3.4. *The endemic equilibrium D^* is globally asymptotically stable when $R_0 > 1$.*

Proof. Refer to Appendix A. □

Remark 3.1. *1. One can observe that in the absence of intervention strategies, i.e., $f(I) = 1$, the basic reproduction number is given by $R_0 = \frac{\beta A q}{\mu(\mu+q)(\mu+\delta+\frac{\gamma}{g(0)})}$. Thus if $f(0) = 1$, which means that if we perform intervention strategies at a suitable level of infection, R_0 remains same. However, by*

our assumption, f is an increasing function, which means R_0 is greater than that in the presence of interventions. From Theorem 3.4, *D^* is globally asymptotically stable, thus intervention strategies decreases the endemic level of disease.*

2. *Further, if there is no limitation on resources of treatment for large infective individuals, i.e., $g(I) = 1$, the basic reproduction number is given by $R_0 = \frac{\beta A q}{\mu f(0)(\mu+q)(\mu+\delta+\gamma)}$. Thus if $g(0) = 1$, which means that if there are low availability of resources for treatment at some level of infection, R_0 remains same. However, by our assumption, g is an increasing function, which means R_0 would be less than that in case of low availability of resources for treatment. Since from Theorem* 3.4, *D^* is globally asymptotically stable, therefore, low resources of treatment increase the endemic level of disease. Clearly, it could be concluded that the disease persists along with the low availability of resources for treatment when the basic reproduction number is greater than one.*

4. Dynamics of delayed system (2.3)

4.1. Positivity and boundedness

Define $L(t) = \min_{t\geq 0}\{S(t), E(t), I(t), R(t)\}$. Clearly, $L(0) = \min\{S(0), E(0), I(0), R(0)\} > 0$. We need to show that $L(t) > 0$ for all $t \geq 0$. Suppose that there exists a $t_0 > 0$ such that $L(t_0) = 0$ and $L(t) > 0$ for all $t \in [0, t_0)$. Here, we need to discuss the following four cases: (*i*) $L(t_0) = S(t_0)$; (*ii*) $L(t_0) = E(t_0)$; (*iii*) $L(t_0) = I(t_0)$; (*iv*) $L(t_0) = R(t_0)$. We only give the proof of case (*iv*). The remaining cases could be discussed similarly.
Let $L(t_0) = R(t_0)$. Since $L(t) > 0$ for all $t \in [0, t_0)$, $I(t - \tau_2) > 0$,

$$\frac{dR}{dt} \geq -\mu R(t) \quad \forall \quad t \in [0, t_0),$$

integrating from 0 to t_0, we obtain

$$0 = R(t_0) \geq R(0)e^{-\mu t_0} > 0,$$

which leads a contradiction. Hence $S(t), E(t), I(t), R(t)$ are positive for all $t \geq 0$. For the boundedness of system (2.3), one can follow Section 3. The closed region $\mho$ defined in (3.1) is also invariant for system (2.3).

4.2. Disease-free equilibrium and its stability

The first three equations of system (2.3) do not include the variable R. Therefore, for simplicity, we ignore the forth equation and analyze the following reduced system containing only first three equations:

$$\begin{aligned}
\frac{dS}{dt} &= A - \mu S - \frac{\beta I}{f(I(t-\tau_1))}S,\\
\frac{dE}{dt} &= \frac{\beta I}{f(I(t-\tau_1))}S - (\mu+q)E,\\
\frac{dI}{dt} &= qE - (\mu+\delta)I - \frac{\gamma I(t-\tau_2)}{g(I(t-\tau_2))}.
\end{aligned} \tag{4.1}$$

Since delay does not affect the number of equilibria, system (4.1) always has a disease-free equilibrium D_0 and a unique endemic equilibrium D^*, which have already been defined in Section 3. The basic reproduction number R_0 has also been defined in Section 3.

Theorem 4.1. *1. If $V_{11}^2 - V_{13}^2 - 2V_{12} > 0$ and $V_{12}^2 - V_{14}^2 > 0$, D_0 is locally asymptotically stable when $\tau_1 > 0, \tau_2 > 0$ and $R_0 < 1$.*

2. D_0 is unstable when $R_0 > 1$.

Proof. For the proof of Theorem 4.1, one may refer to Appendix A. □

Remark 4.1. *From the proof of Theorem* 4.1 *in Appendix A, we observe that if $\tau_1 > 0, \tau_2 = 0$, D_0 is locally asymptotically stable when $R_0 < 1$. Further if $\tau_1 = 0$ and $\tau_2 > 0$, then D_0 is not locally asymptotically stable. Thus the result of Theorem* 4.1 *shows that time delay in the interventions (τ_1) does not affect the stability of D_0, however, the result for the time delay in the recovery (τ_2) suggests that only a restriction on the basic reproduction number R_0 will not be sufficient for the local stability of disease free equilibrium.*

4.3. Stability of D^* and local Hopf bifurcation

In this subsection, we discuss the stability of D^* and establish the local Hopf bifurcation of system (4.1). The characteristic equation of system (4.1) at D^* is given by

$$\det\begin{pmatrix} J_{11}-\lambda & 0 & J_{12}+J_{18}e^{-\lambda\tau_1} \\ J_{13} & J_{14}-\lambda & J_{15}+J_{19}e^{-\lambda\tau_1} \\ 0 & J_{16} & J_{17}+J_{20}e^{-\lambda\tau_2}-\lambda \end{pmatrix} = 0, \tag{4.2}$$

where

$$\begin{aligned} J_{11} =& -\mu - \frac{\beta I^*}{f(I^*)}, \quad J_{12} = -\frac{\beta S^*}{f(I^*)}, \quad J_{13} = \frac{\beta I^*}{f(I^*)}, \quad J_{14} = -(\mu+q), \\ J_{18} =& \frac{\beta I^* S^*}{f(I^*)^2} f'(I^*), \quad J_{19} = -\frac{\beta I^* S^*}{f(I^*)^2} f'(I^*), \quad J_{15} = \frac{\beta S^*}{f(I^*)}, \\ J_{16} =& q, \quad J_{17} = -(\mu+\delta), \quad J_{20} = \gamma \frac{[I^* g'(I^*) - g(I^*)]}{g(I^*)^2}. \end{aligned}$$

Eq. (4.2) is equivalent to

$$\lambda^3 + P_{11}\lambda^2 + P_{12}\lambda + P_{13} + (P_{14}\lambda + P_{15})e^{-\lambda\tau_1} + (P_{16}\lambda^2 + P_{17}\lambda + P_{18})e^{-\lambda\tau_2} = 0, \tag{4.3}$$

where

$$\begin{aligned} P_{11} =& -(J_{11}+J_{14}+J_{17}),\ P_{12} = J_{11}(J_{14}+J_{17}) + J_{14}J_{17} - J_{15}J_{16}, \\ P_{13} =& J_{11}(J_{14}J_{17} + J_{15}J_{16}) - J_{12}J_{13}J_{16},\ P_{14} = -J_{16}J_{19}, \\ P_{15} =& J_{16}(J_{11}J_{19} - J_{13}J_{18}),\ P_{16} = -J_{20},\ P_{17} = J_{20}(J_{11}+J_{14}),\ P_{18} = -J_{11}J_{14}J_{20}. \end{aligned}$$

For the stability and Hopf bifurcation, we have the following results:

Remark 4.2. *If $\tau_1 = \tau_2 = 0$. In this case, system* (4.1) *becomes the non-delayed system* (2.2). *We have already discussed this case in Section* 3.

Lemma 4.2. *[54] For the transcendental equation*

$$\begin{aligned} x(\lambda, e^{-\lambda\tau_1}, \ldots, e^{-\lambda\tau_m}) =& \lambda^n + x_1^{(0)}\lambda^{n-1} + \ldots + x_{n-1}^{(0)}\lambda + x_n^{(0)} \\ &+ \left[x_1^{(1)}\lambda^{n-1} + \ldots + x_{n-1}^{(1)}\lambda + x_n^{(1)}\right] e^{-\lambda\tau_1} + \ldots \\ &+ \left[x_1^{(m)}\lambda^{n-1} + \ldots + x_{n-1}^{(m)}\lambda + x_n^{(m)}\right] e^{-\lambda\tau_m} = 0, \end{aligned}$$

as $\tau_1, \tau_2, \ldots \tau_m$ vary, the sum of the orders of the zeros of $x(\lambda, e^{-\lambda\tau_1}, \ldots, e^{-\lambda\tau_m})$ in the open right half plane can change only if a zero occurs on or crosses the imaginary axis.

Lemma 4.3. *If $M_{11}M_{13} + M_{12}M_{14} > 0$, then $\left(\frac{d\lambda}{d\tau_1}\right)^{-1}_{\lambda=i\omega_1', \tau_1=\tau_{1_j}} > 0$ $(j = 0, 1, 2, \ldots)$ holds.*

Similarly one can prove $\left(\frac{d\lambda}{d\tau_1}\right)^{-1}_{\lambda=i\omega_1^{\pm}, \tau_1=\tau_{1_k}} > 0$ $(k = 0, 1, 2, \ldots)$ and $\left(\frac{d\lambda}{d\tau_1}\right)^{-1}_{\lambda=i\omega_1^{1,2,3}, \tau_1=\tau_{1_l}} > 0$ $(l = 0, 1, 2, \ldots)$.

Theorem 4.4. *For reduced system* (4.1)*, the following conclusions hold:*

1. *If $c_{11} > 0, c_{12} > 0, c_{13} > 0$, then D^* is locally asymptotically stable for $\tau_1 \in (0, +\infty)$.*
2. *If $c_{13} < 0, c_{11} > 0, c_{12} > 0$ or $c_{13} < 0, c_{11} > 0, c_{12} < 0$ or $c_{13} < 0, c_{11} < 0, c_{12} < 0$, there exists a ξ_{1_j} such that $0 < \xi_{1_j} \leq \tau_{1_j}$. Then D^* is locally asymptotically stable for $\xi_{1_j} < \tau_1 < \tau_{1_j}$ and unstable for $\xi_{1_{j+1}} > \tau_1 > \tau_{1_j}$. Additionally, system* (4.1) *undergoes a supercritical Hopf bifurcation at D^* when $\tau_1 = \tau_{1_j}$.*
3. *If $c_{11} > 0$, $c_{12} < 0, c_{13} > 0$ or $c_{11} < 0$, $c_{12} > 0, c_{13} > 0$ or $c_{11} < 0$, $c_{12} < 0, c_{13} > 0$, there exists a σ_{1_k} such that $0 < \sigma_{1_k} \leq \tau_{1_k}$. Then D^* is locally asymptotically stable for $\sigma_{1_k} < \tau_1 < \tau_{1_k}$ and unstable for $\sigma_{1_{k+1}} > \tau_1 > \tau_{1_k}$. Additionally, system* (4.1) *undergoes a supercritical Hopf bifurcation at D^* when $\tau_1 = \tau_{1_k}$.*
4. *If $c_{11} < 0$, $c_{12} > 0, c_{13} < 0$, there exists a σ_{1_l} such that $0 < \sigma_{1_l} \leq \tau_{1_l}$. Then D^* is locally asymptotically stable for $\sigma_{1_l} < \tau_1 < \tau_{1_l}$ and unstable for $\sigma_{1_{l+1}} > \tau_1 > \tau_{1_l}$. Additionally, system* (4.1) *undergoes a supercritical Hopf bifurcation at D^* when $\tau_1 = \tau_{1_l}$.*

Lemma 4.5. *If $M_{21}M_{23} + M_{22}M_{24} > 0$, then $Re\left(\frac{d\lambda}{d\tau_2}\right)^{-1}_{\lambda=i\omega_2', \tau_2=\tau_{2_j}} > 0$ $(j = 0, 1, 2, \ldots)$ holds.*

Similarly one can also prove $\left(\frac{d\lambda}{d\tau_2}\right)^{-1}_{\lambda=i\omega_2^{\pm}, \tau_2=\tau_{2_k}} > 0$ $(k = 0, 1, 2, \ldots)$ and $\left(\frac{d\lambda}{d\tau_2}\right)^{-1}_{\lambda=i\omega_2^{1,2,3}, \tau_2=\tau_{2_l}} > 0$ $(l = 0, 1, 2, \ldots)$.

Theorem 4.6. *For reduced system* (4.1)*, the following conclusions hold:*

1. *If $d_{11} > 0, d_{12} > 0, d_{13} > 0$, then D^* is locally asymptotically stable for $\tau_2 \in (0, +\infty)$.*
2. *If $d_{13} < 0, d_{11} > 0, d_{12} > 0$ or $d_{13} < 0, d_{11} > 0, d_{12} < 0$ or $d_{13} < 0, d_{11} < 0, d_{12} < 0$, there exists a ξ_{2_j} such that $0 < \xi_{2_j} \leq \tau_{2_j}$. Then D^* is locally asymptotically stable for $\xi_{2_j} < \tau_2 < \tau_{2_j}$ and unstable for $\xi_{2_{j+1}} > \tau_2 > \tau_{2_j}$. Additionally, system* (4.1) *undergoes a supercritical Hopf bifurcation at D^* when $\tau_2 = \tau_{2_j}$.*

3. *If* $d_{11} > 0$, $d_{12} < 0, d_{13} > 0$ *or* $d_{11} < 0$, $d_{12} > 0, d_{13} > 0$ *or* $d_{11} < 0$, $d_{12} < 0, d_{13} > 0$, *there exists a* σ_{2_k} *such that* $0 < \sigma_{2_k} \leq \tau_{2_k}$. *Then* D^* *is locally asymptotically stable for* $\sigma_{2_k} < \tau_2 < \tau_{2_k}$ *and unstable for* $\sigma_{2_{k+1}} > \tau_2 > \tau_{2_k}$. *Additionally, system* (4.1) *undergoes a supercritical Hopf bifurcation at* D^* *when* $\tau_2 = \tau_{2_k}$.

4. *If* $d_{11} < 0$, $d_{12} > 0, d_{13} < 0$ *there exists a* σ_{2_l} *such that* $0 < \sigma_{2_l} \leq \tau_{2_l}$. *Then* D^* *is locally asymptotically stable for* $\sigma_{2_l} < \tau_2 < \tau_{2_l}$ *and unstable for* $\sigma_{2_{l+1}} > \tau_2 > \tau_{2_l}$. *Additionally, system* (4.1) *undergoes a supercritical Hopf bifurcation at* D^* *when* $\tau_2 = \tau_{2_l}$.

Lemma 4.7. *If* $M_{31}M_{33} + M_{32}M_{34} > 0$, *then* $Re\left(\frac{d\lambda}{d\tau}\right)^{-1}_{\lambda=i\omega_3', \tau=\tau_j} > 0$ $(j = 0, 1, 2, \dots)$ *holds.*

Similarly we can also prove $\left(\frac{d\lambda}{d\tau}\right)^{-1}_{\lambda=i\omega_3^{\pm}, \tau=\tau_k} > 0$ $(k = 0, 1, 2, \dots)$ and $\left(\frac{d\lambda}{d\tau}\right)^{-1}_{\lambda=i\omega_3^{1,2,3}, \tau=\tau_l} > 0$ $(l = 0, 1, 2, \dots)$.

Theorem 4.8. *For reduced system* (4.1), *the following conclusions hold:*

1. *If* $e_{11} > 0, e_{12} > 0, e_{13} > 0$, *then* D^* *is locally asymptotically stable for* $\tau \in (0, +\infty)$.

2. *If* $e_{13} < 0, e_{11} > 0, e_{12} > 0$ *or* $e_{13} < 0, e_{11} > 0, e_{12} < 0$ *or* $e_{13} < 0, e_{11} < 0, e_{12} < 0$, *there exists a* ξ_{3_j} *such that* $0 < \xi_{3_j} \leq \tau_j$. *Then* D^* *is locally asymptotically stable for* $\xi_{3_j} < \tau < \tau_j$ *and unstable for* $\xi_{3_{j+1}} > \tau > \tau_j$. *Additionally, system* (4.1) *undergoes a supercritical Hopf bifurcation at* D^* *when* $\tau = \tau_j$.

3. *If* $e_{11} > 0$, $e_{12} < 0, e_{13} > 0$ *or* $e_{11} < 0$, $e_{12} > 0, e_{13} > 0$ *or* $e_{11} < 0$, $e_{12} < 0, e_{13} > 0$, *there exists a* σ_{3_k} *such that* $0 < \sigma_{3_k} \leq \tau_k$. *Then* D^* *is locally asymptotically stable for* $\sigma_{3_k} < \tau < \tau_k$ *and unstable for* $\sigma_{3_{k+1}} > \tau > \tau_k$. *Additionally, system* (4.1) *undergoes a supercritical Hopf bifurcation at* D^* *when* $\tau = \tau_k$.

4. *If* $e_{11} < 0$, $e_{12} > 0, e_{13} < 0$, *there exists a* σ_{3_l} *such that* $0 < \sigma_{3_l} \leq \tau_l$. *Then* D^* *is locally asymptotically stable for* $\sigma_{3_l} < \tau < \tau_l$ *and unstable for* $\sigma_{3_{l+1}} > \tau > \tau_l$. *Additionally, system* (4.1) *undergoes a supercritical Hopf bifurcation at* D^* *when* $\tau = \tau_l$.

Lemma 4.9. *If* $M_{41}M_{43} + M_{42}M_{44} > 0$, *then* $Re\left(\frac{d\lambda}{d\tau_1}\right)^{-1}_{\lambda=i\omega_4^*, \tau_1=\tau_{1_j}^*} > 0$ $(j = 0, 1, 2, \dots)$ *holds.*

Theorem 4.10. *For reduced system* (4.1), *If* ***H1*** *holds, there exists a* ξ_{4_j} *such that* $0 < \xi_{4_j} \leq \tau_{1_j}^*$. *Then* D^* *is locally asymptotically stable for* $\xi_{4_j} < \tau_1 < \tau_{1_j}^*$ *and unstable for* $\xi_{4_{j+1}} > \tau_1 > \tau_{1_j}^*$. *Additionally, system* (4.1) *undergoes a supercritical Hopf bifurcation at* D^* *when* $\tau_1 = \tau_{1_j}^*$.

Remark For the proofs of Lemmas 4.3, 4.5, 4.7, 4.9, and Theorems 4.4, 4.6, 4.8, 4.10, interested readers may refer to Appendix A.

Remark 4.3. *Without loss of generality, in Subsection* 4.3 *we only discussed the case* $Re\left(\frac{d\lambda}{d\tau_j}\right)^{-1}_{\lambda=i\omega, \tau=\tau_j} > 0$ $(j = 1, 2)$. *Similarly, for the case of* $Re\left(\frac{d\lambda}{d\tau_j}\right)^{-1}_{\lambda=i\omega, \tau=\tau_j} < 0$ $(j = 1, 2)$, *subcritical Hopf bifurcation will appear instead of supercritical Hopf bifurcation. We do not provide details here.*

4.4. Stability and direction of Hopf bifurcation

In Subsection 4.3, we have established that the reduced system (4.1) possesses a family of periodic solutions bifurcating from D^* at the different critical values of delay parameters τ_1 and τ_2. In this subsection, by using the center manifold theorem and normal form theory [57], the properties of the Hopf bifurcation at the critical value τ_1^* are determined. Throughout the section, we consider that $\tau_2^* < \tau_1^*$, where $\tau_2^* \in (0, \tau_{2j})$. For detailed discussion related to properties of the Hopf bifurcation (direction and stability of Hopf bifurcation), one may refer to Appendix B.

Remark 4.4. *The disappearance or appearance of a periodic orbit through a local change in the stability properties of a steady point is called Hopf bifurcation. There are two types of Hopf bifurcation, the bifurcation is known as supercritical if the bifurcated periodic solutions are stable and subcritical if they are unstable. The parameter μ_2 determines the directions of the Hopf bifurcation: if $\mu_2 > 0$ ($\mu_2 < 0$), then the Hopf bifurcation is supercritical (subcritical).*

Theorem 4.11. *If $Re\{c_1(0)\} < 0$ ($Re\{c_1(0)\} > 0$), then the reduced system* (4.1) *undergoes a supercritical (subcritical) Hopf bifurcation at D^* when τ_1 crosses its critical value τ_1^*. Furthermore, the bifurcated periodic solutions occurring through Hopf bifurcations are orbitally asymptotically stable on the center manifold if $Re\{c_1(0)\} < 0$ and unstable if $Re\{c_1(0)\} > 0$.*

4.5. Global continuation of local Hopf bifurcation

In this subsection, we investigate the global continuation of periodic solutions bifurcating from D^* for system (2.3) for fixed τ_2 in the interval $(0, \tau_{2j})$. Throughout this subsection, we follow the notations in Wu [59]. For simplification, we denote $\tau = \tau_1$. Let $z(t) = (z_1(t), z_2(t), z_3(t)) = (S(t), E(t), I(t))$, then system (2.3) can be rewritten as

$$\dot{z} = F(z_t, \tau, p), \tag{4.4}$$

where $z_t(\theta) = (z_1(t+\theta), z_2(t+\theta), z_3(t+\theta))^T = (z_{1t}(\theta), z_{2t}(\theta), z_{3t}(\theta))^T \in C([-\tau, 0], \mathbb{R}^3)$. It is clear that if $R_0 > 1$, then system (2.3) has a disease-free equilibrium (D_0) and an endemic equilibrium (D^*). Following Wu [59], we define

$$\begin{aligned} X =& C([-\tau, 0], \mathbb{R}^3), \\ \mho =& Cl\{(z, \tau, p) \in X \times \mathbb{R} \times \mathbb{R}_+; z \text{ is a nonconstant periodic solution of (4.4)}\}, \\ M =& \{(\bar{z}, \tau, p); F(\bar{z}, \tau, p) = 0\}. \end{aligned}$$

Lemma 4.12. *Assume that $(\bar{z}, \tau, p)$ is an isolated center satisfying (A1-A4) in [59]. Denote by $l_{(\bar{z},\tau,p)}$ the connected component of $(\bar{z}, \tau, p)$ in $\mho$. Then either*

(i) $l_{(\bar{z},\tau,p)}$ is unbounded, or

(ii) $l_{(\bar{z},\tau,p)}$ is bounded, $l_{(\bar{z},\tau,p)} \cap M$ is finite, and $\sum_{(\bar{z},\tau,p) \in l_{(\bar{z},\tau,p)} \cap M} \gamma_m(\bar{z}, \tau, p) = 0$ for all $m = 1, 2, 3, \ldots$, where $\gamma_m(\bar{z}, \tau, p)$ is the m^{th} crossing number of $(\bar{z}, \tau, p)$, if $m \in J(\bar{z}, \tau, p)$, or it is zero otherwise.

It is well recognized that if the condition (ii) of above lemma is not true, then $l_{(\bar{z},\tau,p)}$ is unbounded. Thus, if the projections of $l_{(\bar{z},\tau,p)}$ onto p-space and onto z-space are bounded, then the projection onto τ-space is unbounded. Further, if we can show that the projection of $l_{(\bar{z},\tau,p)}$ onto τ-space is away from zero, then the projection of $l_{(\bar{z},\tau,p)}$ onto τ-space must include interval $[\tau, +\infty)$. Following this concept, we can prove our consequences on the global continuation of local Hopf bifurcation.

Lemma 4.13. *If $R_0 > 1$, then all non-constant periodic solutions of system* (2.3) *with initial conditions* (2.4) *are uniformly bounded.*

Lemma 4.14. *If $R_0 > 1$, then there does not exist any non-constant periodic solution of system* (2.3) *with period τ.*

Proof. Suppose there exists a non-constant periodic solution of system (2.3) with period τ. Then system (2.2) also has a non-constant periodic solution. Both systems (2.2) and (2.3) have same equilibria, i.e., D_0 and D^*. Note that E-axis and I-axis are the invariable manifolds of system (2.2) and the orbits of system (2.2) do not cross each other. Thus, there is no solution that intersects the coordinate axis.

On the other hand, if system (2.2) has a periodic solution, then there must be an equilibrium in its interior [41] and D_0 is located on the coordinate axis. Thus, it can be concluded that the periodic orbit of system (2.2) must lie in the first octant. From Theorem 3.4, the positive equilibrium is globally asymptotically stable in $\mathbb{R}^4_+$, thus, there is no periodic orbit in the first quadrant. This completes the proof. □

Theorem 4.15. *Let ω_4^* and τ_{1j}^* $(j = 0, 1, 2, \ldots)$ be defined in case 5 in subsection* 4.3. *Then for each $\tau > \tau_{1j}^*$ $(j \geq 1)$, system* (2.3) *has at least $j + 1$ periodic solutions.*

Proof. It is sufficient to prove that the projection of $l_{(D^*,\tau_{1j}^*,2\pi/\omega_4^*)}$ onto τ-space is $[\tau, +\infty)$ for each $j > 0$, where $\bar{\tau} \leq \tau_{1j}^*$. The characteristic matrix of (4.4) at positive equilibrium D^* takes the following form

$$\Delta(D^*, \tau, p)(\lambda) = \begin{pmatrix} J_{11} - \lambda & 0 & J_{12} + J_{18}e^{-\lambda\tau} \\ J_{13} & J_{14} - \lambda & J_{15} + J_{19}e^{-\lambda\tau} \\ 0 & J_{16} & J_{17} + J_{20}e^{-\lambda\tau_2} - \lambda \end{pmatrix}, \tag{4.5}$$

where $J_{1i}, i = 1, 2, 3, 4, 5, 6, 7, 8, 9$ and J_{20} are defined in subsection 4.3. From the discussion of local Hopf bifurcation, it is easy to verify that $(D^*, \tau_{1j}^*, 2\pi/\omega_4^*)$, $j = 1, 2, ...$ are isolated centers. There exists $\epsilon > 0, \delta > 0$ and a smooth curve $\lambda : (\tau_{1j}^* - \delta, \tau_{1j}^* + \delta) \to C$, such that $det(\Delta(\lambda(\tau))) = 0, |\lambda(\tau) - \omega_4^*| < \epsilon$ for all $\tau \in [\tau_{1j}^* - \delta, \tau_{1j}^* + \delta]$ and

$$\lambda(\tau_{1j}^*) = i\omega_4^*, \quad \frac{dRe(\lambda(\tau))}{d\tau}\Big|_{\tau=\tau_{1j}^*} > 0.$$

Let

$$\Omega_{\epsilon,2\pi/\omega_4^*} = \Big\{(\eta, p) : 0 < \eta < \epsilon, \Big|p - \frac{2\pi}{\omega_4^*}\Big| < \epsilon\Big\}.$$

It is easy to verify that on $[\tau_{1j}^* - \delta, \tau_{1j}^* + \delta] \times \partial\Omega_{\epsilon,2\pi/\omega_4^*}$,

$$det\Big(\Delta(D^*, \tau, p)\Big(\eta + \frac{2\pi}{p}i\Big)\Big) = 0$$

if and only if $\eta = 0, \tau = \tau_{1j}^*, p = 2\pi/\omega_4^*$. Thus, the hypotheses (A1-A4) in [59] are satisfied. Moreover, if we define

$$H^{\pm}\Big(D^*, \tau_{1j}^*, \frac{2\pi}{\omega_4^*}\Big)(\eta, p) = det\Big(\Delta(D^*, \tau_{1j}^* \pm \delta, p)\Big(\eta + \frac{2\pi}{p}i\Big)\Big),$$

then we have the crossing number of isolated center $\left(D^*, \tau^*_{1j}, \frac{2\pi}{\omega^*_4}\right)$ as follows:

$$\begin{aligned}\gamma\Big(D^*, \tau^*_{1j}, \frac{2\pi}{\omega^*_4}\Big) &= \deg_B\Big(H^-\Big(D^*, \tau^*_{1j}, \frac{2\pi}{\omega^*_4}\Big), \Omega_{\epsilon,2\pi/\omega^*_4}\Big) - \deg_B\Big(H^+\Big(D^*, \tau^*_{1j}, \frac{2\pi}{\omega^*_4}\Big), \Omega_{\epsilon,2\pi/\omega^*_4}\Big)\\ &= -1.\end{aligned}$$

By Theorem 3.2 in Wu [59], we conclude that the connected $l_{(D^*,\tau^*_{1j},2\pi/\omega^*_4)}$ through $(D^*, \tau^*_{1j}, 2\pi/\omega^*_4)$ in $\mathfrak{V}$ is nonempty. We have

$$\sum_{(\bar{z},\tau,p)\in l_{(D^*,\tau^*_{1j},2\pi/\omega^*_4)}} \gamma(\bar{z}, \tau, p) < 0.$$

Hence $l_{(D^*,\tau^*_{1j},2\pi/\omega^*_4)}$ is unbounded.

From Eq. (.34), we see that, for $j \geq 1, 2\pi/\omega^*_4 < \tau^*_{1j}$. Then, we are in a position to show that the projection of $l_{(D^*,\tau^*_{1j},2\pi/\omega^*_4)}$ onto τ-space is $[\bar{\tau}, +\infty)$, where $\bar{\tau} < \tau^*_{1j}$. Clearly, it follows from the proof of Lemma 4.14 that system (2.3) with $\tau = 0$ has no non-constant periodic solution. Hence, the projection of $l_{(D^*,\tau^*_{1j},2\pi/\omega^*_4)}$ onto τ-space is away from zero.

For a contradiction, we suppose that the projection of $l_{(D^*,\tau^*_{1j},2\pi/\omega^*_4)}$ onto τ-space is bounded. This means that the projection of $l_{(D^*,\tau^*_{1j},2\pi/\omega^*_4)}$ onto τ-space is included in an interval $(0, \tau^*)$. Note that $2\pi/\omega^*_4 < \tau^*_{1j}$ and applying Lemma 4.14, we have $p < \tau^*$ for (z, τ, p) belonging to $l_{(D^*,\tau^*_{1j},2\pi/\omega^*_4)}$. This implies that the projection of the connected component $l_{(D^*,\tau^*_{1j},2\pi/\omega^*_4)}$ onto p-space is bounded. In addition, from Lemma 4.13, we obtain that the projection of $l_{(D^*,\tau^*_{1j},2\pi/\omega^*_4)}$ onto z-space is bounded if the projection of $l_{(D^*,\tau^*_{1j},2\pi/\omega^*_4)}$ onto τ-space is bounded. Thus, the connected component $l_{(D^*,\tau^*_{1j},2\pi/\omega^*_4)}$ crossing through $(D^*, \tau^*_{1j}, 2\pi/\omega^*_4)$ is bounded, which is a contradiction. This implies that the projection of $l_{(D^*,\tau^*_{1j},2\pi/\omega^*_4)}$ onto τ-space is $[\bar{\tau}, +\infty)$ for each $j \geq 1$, where $\bar{\tau} < \tau^*_{1j}$. This completes the proof. □

4.6. Estimation of the length of delay to preserve stability

In this subsection, we determine the length of delay to preserve the stability of system (4.1) by the Nyquist criterion [55]. We consider the system (4.1) and space of all real-valued continuous functions on $[-\tau, +\infty)$ satisfying the initial conditions on $[-\tau, 0]$. We use the transformations $S = S^* + u_1, E = E^* + u_2, I = I^* + u_3$ and obtain the following linearized system:

$$\begin{aligned}\frac{du_1}{dt} &= a_{11}u_1 + a_{12}u_3 + a_{13}u_3(t-\tau_1),\\ \frac{du_2}{dt} &= a_{21}u_1 + a_{22}u_2 + a_{23}u_3 + a_{24}u_3(t-\tau_1),\\ \frac{du_3}{dt} &= a_{31}u_2 + a_{32}u_3 + a_{33}u_3(t-\tau_2),\end{aligned} \tag{4.6}$$

where

$$\begin{aligned}a_{11} &= -\left(\mu + \frac{\beta I^*}{f(I^*)}\right), \quad a_{12} = -\frac{\beta S^*}{f(I^*)}, \quad a_{13} = \frac{\beta S^* I^* f'(I^*)}{f(I^*)^2},\\ a_{21} &= \frac{\beta I^*}{f(I^*)}, \quad a_{22} = -(\mu + q), \quad a_{23} = \frac{\beta S^*}{f(I^*)}, \quad a_{24} = -\frac{\beta S^* I^* f'(I^*)}{f(I^*)^2},\end{aligned}$$

$$a_{31} = q, \quad a_{32} = (\mu + \delta + \frac{\gamma}{g(I^*)}), \quad a_{33} = \frac{\gamma g'(I^*)}{(g(I^*))^2}.$$

Now taking Laplace transform of system (4.6), we obtain

$$\begin{aligned}
(s - a_{11})\bar{u}_1(s) &= u_1(0) + a_{12}\bar{u}_3(s) + a_{13}e^{-s\tau_1}\bar{u}_3(s) + a_{13}e^{-s\tau_1}K_1(s),\\
(s - a_{22})\bar{u}_2(s) &= u_2(0) + a_{21}\bar{u}_1(s) + a_{23}\bar{u}_3(s) + a_{24}e^{-s\tau_1}\bar{u}_3(s) + a_{24}e^{-s\tau_1}K_1(s),\\
(s - a_{32} - a_{33}e^{-s\tau_2})\bar{u}_3(s) &= u_3(0) + a_{31}\bar{u}_2(s) + a_{33}e^{-s\tau_2}K_2(s),
\end{aligned} \tag{4.7}$$

where $K_1(s) = \int_{-\tau_1}^{0} e^{-s\tau_1}u_3(t)dt$, $K_2(s) = \int_{-\tau_2}^{0} e^{-s\tau_2}u_3(t)dt$, and $\bar{u}_i(s)$ are the Laplace transforms of $u_i(t), i = 1, 2, 3$, respectively. The characteristic equation of Eq. (4.7) is

$$\Psi(s) = s^3 + P_{11}s^2 + P_{12}s + P_{13} + (P_{14}s + P_{15})e^{-s\tau_1} + (P_{16}s^2 + P_{17}s + P_{18})e^{-s\tau_2} = 0, \tag{4.8}$$

where $P_{1i}, i = 1, 2, 3, 4, 5, 6, 7, 8$ are given in subsection 4.3. The conditions for local asymptotic stability of D^* are given by

$$Re(\Psi(i\eta_0)) = 0, \tag{4.9}$$

$$Im(\Psi(i\eta_0)) > 0, \tag{4.10}$$

where η_0 is the smallest positive root of Eq. (4.9).

We have already revealed that D^* is locally asymptotically stable when $\tau_1 = \tau_2 = 0$. Hence, by continuity, all eigenvalues will have negative real parts for sufficiently small $\tau_1 > 0, \tau_2 > 0$ provided one can assure that no eigenvalues with positive real parts bifurcates from infinity as τ_1 and τ_2 increase from zero. This can be proved by Butler's lemma [56]. Now, we consider the conditions of Case 5, i.e., $\tau_1 > 0$ and τ_2 is in stable interval. Eq. (4.9) and (4.10) gives

$$P_{11}\eta_0^2 - P_{13} - (P_{18} - P_{16}\eta_0^2)\cos(\eta_0\tau_2) - P_{17}\eta_0\sin(\eta_0\tau_2) = \quad P_{15}\cos(\eta_0\tau_1) + P_{14}\eta_0\sin(\eta_0\tau_1), \tag{4.11}$$

$$-P_{12}\eta_0 + \eta_0^3 - P_{17}\eta_0\cos(\eta_0\tau_2) + (P_{18} - P_{16}\eta_0^2)\sin(\eta_0\tau_2) > \quad P_{14}\eta_0\cos(\eta_0\tau_1) - P_{15}\sin(\eta_0\tau_1). \tag{4.12}$$

If Eq. (4.11) and (4.12) hold simultaneously, these are sufficient conditions to assure stability. We shall use them to obtain an estimation of the length of delay. Our goal is to discover an upper bound η^+ on η_0 free of τ_1 and τ_2, and then estimate τ_1 so that Eq. (4.12) holds for all values of η, $0 \le \eta \le \eta^+$ and hence in particular at $\eta = \eta_0$. From (4.11), we obtain

$$P_{11}\eta_0^2 = P_{13} + (P_{18} - P_{16}\eta_0^2)\cos(\eta_0\tau_2) + P_{17}\eta_0\sin(\eta_0\tau_2) + P_{15}\cos(\eta_0\tau_1) + P_{14}\eta_0\sin(\eta_0\tau_1). \tag{4.13}$$

Maximize $P_{13} + (P_{18} - P_{16}\eta_0^2)\cos(\eta_0\tau_2) + P_{17}\eta_0\sin(\eta_0\tau_2) + P_{15}\cos(\eta_0\tau_1) + P_{14}\eta_0\sin(\eta_0\tau_1)$ subject to $|\sin(\eta_0\tau_1)| \le 1, |\sin(\eta_0\tau_2)| \le 1, |\cos(\eta_0\tau_1)| \le 1, |\cos(\eta_0\tau_2)| \le 1$, we obtain

$$P_{11}\eta_0^2 \le |P_{13}| + |(P_{18} - P_{16}\eta_0^2)| + |P_{17}|\eta_0 + |P_{15}| + |P_{14}|\eta_0. \tag{4.14}$$

Assume that Eq. (4.14) has a positive root such η^+, then obviously from inequality (4.14), we have $\eta_0 \le \eta^+$.

Now, rearranging the inequality (4.12), using Eq. (4.11), and assuming $|\sin(\eta_0\tau_2)| \leq 1, |\cos(\eta_0\tau_2)| \leq 1$, we obtain

$$\begin{aligned}(P_{14} - \frac{P_{15}}{P_{11}})\eta_0[\cos(\eta_0\tau_1) - 1] - (P_{15} + \frac{P_{14}}{P_{11}})\eta_0^2 \sin(\eta_0\tau_1) <& |\frac{P_{13}}{P_{11}} - P_{12}|\eta_0 + | - P_{17} \\ &+ \frac{P_{18} - P_{16}\eta_0^2}{P_{11}}|\eta_0 \\ &+ |P_{18} - (\frac{P_{17}}{P_{11}} - P_{16})\eta_0^2| \\ &- (P_{14} - \frac{P_{15}}{P_{11}}).\end{aligned} \tag{4.15}$$

Using the bounds, we obtain

$$(P_{14} - \frac{P_{15}}{P_{11}})\eta_0[1 - \cos(\eta_0\tau_1)] = (P_{14} - \frac{P_{15}}{P_{11}})\eta_0 2\sin^2\left(\frac{\eta_0\tau_1}{2}\right) \leq \frac{1}{2}|(P_{14} - \frac{P_{15}}{P_{11}})\eta^+|\eta^{+2}\tau_1^2,$$

and

$$-(P_{15} + \frac{P_{14}}{P_{11}})\eta_0^2 \sin(\eta_0\tau_1) \leq |(P_{15} + \frac{P_{14}}{P_{11}})|\eta^{+3}\tau_1.$$

Hence, from inequality (4.15), we obtain

$$L_{11}\tau_1^2 + L_{12}\tau_1 < L_{13}, \tag{4.16}$$

where

$$\begin{aligned}L_{11} =& \frac{1}{2}|(P_{14} - \frac{P_{15}}{P_{11}})\eta^+|\eta^{+2}, \quad L_{12} = |(P_{15} + \frac{P_{14}}{P_{11}})|\eta^{+3}, \\ L_{13} =& |\frac{P_{13}}{P_{11}} - P_{12}|\eta_0 + | - P_{17} + \frac{P_{18} - P_{16}\eta_0^2}{P_{11}}|\eta_0 + |P_{18} - (\frac{P_{17}}{P_{11}} - P_{16})\eta_0^2| - (P_{14} - \frac{P_{15}}{P_{11}}).\end{aligned}$$

Hence, if

$$\tau_1^+ = \frac{1}{2L_{11}}\left(-L_{12} + \sqrt{L_{12}^2 + 4L_{11}L_{13}}\right) \tag{4.17}$$

then the stability is preserved for $0 \leq \tau_1 < \tau_1^+$.

Similarly, one can follow the above calculation to determine the length of delay τ_2 where the stability is preserved, taking τ_1 in its stable interval.

4.7. Stability switching curves and crossing directions

To study stability switching, we need to seek purely imaginary characteristic roots. For this, we assume $\lambda = i\omega(\omega > 0)$ and substituting this in Eq. (4.3), we obtain

$$m_1(i\omega) + m_2(i\omega)e^{-i\omega\tau_1} + m_3(i\omega)e^{-i\omega\tau_2}, \tag{4.18}$$

with

$$m_1(i\omega) = (i\omega)^3 + P_{11}(i\omega)^2 + P_{12}(i\omega) + P_{13}, \quad m_2(i\omega) = P_{14}(i\omega) + P_{15},$$

$$m_3(i\omega) = P_{16}(i\omega)^2 + P_{17}(i\omega) + P_{18}.$$

Since $|e^{-i\omega\tau_2}| = 1$, we have

$$|m_1 + m_2 e^{-i\omega\tau_1}| = |m_3|, \tag{4.19}$$

which is equivalent to

$$(m_1 + m_2 e^{-i\omega\tau_1})(\bar{m}_1 + \bar{m}_2 e^{i\omega\tau_1}) = m_3\bar{m}_3.$$

After simplification, we obtain

$$|m_1|^2 + |m_2|^2 + 2\mathrm{Re}(m_1\bar{m}_2)\cos(\omega\tau_1) - 2\mathrm{Im}(m_1\bar{m}_2)\sin(\omega\tau_1) = |m_3|^2.$$

Thus,

$$|m_3|^2 - |m_1|^2 - |m_2|^2 = 2K_1(\omega)\cos(\omega\tau_1) - 2K_2(\omega)\sin(\omega\tau_1), \tag{4.20}$$

where $K_1(\omega) = \mathrm{Re}(m_1\bar{m}_2)$ and $K_2(\omega) = \mathrm{Im}(m_1\bar{m}_2)$.

If there is some ω such that $K_1(\omega)^2 + K_2(\omega)^2 = 0$, then

$$K_1(\omega) = K_2(\omega) = 0 \Leftrightarrow m_1\bar{m}_2 = 0. \tag{4.21}$$

The right hand side of Eq. (4.20) is zero with any τ_1, and

$$|m_3|^2 = |m_1|^2 + |m_2|^2. \tag{4.22}$$

Therefore, if there is an ω such that both (4.21) and (4.22) are satisfied, then all $\tau_1 \in \mathbb{R}_+$ are solution of (4.19).

If $K_1(\omega)^2 + K_2(\omega)^2 > 0$, then there exists some continuous function $\chi_1(\omega)$ such that

$$\begin{aligned} K_1(\omega) &= \sqrt{K_1(\omega)^2 + K_2(\omega)^2}\cos(\chi(\omega)), \\ K_2(\omega) &= \sqrt{K_1(\omega)^2 + K_2(\omega)^2}\sin(\chi(\omega)). \end{aligned}$$

Indeed,

$$\chi_1(\omega) = \arg(m_1\bar{m}_2).$$

Therefore, Eq. (4.20) becomes

$$|m_3|^2 - |m_1|^2 - |m_2|^2 = 2\sqrt{K_1(\omega)^2 + K_2(\omega)^2}\cos(\chi_1(\omega) + \omega\tau_1). \tag{4.23}$$

Obviously, a sufficient and necessary condition for the existence of $\tau_1 \in \mathbb{R}_+$ satisfying the above equation is

$$||m_3|^2 - |m_1|^2 - |m_2|^2| \le 2\sqrt{K_1^2 + K_2^2}. \tag{4.24}$$

Denote Ω^1 to be $\omega \in \mathbb{R}_+$ satisfying (4.24). We note that (4.24) includes the case $K_1^2 + K_2^2 = 0$ which leads to (4.21) and (4.22).

Let

$$\cos(\Theta_1(\omega)) = \frac{|m_3|^2 - |m_1|^2 - |m_2|^2}{2\sqrt{K_1^2 + K_2^2}}, \quad \Theta_1 \in [0, \pi].$$

We have

$$\tau^{\pm}_{1,k_1}(\omega) = \frac{\pm\Theta_1(\omega) - \chi_1(\omega) + 2k_1\pi}{\omega}, \quad k_1 \in \mathbb{Z}. \tag{4.25}$$

By substituting the value of $\tau_1(\omega)$ given by (4.25), into (4.18) and we obtain an explicit formula for $\tau_2(\omega)$ unconditionally with each $\omega \in \Omega^1$, i.e.,

$$\tau^{\pm}_{2,k_2}(\omega) = \frac{1}{\omega}\arg\left\{\frac{-m_3}{m_1 + m_2 e^{-i\omega\tau_1^{\pm}}}\right\} + 2k_2\pi, \quad k_2 \in \mathbb{Z}. \tag{4.26}$$

Hence, the stability crossing curves are

$$\Gamma = \left\{(\tau^{\pm}_{1,k_1}(\omega), \tau^{\pm}_{2,k_2}(\omega)) \in \mathbb{R}^2_+ : \omega \in \Omega^1, k_1, k_2 \in \mathbb{Z}\right\}. \tag{4.27}$$

Another way to find τ_2 is similarly to the analysis of τ_1, which gives

$$\tau^{\pm}_{2,k_2}(\omega) = \frac{\pm\Theta_2(\omega) - \chi_2(\omega) + 2k_2\pi}{\omega}, \quad k_2 \in \mathbb{Z}, \tag{4.28}$$

where

$$\begin{aligned}
\cos(\Theta_2(\omega)) &= \frac{|m_2|^2 - |m_1|^2 - |m_3|^2}{2\sqrt{K_3^2 + K_4^2}}, \quad \Theta_2 \in [0, \pi],\\
K_3(\omega) &= \sqrt{K_3(\omega)^2 + K_4(\omega)^2}\cos(\chi_2(\omega)),\\
K_4(\omega) &= \sqrt{K_3(\omega)^2 + K_4(\omega)^2}\sin(\chi_2(\omega)),\\
K_3(\omega) &= \mathrm{Re}(m_1\bar{m}_3),\\
K_4(\omega) &= \mathrm{Im}(m_1\bar{m}_3),
\end{aligned}$$

with the condition on ω:

$$||m_2|^2 - |m_1|^2 - |m_3|^2| \le 2\sqrt{K_3^2 + K_4^2}, \tag{4.29}$$

which defines a region Ω^2.

By squaring both sides of the conditions (4.24) and (4.29), one can observe that (4.24) and (4.29) are equivalent. Hence

$$\Omega = \Omega^1 = \Omega^2,$$

and Ω is called the crossing set.

Lemma 4.16. *Ω consists of a finite number of intervals of finite length.*

Proof. The theoretical proof of this lemma can easily be established similarly as Lemma 3.2 of [64]. Numerically, we show that $F(\omega) = (|m_3|^2 - |m_1|^2 - |m_2|^2)^2 - 4(K_1^2 + K_2^2)$ has finite number of roots on $\mathbb{R}_+$ in Figure 21. □

If $F(0) > 0$, then $F(\omega)$ has roots $0 < a_1 < b_1 < a_2 < b_2 < ... < a_N < b_N < +\infty$ and

$$\Omega = \bigcup_{n=1}^{N} \Omega_n, \quad \Omega_n = [a_n, b_n].$$

If $F(0) < 0$, then $F(\omega)$ has roots $0 < b_1 < a_2 < b_2 < ... < a_N < b_N < +\infty$ and

$$\Omega = \bigcup_{n=1}^{N} \Omega_n, \quad \Omega_1 = (0, b_1], \ \Omega_n = [a_n, b_n] \ (n \geq 2).$$

For any Ω_n, we have a restriction on the range of $\chi_i(\omega), i = 1, 2$. We require $\chi_i(\omega)$ to be the smallest continuous branch with the property that there exists an $\omega_i \in \Omega_n$, such that

$$\chi_i(\omega_i) > 0.$$

Therefore, k_i has a lower bound, denoted by $M_{i,n}$.

By (4.26), one can obtain either τ^+_{2,k_2} or τ^-_{2,k_2} (but not both) for a given τ^+_{1,k_1}, and similarly for τ^-_{1,k_1}. By knotty computation, one can verify that when $\tau_1 = \tau^+_{1,k_1}(\omega)$, we have $\tau_2 = \tau^-_{2,k_2}(\omega)$, and when $\tau_1 = \tau^-_{1,k_1}(\omega)$, we have $\tau_2 = \tau^+_{2,k_2}(\omega)$. Therefore

$$\Gamma = \bigcup_{\substack{n=1,2,...N \\ k_1 \geq M_{1,n}, M_{1,n+1}, ... \\ k_2 \geq M_{2,n}, M_{2,n+1}, ...}} \Gamma^{\pm n}_{k_1,k_2} \bigcap \mathbb{R}^2_+, \tag{4.30}$$

$$\Gamma^{\pm n}_{k_1,k_2} = \left\{ \left(\frac{\pm\Theta_1(\omega) - \chi_1(\omega) + 2k_1\pi}{\omega}, \frac{\mp\Theta_2(\omega) - \chi_2(\omega) + 2k_2\pi}{\omega} \right) : \omega \in \Omega_n \right\}. \tag{4.31}$$

Γ defined in (4.30) is the set of all stability switching curves on the (τ_1, τ_2)-plane and $\Gamma^{\pm n}_{k_1,k_2}$ is continuous in $\mathbb{R}^2$.

For the crossing directions, we directly use Theorem 4.1 of [64] which is shown in Figure 22.

5. Persistence

In this section, we prove the persistence result for both systems (2.2) and (2.3). Biologically, persistence means the survival of all populations in the future time. Mathematically, persistence means positive solutions do not have omega limit points on the boundary of the non-negative set. A population $x(t)$ is called uniformly persistent if there is an $\delta > 0$, free of $x(0) > 0$ such that $\lim_{t\to\infty} x(t) > \delta$. A system is called uniformly persistent if each component persists uniformly.

Theorem 5.1. *Both systems* (2.2) *and* (2.3) *are uniformly persistent in the interior of* $\mho$ *whenever* $R_0 > 1$.

Proof. Refer the Appendix C. □

6. Numerical simulations

In this section, we present some numerical evaluations to verify our theoretical results and to exhibit different dynamics of systems (2.2) and (2.3).

6.1. Model system (2.2)

First, we numerically validate the theoretical results obtained for non-delayed system (2.2). We consider $f(I) = 1 + \alpha_1 I^2$ and $g(I) = 1 + \alpha_2 I^2$ and set the following parameter values (there may exist another set of parameter values):

$$A = 5, \mu = 0.5, \beta = 0.2, \delta = 0.05, q = 0.2, \gamma = 0.2, \alpha_1 = 0.02, \alpha_2 = 0.02. \tag{6.1}$$

In this way, the system (2.2) can be rewritten as

$$\begin{aligned} \frac{dS}{dt} &= 5 - 0.5S - \frac{0.2I}{1 + 0.02I^2}S, \\ \frac{dE}{dt} &= \frac{0.2I}{1 + 0.02I^2}S - (0.5 + 0.2)E, \\ \frac{dI}{dt} &= 0.2E - (0.5 + 0.05)I - \frac{0.2I}{1 + 0.02I^2}, \\ \frac{dR}{dt} &= \frac{0.2I}{1 + 0.02I^2} - 0.5R. \end{aligned} \tag{6.2}$$

In this case, $R_0 = 0.7619 < 1$ and the system (6.2) has a disease-free equilibrium $D_0(10.00, 0, 0, 0)$, which is globally asymptotically stable as shown in Figure 5(a). We observe that curve S starts up very quickly, attains its maximum value and stabilize. The curves E, I, R go down to zero.

Further, we increase the incidence rate as $\beta = 0.5$. By simple calculation, we obtain $R_0 = 1.9048 > 1$ and endemic equilibrium $D^*(5.313, 3.348, 0.896, 0.353)$, which is globally asymptotically stable as shown in Figure 5(b). We observe that curve S starts up very quickly, attains its maximum value and then goes down and stabilize at a certain value. The curves E, I, R go up to a certain value and stabilize. We plot a transcritical bifurcation diagram in Figure 6.

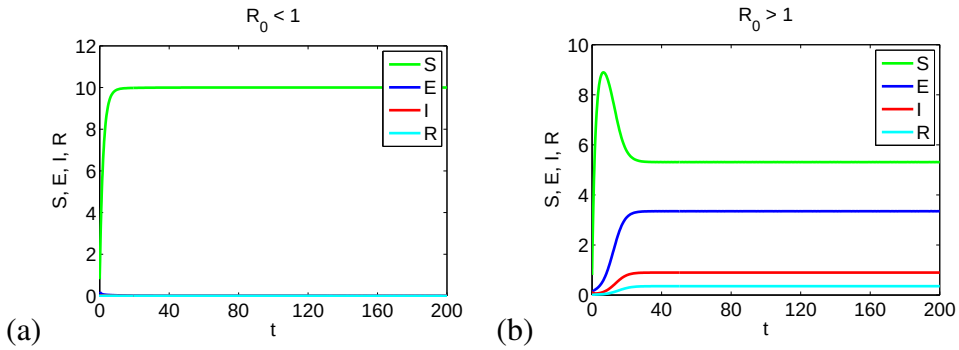

Figure 5. The graphs show the stability behavior of disease free equilibrium (D_0) and endemic equilibrium (D^*) of system (2.2). Panel (a) shows that D_0 is stable when $R_0 < 1$ and Panel (b) shows that D^* is stable when $R_0 > 1$.

In Figure 7, we show that by increasing the value of recovery rate (γ), the level of infected population decreases and by increasing the value of contact rate (β), the level of infected population increases. From this observation, it could also be concluded that if we increase the recovery rate (by increasing the availability of resources for treatment), the level of infected population could be reduced. Similarly, if we decrease the contact rate (by increasing the intervention strategies), the level

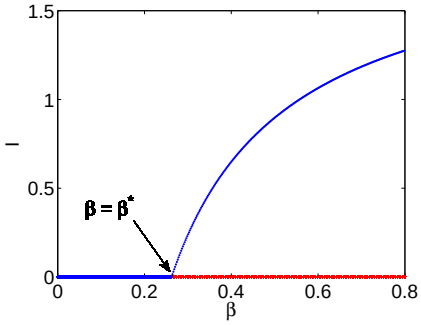

Figure 6. The graph demonstrates the transcritical bifurcation with respect to β. The blue line depicts the stable equilibrium points and red line depicts the unstable equilibrium. Before a critical value of $\beta = \beta^*$, D_0 is locally asymptotically stable and after a critical value of $\beta = \beta^*$, D_0 is unstable and D^* exists and locally asymptotically stable.

of infected population could be reduced. In Figure 8, we plot the infected population with respect to time for different values of α_1 and α_2. We observe that for greater values of α_1, the trajectory of the infected population settles down at a lower level, which means by imposing more intervention, the infection level can be reduced. For higher values of α_2, the infected population settles down at a high level, which means the level of infection increases with the limitation of treatment. In Figure 9, we show that the value of R_0 with respect to β and γ. Here we observe that β increases the value of R_0 and γ decreases the value of R_0, which means the disease can be extinct by reducing the value of β (by reducing contact between susceptible and infected individuals) and by increasing the value of γ (by increasing the treatment). From Figure 9, it can also be observed that β has more influence than γ on R_0.

In Figure 10(a)(b), 11(a)(b) and 12(a)(b), we show the combined effect of various parameters on endemic level. Figure 10(a) represents the variation of endemic level with respect to two parameters β and γ. We observe that by decreasing the value of contact rate β and by increasing the value of recovery rate (γ), endemic level could be reduced. Figure 10(b) represents the variation of endemic level with respect to two parameters β and α_1. We observe that the parameters β and α_1 have equal impact on endemic level. From this observation, it can be concluded that by increasing the interventions and reducing the contact rate between susceptible and infected individuals, endemic level can be reduced. Figure 11(a) shows that by increasing the value of recovery rate γ and increasing the strength of interventions (α_1), number of infected individuals could be reduced. Figure 11(b) demonstrates that by decreasing the value of contact rate β and reducing the limitation on resources availability (α_2), number of infected individuals could be reduced. Figure 12(a) depicts the variation of endemic level with respect to two parameters γ and α_2. We note that by increasing the recovery rate (γ) and by reducing the limitation on resources availability (α_2), endemic level can be reduced. Figure 12(b) declares that number of infected individuals could be reduced by increasing the value of α_1 (by increasing the strength of interventions) and decreasing the value of α_2 (by decreasing the limitation on resources availability). These results are suitable in real life when the disease spread fast and the infection level is high, for example, COVID-19, H1N1 influenza, SARS. Our study suggests that treatment resources should be available with intervention strategies.

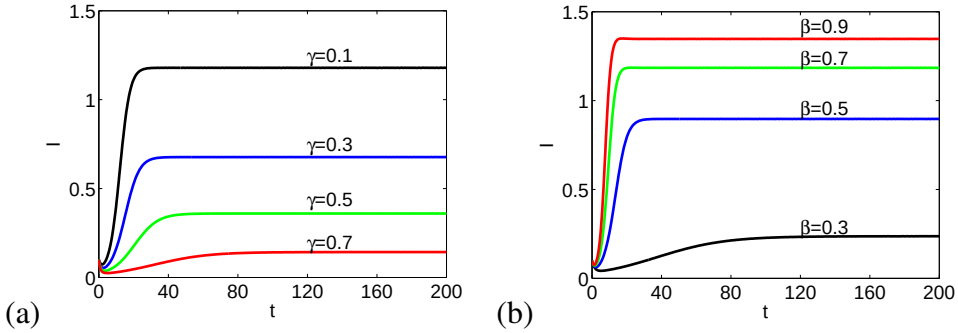

Figure 7. The graphs show the variation of infected population with respect to recovery rate (γ) and contact rate (β). Panel (a) shows that the level of infected population decreases as γ increases. Panel (b) shows that the level of infected population increases as β increases.

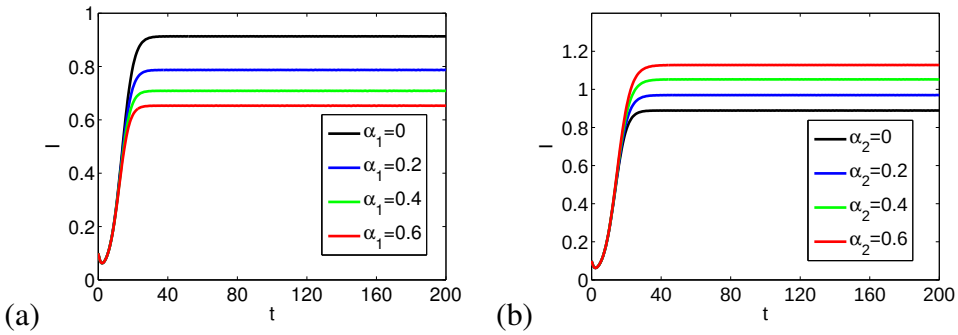

Figure 8. The graphs depict the variation of infected population with respect to measure of interventions (α_1) and limitation of resources for treatment (α_2). Panel (a) shows that the level of infected population decreases as α_1 increases. Panel (b) shows that the level of infected population increases as α_2 increases.

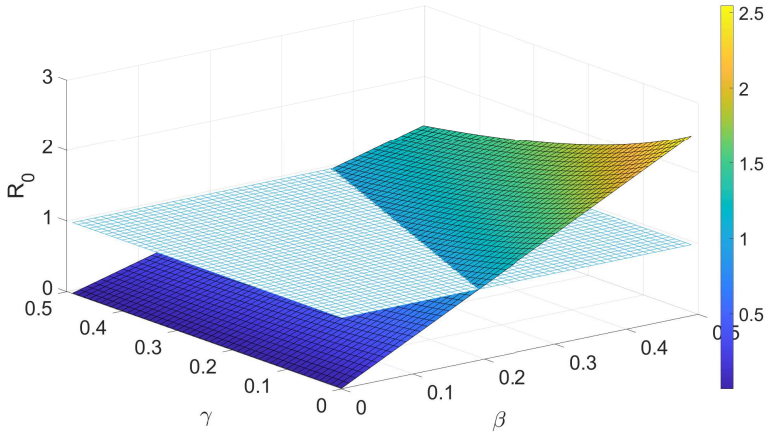

Figure 9. Surface plot shows the impact of β and γ on R_0.

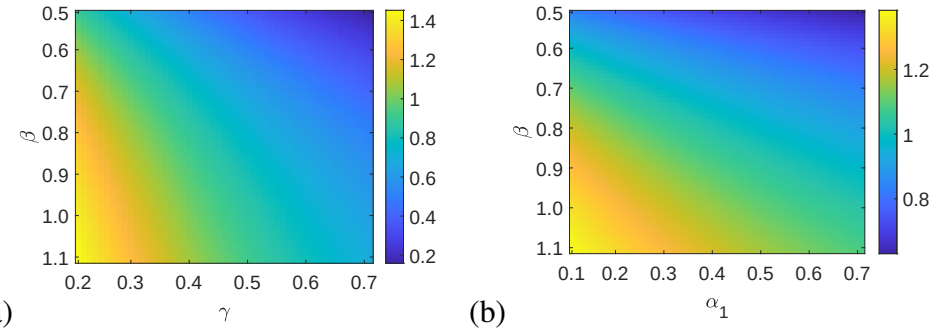

(a) (b)

Figure 10. The graphs show the impact of different parameters on prevalence. Panel (a) shows the variation of infected individuals with respect to β and γ. Panel (b) shows the variation of infected individuals with respect to β and α_1.

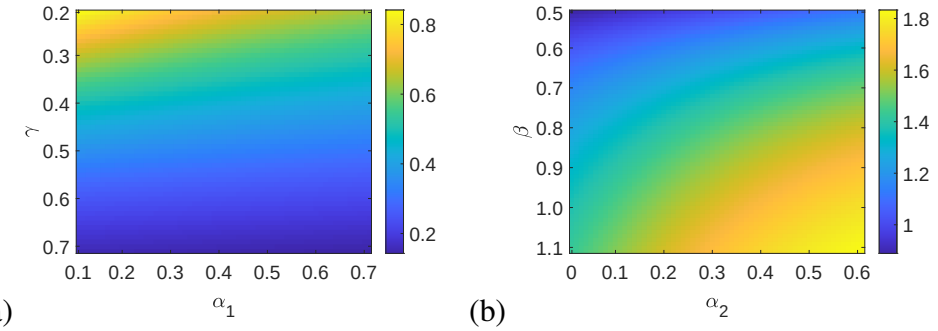

(a) (b)

Figure 11. The graphs show the impact of different parameters on prevalence. Panel (a) shows the variation of infected individuals with respect to γ and α_1. Panel (b) shows the variation of infected individuals with respect to β and α_2.

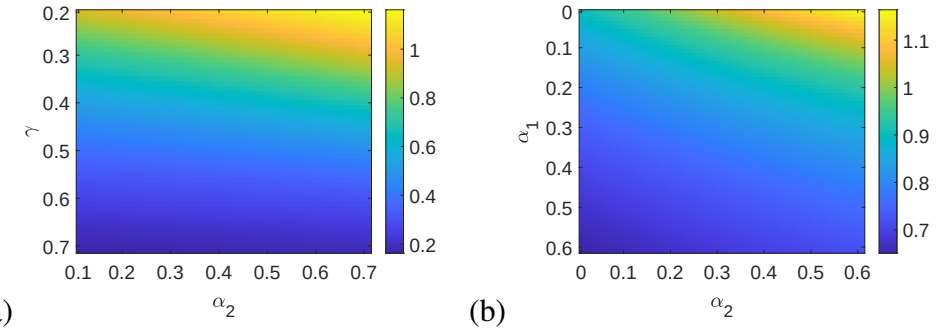

(a) (b)

Figure 12. The graphs show the impact of different parameters on prevalence. Panel (a) shows the variation of infected individuals with respect to γ and α_2. Panel (b) shows the variation of infected individuals with respect to α_1 and α_2.

6.2. *Model system* (2.3)

In this section, we perform some numerical simulations to verify our theoretical results of system (2.3) in Section 3. We set the parameter values as

$$A = 500, \mu = 0.7, \beta = 0.9, \delta = 0.05, q = 0.2, \gamma = 1.45, \alpha_1 = 0.02, \alpha_2 = 2 \times 10^{-12}, \tag{6.3}$$

and then the system (2.3) can be rewritten as

$$\begin{aligned}
\frac{dS}{dt} &= 500 - 0.7S - \frac{0.9I}{1 + 0.02I(t-\tau_1)^2}S,\\
\frac{dE}{dt} &= \frac{0.9I}{1 + 0.02I(t-\tau_1)^2}S - (0.7 + 0.2)E,\\
\frac{dI}{dt} &= 0.2E - (0.7 + 0.05)I - \frac{1.45I(t-\tau_2)}{1 + 2\times 10^{-12}I(t-\tau_2)^2},\\
\frac{dR}{dt} &= \frac{1.45I(t-\tau_2)}{1 + 2\times 10^{-12}I(t-\tau_2)^2} - 0.7R.
\end{aligned} \tag{6.4}$$

By simple calculation, we obtain that $R_0 = 64.9351$ and the endemic equilibrium $D^*(248, 362, 32.93, 68.12)$.

For $\tau_2 = 0, \tau_1 > 0$, by simple calculations, we obtain the critical value of $\tau_1 = 3.2$. By Theorem 4.4, we can deduce that D^* is locally asymptotically stable when $\tau_1 = [0, 3.2)$ and a supercritical Hopf bifurcation occur at the critical value $\tau_1 = 3.2$. Figure 13 also depicts that D^* is locally asymptotically stable for $\tau_1 = 2 < \tau_1^* = 3.2$ and bifurcated periodic solutions feasible for $\tau_1 = 10 > \tau_1^* = 3.2$.

For $\tau_1 = 0, \tau_2 > 0$, we obtain the critical value of $\tau_2 = 3.74$. By Theorem 4.6, we can deduce that D^* is locally asymptotically stable when $\tau_2 = [0, 3.74)$ and a supercritical Hopf bifurcation occur at the critical value $\tau_2 = 3.74$. It has been presented in Figure 14 that D^* is locally asymptotically stable for $\tau_2 = 1 < \tau_2^* = 3.74$ and bifurcated periodic solutions feasible for $\tau_2 = 10 > \tau_1^* = 3.74$.

For $\tau_1 = \tau_2 = \tau > 0$, we obtain the critical value of $\tau = 0.63$. By Theorem 4.8, we can deduce that D^* is locally asymptotically stable when $\tau = [0, 0.63)$ and a supercritical Hopf bifurcation occur at the critical value $\tau = 0.63$. It has been shown in Figure 15 that D^* is locally asymptotically stable for $\tau = 0.5 < \tau^* = 0.63$ and bifurcated periodic solutions feasible for $\tau = 0.65 > \tau^* = 0.63$.

For $\tau_1 > 0, \tau_2 \in (0, 3.74]$, by simple calculations we obtain the critical value of $\tau_1 = 0.05$. By Theorem 4.10, we can deduce that D^* is locally asymptotically stable when $\tau_1 = [0, 0.05)$ and a supercritical Hopf bifurcation occur at the critical value $\tau_1 = 0.05$. Figure 16 illustrates that D^* is locally asymptotically stable for $\tau_1 = 0.04 < \tau_1^* = 0.05$ and bifurcated periodic solutions feasible for $\tau_1 = 0.16 > \tau_1^* = 0.05$.

Furthermore, we plot bifurcation diagrams using the time delays as bifurcation parameters for different cases in Figure 17 and obtain that D^* is locally asymptotically stable before the critical values of delays and bifurcated periodic solutions occur after the critical values of delays. We also plot global branches of Hopf bifurcation in Figure 18 and obtain the global existence of periodic solutions.

Figure 19 represents the changes in critical value of τ_1 with respect to β and α_1. The critical value of τ_1 decreases with an increase in β while increases with an increase in α_1. Figure 20 represents the changes in critical value of τ_2 with respect to γ and α_2. The critical value of τ_2 increases with an increase in γ while decreases with an increase in α_2. At the same time, we give the variation values of τ_1 and τ_2 with respect to parameters β, α_1, γ and α_2 in Table 1 and 2. These results indicate that these parameters also significantly influence the dynamics of the system with time delays such as critical value of bifurcation parameters.

For stability switching curves, we obtain that $F(0) = -158.96 < 0$ and $F(\omega)$ has three roots $b_1 =$

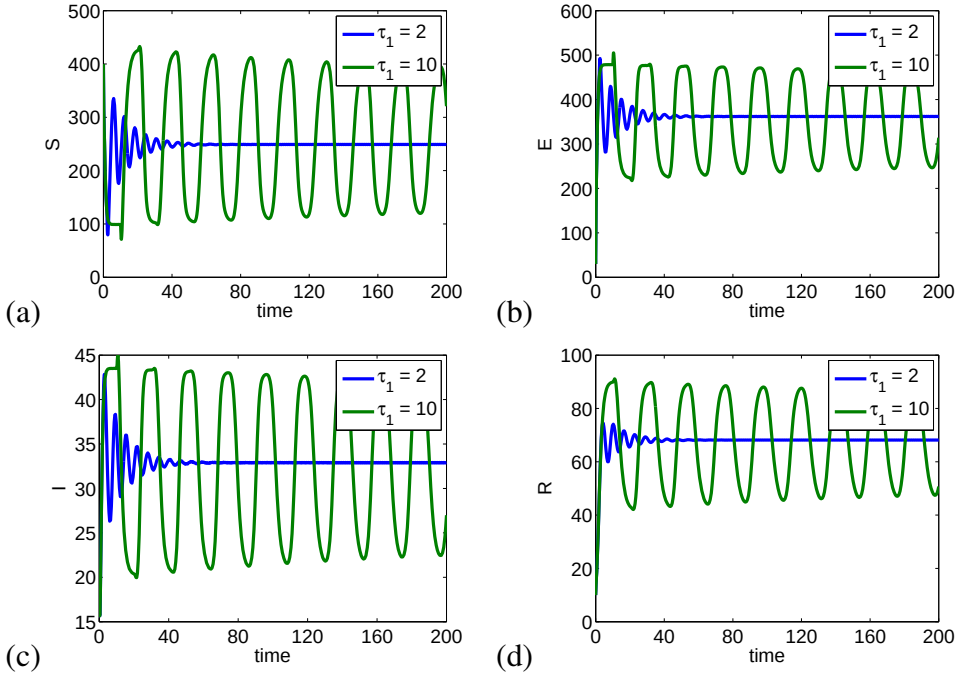

Figure 13. The graphs show the stability behavior of system (2.3) for $\tau_1 = 2 < \tau_1^* = 3.2$ and oscillatory behavior for $\tau_1 = 10 > \tau_1^* = 3.2$ when $\tau_2 = 0$.

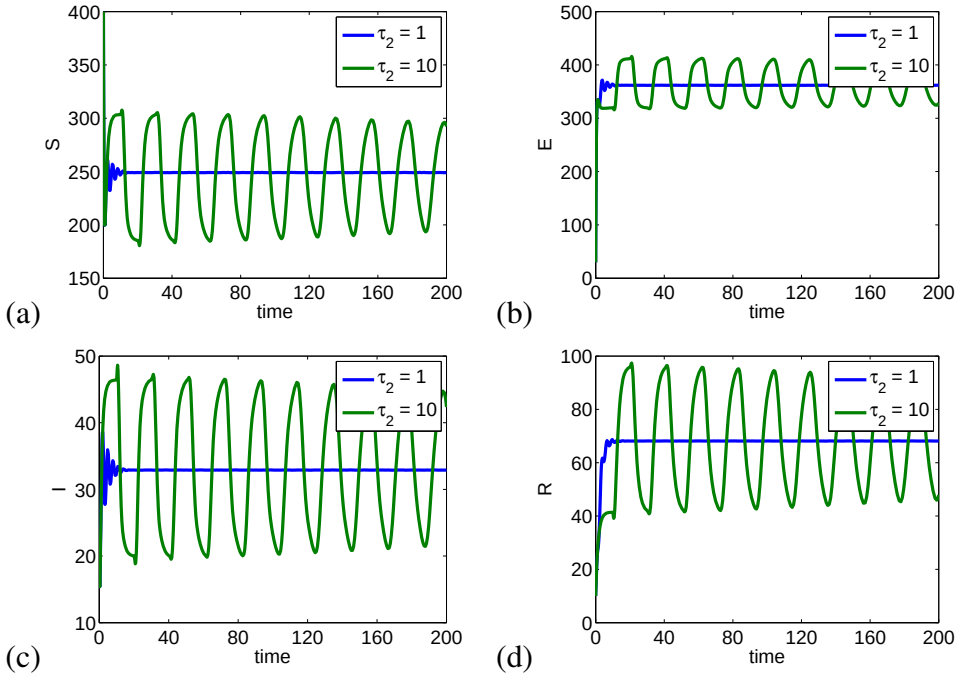

Figure 14. The graphs show the stability behavior of system (2.3) for $\tau_2 = 1 < \tau_2^* = 3.74$ and oscillatory behavior for $\tau_2 = 10 > \tau_2^* = 3.74$ when $\tau_1 = 0$.

$0.01575, a_2 = 0.02216$, and $b_2 = 0.0667$ (see Figure 21). Thus

$$\Omega = \bigcup_{n=1}^{2} \Omega_n, \quad \Omega_1 = (0, b_1], \ \Omega_2 = [a_2, b_2].$$

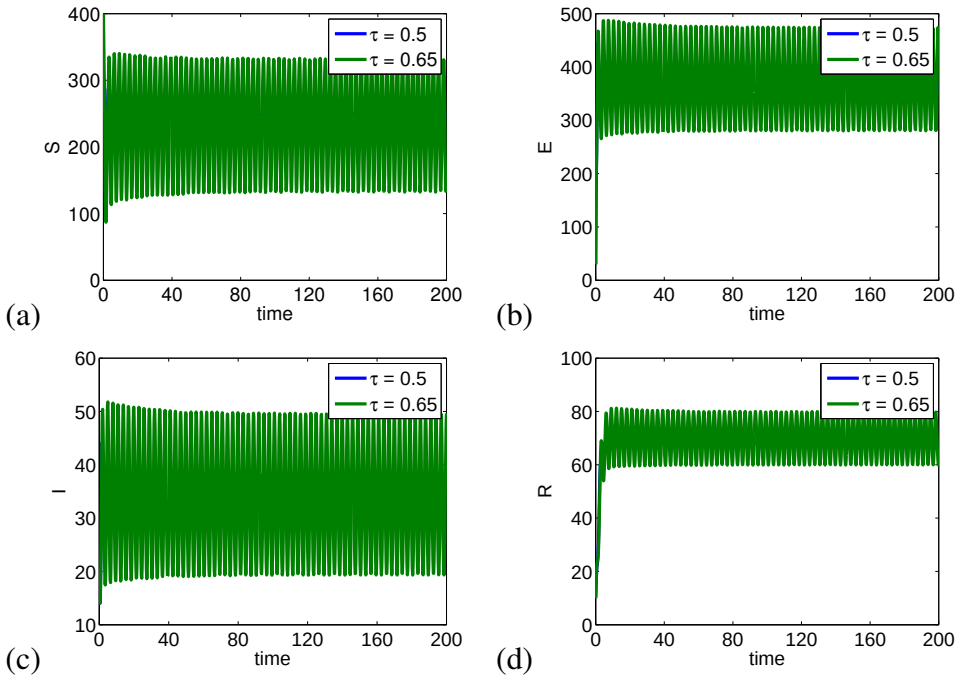

Figure 15. The graphs show the stability behavior of system (2.3) for $\tau = 0.5 < \tau^* = 0.63$ and oscillatory behavior for $\tau = 0.65 > \tau^* = 0.63$ when $\tau_1 = \tau_2 = \tau$.

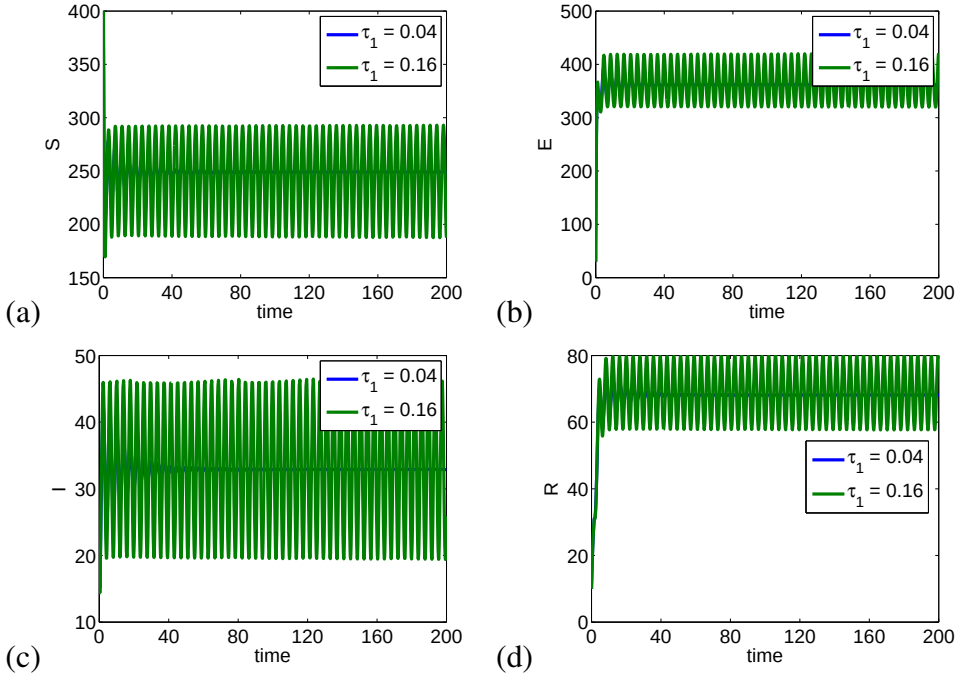

Figure 16. The graphs show the stability behavior of system (2.3) for $\tau_1 = 0.04 < \tau_1^* = 0.05$ and oscillatory behavior for $\tau_1 = 0.16 > \tau_1^* = 0.05$ when $\tau_2 = 1.5 < \tau_2^*$.

We have

$$\delta_1^a = 0, \quad \delta_2^a = 1, \quad \delta_1^b = 1, \quad \delta_2^b = 1.$$

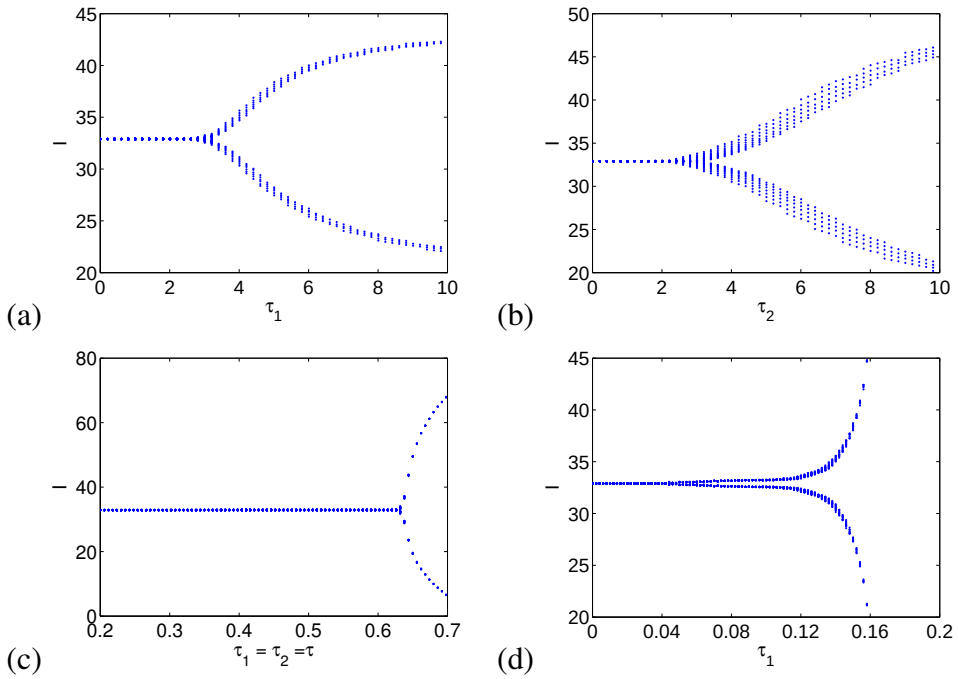

Figure 17. The graphs demonstrate the bifurcation diagrams of system (2.3) with respect to time delays. Panel (a) depicts the infected population with respect to τ_1 when $\tau_2 = 0$. Panel (b) depicts the infected population with respect to τ_2 when $\tau_1 = 0$. Panel (c) depicts the infected population with respect to τ when $\tau_2 = \tau_1 = \tau$. Panel (d) depicts the infected population with respect to τ_1 when $\tau_2 = 1.5 < \tau_2^*$.

Table 1. The changes in critical value of τ_1 with respect to β and α_1.

β	Critical value of τ_1	α_1	Critical value of τ_1
0.3	3.32	0.1	3.76
0.5	3.25	0.2	3.86
0.7	3.22	0.3	4.28
0.9	3.20	0.4	4.50

Table 2. The changes in critical value of τ_2 with respect to γ and α_2.

γ	Critical value of τ_2	α_2	Critical value of τ_2
1.4	0.474	3×10^{-7}	0.5426
1.5	0.601	5.3×10^{-6}	0.5093
1.6	0.676	1.13×10^{-5}	0.4625
1.7	0.720	1.74×10^{-5}	0.4057

Since $(\delta_1^a, \delta_2^a) \neq (\delta_1^b, \delta_2^b)$, therefore by Theorem 3.1 of [64], Γ is a set of continuous curves with their two end points on the axises (class II) (see Figure 22).

We know that for system (2.3), the interior equilibrium is stable when $\tau_1 = \tau_2 = 0$, i.e., no characteristic roots have positive real parts. Hence from Figure 22, the interior equilibrium is stable if and only if (τ_1, τ_2) is on the small bottom-left region of the (τ_1, τ_2)-plane. As τ_1 and τ_2 increase, there

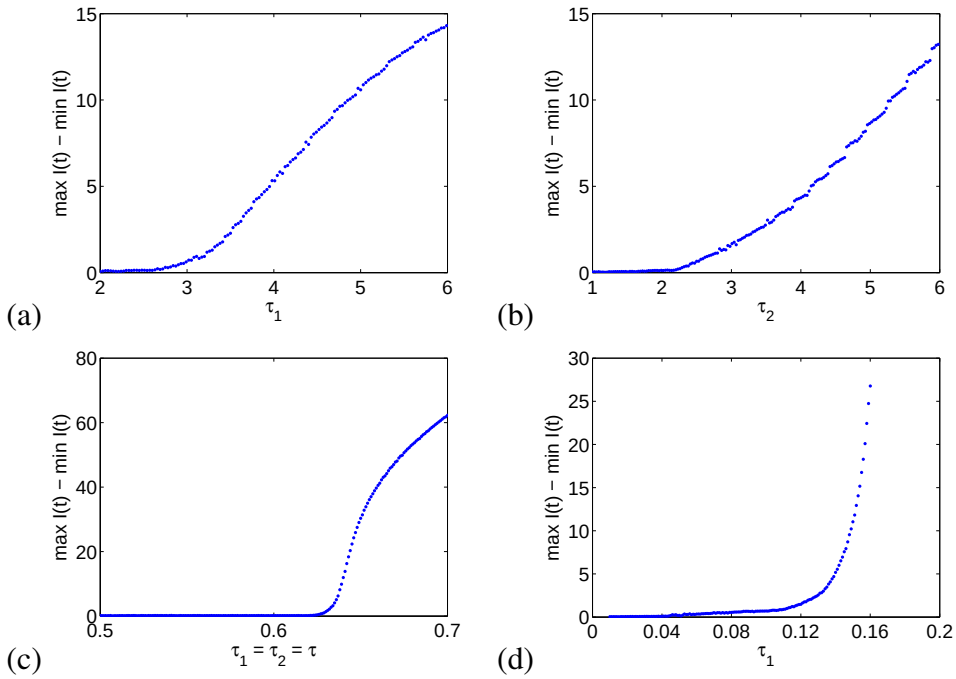

Figure 18. The graphs demonstrate the global Hopf branches of system (2.3) with respect to time delays. Panel (a) shows the global Hopf branches when $\tau_1 = \tau_1^* = 3.2$ and $\tau_2 = 0$. Panel (b) shows the global Hopf branches when $\tau_2 = \tau_2^* = 3.74$ and $\tau_2 = 0$. Panel (c) shows the global Hopf branches when $\tau = \tau^* = 0.63$ and $\tau_2 = \tau_1 = \tau$. Panel (d) shows the global Hopf branches when $\tau_1 = \tau_1^* = 0.05$ and $\tau_2 = 1.5 < \tau_2^*$.

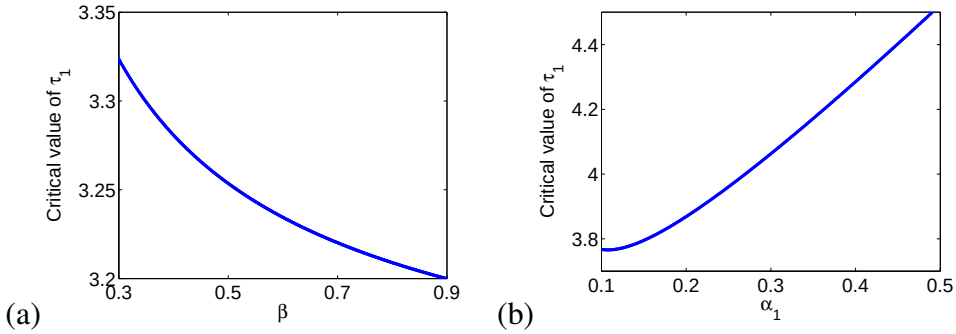

Figure 19. The graphs depict the relation of critical value of delay τ_1 with β and α_1. Other parameter values remain same as (6.3). Panel (a) depicts the changes in critical value of τ_1 with respect to β. Panel (b) depicts the changes in critical value of τ_1 with respect to α_1.

is a trend that there are more and more characteristic roots with positive real parts.

7. Application of the study to COVID-19 in Spain and Italy

Recently, a novel coronavirus (namely COVID-19) spread worldwide. Several countries are in the list of top countries, including the USA, India, Brazil, Russia [61]. But early on the disaster, Spain and Italy emerged as a major global coronavirus hotspot. Both countries have implemented strict

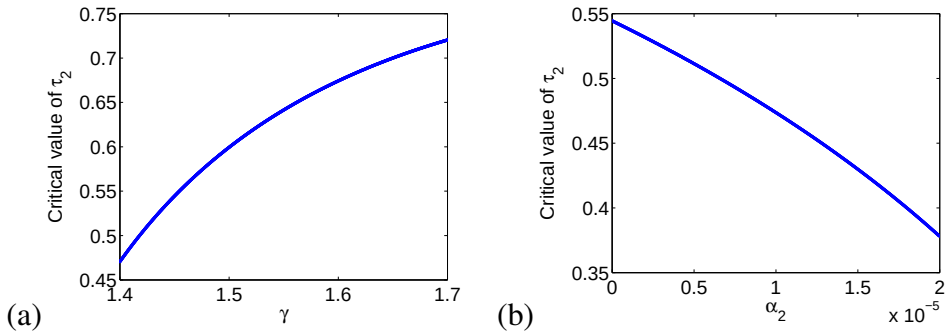

(a) (b)

Figure 20. The graphs depict the relation of critical value of delay τ_2 with γ and α_2. Other parameter values remain same as (6.3). Panel (a) depicts the changes in critical value of τ_2 with respect to γ. Panel (b) depicts the changes in critical value of τ_2 with respect to α_2.

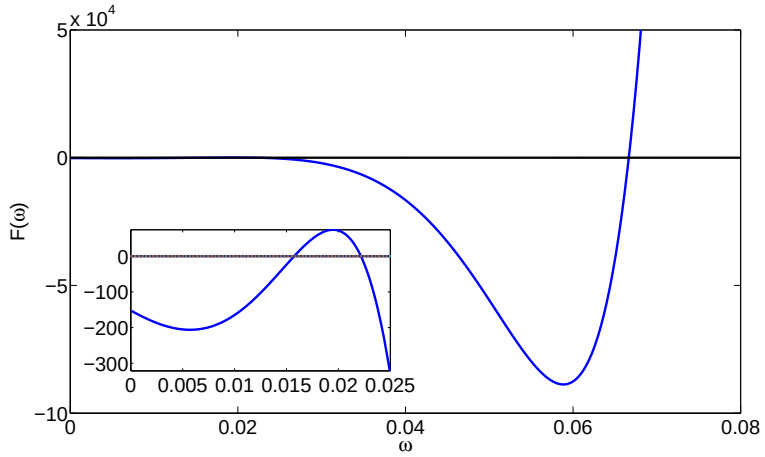

Figure 21. Graph of $F(\omega)$. Other parameter values remain same as (6.3).

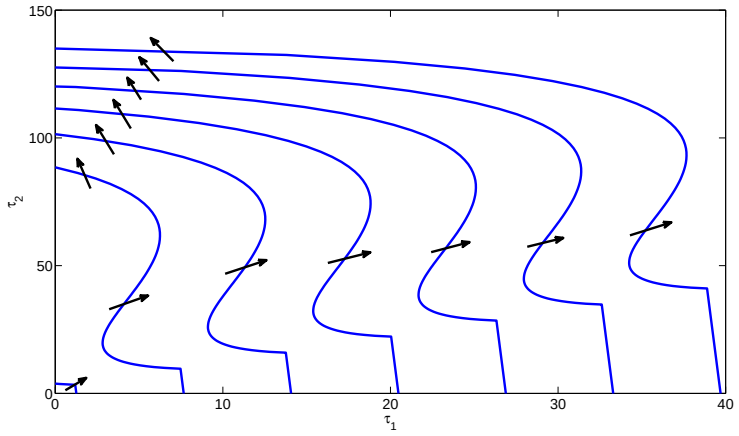

Figure 22. Plot of stability switching curves. Arrows are used to depict the crossing directions, i.e., the region on the end of an arrow has two more characteristic roots with positive real parts. Other parameter values remain same as (6.3).

lockdown from March 2020. Restrictions started in Spain on March 14 and in Italy on March 9 [62]. Following this, the daily new cases are decreased in Spain and Italy after March 2020 [61,63]. In Spain, the maximum number of reported cases was observed on April 2, 2020, which implies the number of infections was on an upward trend till April 2, 2020. After that day, the number of daily cases was observed to decrease asymptotically after imposing interventions, which is the most significant interpretation of the mathematical model. A similar case can be seen in Italy, the maximum number of reported cases was observed on March 21, 2020, after which the number of daily cases was observed to decrease asymptotically. Without loss of generality, we have chosen the data of Spain and Italy during March 1, 2020 to May 31, 2020. We have plotted the bar graph of new daily cases in Spain and Italy from March 1, 2020 to May 31, 2020, i.e., the real cases for 92 days in Figure 23. We calibrate the system (2.3) to fit the new daily cases and cumulative cases of COVID-19 in Spain and Italy and estimate some parameters of the system (2.3) by the least square method using real data of Spain and Italy from March 1, 2020 to May 31, 2020, which is shown in Figure 25. The cumulative number of cases is represented by $C(t)$, which is given as

$$\frac{dC}{dt} = qE, \tag{7.1}$$

and the daily new cases are given by $C_d(t)$, where

$$C_d(t) = C(t) - C(t-1). \tag{7.2}$$

The demographic effects are not considered in this discussion because of the short epidemic time scale in comparison to demographic time scale, i.e., we take $A = 0, \mu = 0$ here. Other estimated parameters and initial conditions for system (2.3) are given in Table 3 and Table 4, respectively.

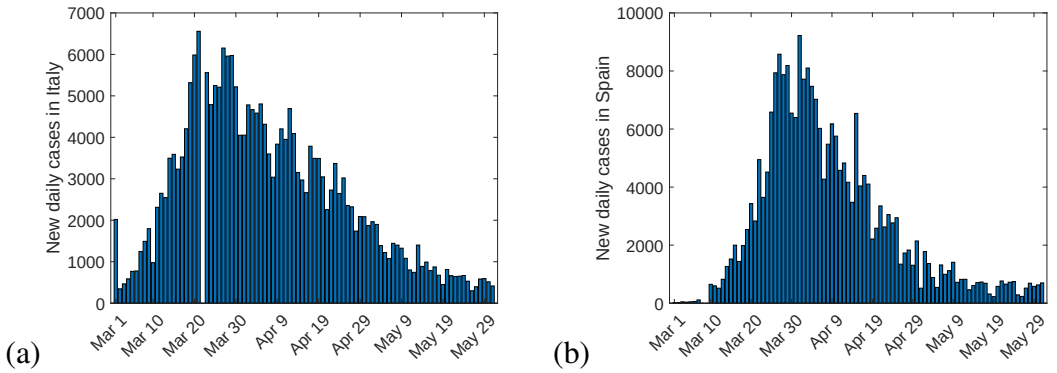

Figure 23. New daily cases of COVID-19 in Italy and Spain from from March 1, 2020 to May 31, 2020. Panel (a) shows the bar plot of data of COVID-19 in Italy. Panel (b) shows the bar plot of data of COVID-19 in Spain.

The basic reproduction number R_0 can be explicitly calculated as $R_0 = \frac{\beta N}{\gamma+\delta}$. Based on the parameter values in Table 3, we calculated the value of R_0 for both countries Spain and Italy are 5.3391 and 9.7921, respectively.

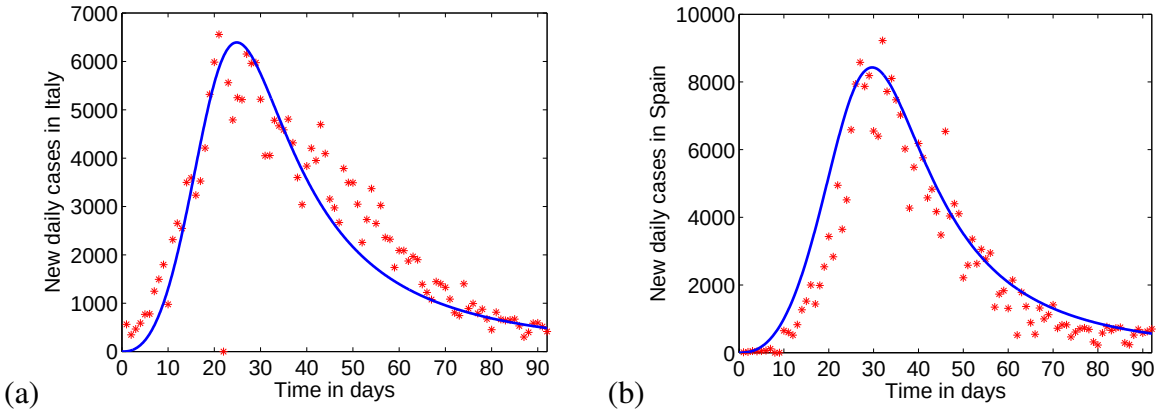

(a) (b)

Figure 24. Outputs of the system (2.3) and new daily cases in Italy and Spain. Red stars represent the data points and blue line represents the output of the system (2.3). Panel (a) shows the fitting of system (2.3) with respect to new daily cases in Italy. Panel (b) shows the fitting of system (2.3) with respect to new daily cases in Spain.

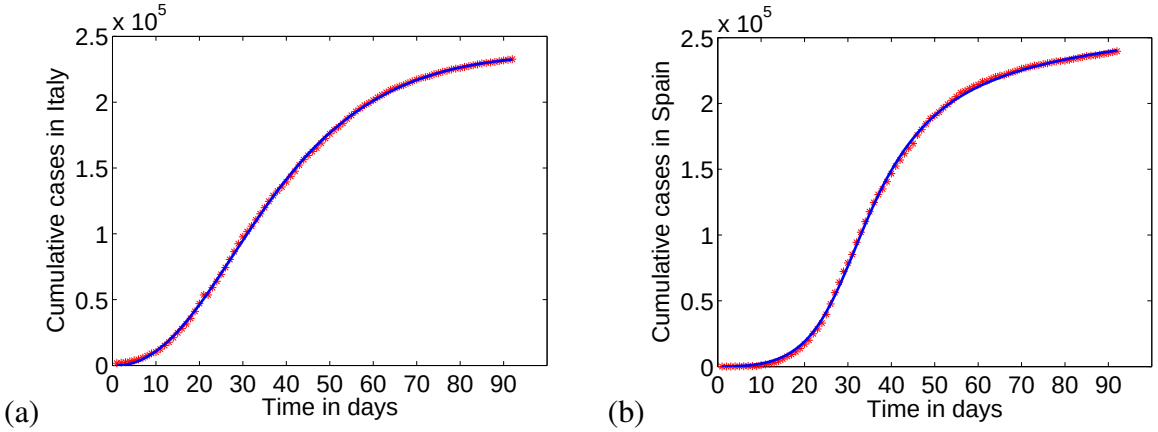

(a) (b)

Figure 25. Outputs of the system (2.3) and cumulative cases in Italy and Spain. Red stars represent the data points and blue line represents the output of the system (2.3). Panel (a) shows the fitting of system (2.3) with respect to cumulative cases in Italy. Panel (b) shows the fitting of system (2.3) with respect to cumulative cases in Spain.

7.1. Impact of intervention strength and time delays on the early phase of COVID-19 in Spain and Italy

This section aims to compare the outcomes of cumulative cases over time in Spain and Italy for different values of different parameters. Here, using the parameter values given in Table 3 as the baseline values, we have shown that how a model could be used to observe the effect of changing strength of interventions and time delays on epidemic dynamics. In particular, we illustrate the impact of the strength of interventions (α_1), time delay in intervention (τ_1), and time delay in recovery (τ_2) on the early phase of pandemic COVID-19. In mathematical terms, we explore how our model dynamics depends on the parameters α_1, τ_1, and τ_2. We compare the total cases generated by the model for different values of strength of interventions (α_1) and time delays τ_1, and τ_2. We observe that if the strength of interventions and time delays in the model alter, total cases generated via models are

Table 3. Estimated values of parameters of system (2.3) with respect to COVID-19 in Spain and Italy.

Parameters	Estimated values in Spain	Estimated values in Italy	Reference
A	0	0	-
μ	0	0	-
q	0.07112	0.0665	Estimated
β	3.1114×10^{-8}	4.9092×10^{-8}	Estimated
γ	0.273	0.3026	Estimated
δ	3.2720×10^{-4}	2.0102×10^{-4}	Estimated
α_1	1×10^{-8}	2×10^{-8}	Assumed
α_2	2×10^{-8}	4×10^{-9}	Assumed
τ_1	3.5	1	Estimated
τ_2	2	3	Estimated

Table 4. Initial population for system (2.3) with respect to COVID-19 in Spain and Italy.

Initial population	$S(0)$	$E(0)$	$I(0)$	$R(0)$
Spain	4.69×10^7	2.18×10^3	13	10
Italy	6.04×10^7	3.10×10^2	561	33

different.

From Figure 26(a), we observe that the strength of intervention (α_1) could have reduced the total number of cases at the early stage of epidemic in Italy. We note that Italy had recorded 2.32×10^5 total number of cases by May 31, 2020. We analyze that if the strength of interventions (α_1) had increased, the total cases of COVID-19 would have decreased than that the actual cases. Figure 26(a) shows that if the strength of interventions had increased by 50%($\alpha_1 = 3 \times 10^{-8}$) from its baseline value ($\alpha_1 = 2 \times 10^{-8}$), then the cumulative cases would have decreased by 12%(2.04×10^5) and if the strength of interventions had increased by 100%($\alpha_1 = 4 \times 10^{-8}$) from its baseline value, then the cumulative cases would have decreased by 18%(1.89×10^5). If the strength of interventions had decreased by 50%($\alpha_1 = 1 \times 10^{-8}$) from its baseline value, then the cumulative cases would have increased by 34%(3.12×10^5). We observe that the strength of interventions would have been beneficial in the early phase of COVID-19 (measured in terms of total confirmed cases of COVID-19).

We also illustrate that how time delays in intervention and recovery influence the outcomes of early cumulative cases in Italy. The results in Figure 26(b) show that the sooner the interventions are imposed, the greater reduction in the cumulative number of cases. We analyzed that if time delay τ_1 increased by 2 times ($\tau_1 = 2$) by its baseline value ($\tau_1 = 1$), then cumulative number of cases would have been increased by 8%(2.52×10^5) and if τ_1 increased by 3 times ($\tau_1 = 3$) by its baseline value, then cumulative number of cases would have been increased by 25%(2.91×10^5). Thus the timing of implementing the interventions is crucial and analyzing the impact of time delay in the system is significant. Imposing the interventions sufficiently early, may have the potential to reduce the total number of infected cases. Figure 27 shows that if the time delay (τ_2) had increased by 3/2 times ($\tau_2 = 3$) by its baseline value ($\tau_2 = 2$) then number of cumulative cases would have been increased by 4% and if the time delay (τ_2) had decreased by 2 times ($\tau_2 = 4$) by its baseline value ($\tau_2 = 2$) then

number of cumulative cases would have been decreased by 2%.

We find the same qualitative result (Figures 28 and 29) when we parameterize the model using the data of COVID-19 in Spain. These results also demonstrate that model system can produce observed disease dynamics, but total cases are different when strength of interventions and time delays are altered. From Figure 28(a), we observe that the strength of intervention (α_1) would have reduced the total number of cases at the early stage of epidemic in Spain. We note that Spain had recorded 2.39×10^5 total number of cases by May 31, 2020. We analyze that if the strength of interventions (α_1) had increased, the total cases of COVID-19 would have decreased. Figure 28(a) shows that if the strength of interventions had increased by 100%($\alpha_1 = 2\times10^{-8}$) from its baseline value ($\alpha_1 = 1\times10^{-8}$), then the cumulative cases would have decreased by 25%(1.796×10^5) and if the strength of interventions had increased by 200%($\alpha_1 = 3 \times 10^{-8}$) from its baseline value, then the cumulative cases would have decreased by 38%(1.48×10^5). If the strength of interventions had increased by 300%($\alpha_1 = 4 \times 10^{-8}$) from its baseline value, then the cumulative cases would have decreased by 45%(1.30×10^5). Figure 28(b) illustrates that how time delay in intervention affects the outcomes of early cumulative cases in Spain. We analyzed that if time delay τ_1 increased by 1.28 times ($\tau_1 = 4.5$) by its baseline value ($\tau_1 = 3.5$), then cumulative number of cases would have been increased by 21%(2.91×10^5) and if τ_1 decreased by 1.4 times ($\tau_1 = 2.5$) by its baseline value, then cumulative number of cases would have been decreased by 7%(2.22×10^5). Figure 29 shows that if the time delay (τ_2) had increased by 3/2 times ($\tau_2 = 3$) by its baseline value ($\tau_2 = 2$) then number of cumulative cases would have been increased by 5% and if the time delay (τ_2) had decreased by 2 times ($\tau_2 = 1$) by its baseline value ($\tau_2 = 2$) then number of cumulative cases would have been decreased by 2%.

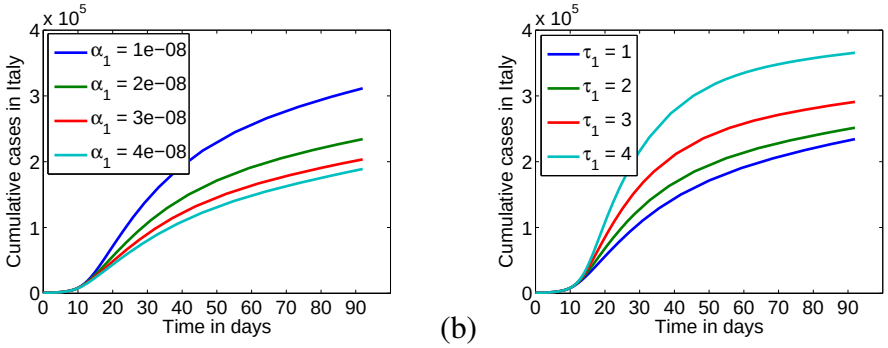

Figure 26. The plots show the dynamics of cumulative cases over time in Italy for different values of α_1 and τ_1. (a) Illustration of what would have happened if time delay τ_1 had changed. (b) Illustration of what would have happened if the strength of intervention α_1 had changed.

8. Discussion

In the case of many infectious diseases, either we are unable to perform sufficient experiments, or a deeper understanding of disease dynamics is essentially required. Therefore, modeling of epidemics (mathematical and computational methods) is one of the important tools to understand the disease dynamics. Mathematical modeling along with precise computations gives new insights about different important issues of disease dynamics and their prevention, e.g., effects of different important

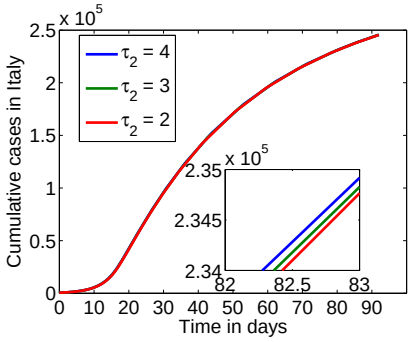

(a)

Figure 27. The plot shows the dynamics of cumulative cases over time in Italy for different values of τ_2.

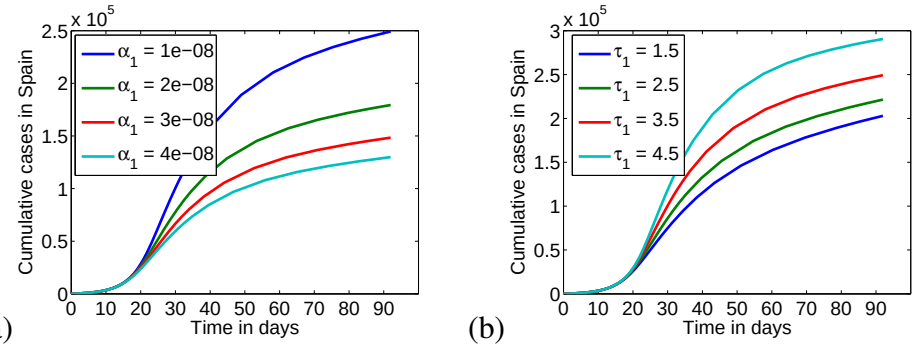

(a) (b)

Figure 28. The plots show the dynamics of cumulative cases over time in Spain for different values of α_1 and τ_1.

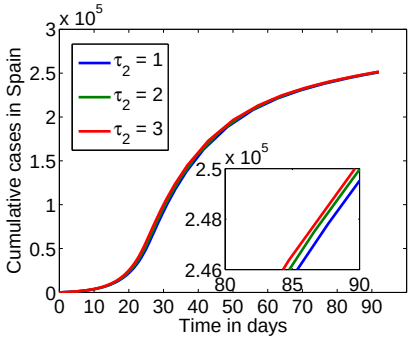

(a)

Figure 29. The plot shows the comparison of the effect of τ_2 on the cumulative cases over time in Spain.

parameters: delay, treatment, epidemic trends, intervention strategies, control, and spread of infections. Intervention strategies and treatment have great impression to control different contagious diseases. In the last few years, models accompanying the impact of intervention strategies on the spread of infectious diseases showed impressive popularity. But these models overlooked the impact of the availability of treatment resources on the dynamics of infectious disease. These models also do not involve different time delays, such as time delay in interventions and cure rate. However, in many biological systems, time delays are inevitably present, and several epidemic model systems have been explored incorporating the delays [35, 46, 47, 49]. Here we put our efforts to understand the impact of

intervention strategies and available resources for the treatment/control of infectious diseases, with special emphasis on the current pandemic COVID-19.

In this work, we have studied an SEIR model system (2.2) with infection force under intervention strategies and recovery rate under the low availability of resources for treatment. Furthermore, we included the two time delays in system (2.2), first-time delay τ_1 represents the latent period of the intervention strategies, and second-time delay τ_2 is due to the period that is used to cure the infected individuals. For systems (2.2) and (2.3), we obtained the various theoretical and epidemiological findings.

(i) We investigated that the system (2.2) has two equilibria, namely, disease-free equilibrium (D_0) and endemic equilibrium (D^*). The existence of equilibria depends on the basic reproduction number (R_0). For the non-delayed model, stability analysis for both disease-free and endemic equilibriums are performed. In particular, it has been shown that for disease spread, the basic reproduction number (R_0) acts as a threshold value. When $R_0 < 1$, only disease-free equilibrium (D_0) exists and locally asymptotically stable. When $R_0 > 1$, there exists two equilibria, disease-free equilibrium (D_0) and endemic equilibrium (D^*).

(ii) System (2.2) undergoes a transcritical bifurcation at $R_0 = 1$, which means disease die out whenever $R_0 < 1$ and disease persists whenever $R_0 > 1$. We have obtained that D_0 is globally stable in its feasible region $R_0 < 1$ and D^* is globally stable if $R_0 > 1$. In numerical analysis, by choosing a particular combination of $f(I)$ and $g(I)$, we have performed the impact of various parameters in the disease dynamics (Figure 7, 8). We have shown the relation of the different parameters with R_0 (Figure 9). We have also illustrated the combined effect of various parameters on the endemic level (Figure 10, 11, 12). Our observations revealed that increasing the interventions, disease level settle down at low level, but limitation on treatment sets the infected population at higher level. We additionally observed that R_0 can be reduced by increasing interventions and decreasing the limitation on resources availability.

(iii) For delayed system (2.3), we have obtained that when $R_0 < 1$, D_0 is locally asymptotically stable with certain conditions (Theorem 4.1) when $\tau_1 > 0$ and $\tau_2 > 0$. Further, when $R_0 > 1$, D_0 remain unstable when $\tau_1 > 0$ and $\tau_2 > 0$. The system (2.3) seems sensitive to delay lengths. It is observed by both theoretical results and numerical simulations. When $R_0 > 1$, the effect of two-time delay has been investigated by taking different cases and the threshold values of both the delays have been obtained in section 4.3. Analytically and numerically, we have shown that system (2.3) is stable when delay parameters are less than their threshold values (Figure 13, 14, 15, 16), which means the disease could be controlled easily. Whenever these parameters cross these threshold values, periodic solutions will occur through Hopf bifurcation. It can also be understood by the bifurcation diagram (Figure 17). In additional, the direction and stability of Hopf bifurcation are studied by normal form theory and center manifold theorem. We have also studied the global continuation of local Hopf bifurcation via both analytically and numerically (section 4.5 and Figure 18). We concluded that the time delays in the system (2.3) affect the structure of the solutions substantially. The time delays play the roles to destabilize the system. Indeed, it is evidenced by our theoretical results. The length of delay to preserve stability has also been estimated by employing the Nyquist criterion. More importantly, the stability crossing curves along with crossing directions [47, 48, 64] have been discussed in two-delay parameter space (refer to the stability switching curve plots in Figure 22). Our system (2.3) demonstrates

rich dynamics, such as Hopf bifurcation, and is suitable for large population densities.

(iv) The dynamics of system (2.3) is also affected by the parameters $\beta, \alpha_1, \gamma, \alpha_2$. Numerical simulations indicate that the critical value of τ_1 decreases with an increase in β (cf. Figure 19 and Table 1). Therefore, we conclude that the impact of an increase in transmission rate is to early the occurrence of Hopf bifurcation. Similarly, the critical value of τ_1 increases with an increase in α_1, which means the impact of increasing the value of the parameter α_1 (imposing more interventions) is to postpone the occurrence of Hopf bifurcation. It can also be concluded that the epidemic cycle is more difficult to occur as the intervention strategies increases. On the other hand, the critical value of τ_2 increases with an increase in γ (cf. Figure 20 and Table 2). Thus, the impact of an increase in recovery rate is to postpone the occurrence of Hopf bifurcation while the impact of the increasing the value of the parameter α_2 (increasing limitations on treatment) is to early the occurrence of Hopf bifurcation because the critical value of τ_2 decreases with increasing α_2.

(v) Furthermore, we have applied our model to a case study based on the data of COVID-19 in Spain and Italy. We estimated the parameters of system (2.3) by using the least-square method. It has also been depicted that if we could be able to increase the strength of interventions sufficiently, total number of cases in Spain and Italy would have reduced in early phase of COVID-19 (refer to Subsection 7.1). In both countries (Spain and Italy), the similar effects could also be achieved by reducing time delays in intervention and recovery. Further, it is expected that the similar scenarios could also be observed in many other European countries such as UK, Germany, and France. As such, the outcomes related to different significant values may differ from actual ones. Here we should note that many attributes of the system also depend on the published/collected data. The data have been collected for a short time span and do not have any future predictions. The quantitative results have been illustrated for the early phase of the pandemic COVID-19 in only two countries, Spain and Italy. Our model could also be applicable for other countries and also for long time periods.

8.1. Epidemiological implications and future scope

Our proposed model systems generalize the study [10, 11] and become more realistic via investigation of recovery rate and delay parameters on the system dynamics. Treatment resources play a significant role in protecting the individuals against a particular disease and to control a contagious disease, for example, COVID-19. Thus, our results are the complement to the study by Zhou et al. [11]. The results found here could be favorable for measuring the effect of the intervention strategies and treatment in the control of infectious diseases. The existence of periodic solutions in epidemic models is significant and interesting both in mathematics and applications since it provides a satisfactory explanation for the breakout and recurrence of a disease, which may have profound implications for the prediction, prevention, and control of disease transmission. If the delay due to the latent period of the intervention strategies is large enough, it will lead to repetitive episodes of endemic and in this situation, the disease would be out of control. Our study suggests that imposing intervention strategies timely may be helpful in controlling the outbreak of disease. Further, our study also suggests that to control and predict the disease spread, we should trim the time delays. When the delay is not too large, ultimately, the epidemic disease will become endemic. Similarly, the time delay due to the period used to cure the infected individuals also leads to periodic solutions. Appropriately,

we should truncate the delays in the model as much as possible so that we could control and predict the disease spread. The outcomes of our results in Section 7 emphasized the importance of the intervention strategies and time delays for the case of COVID-19. Policy makers should take care of reducing the time delays in such biological processes. These policies can be used by policymakers and other professionals to make decisions on how certain interventions such as lockdown, quarantine, isolation, and social distancing can effectively be implemented.

By considering the incidence rate under intervention strategies and recovery rate under low resources availability treatment, the system (2.2) does not have complex dynamics. It will be intriguing to consider the incidence and recovery rate in which the infection and recovery function first increases and attain its maximum, and then eventually tends to a saturation level due to crowding effect and limitation of treatment, respectively. It will be insightful to compare the dynamics of these cases with our results as future work. In future studies, according to the actual situation of COVID-19 in Spain and Italy, the pre-stage exposed and post-stage exposed period [65] can be further considered in the model to analyze the impact of intervention and medical resources on COVID-19 prevention and control.

Acknowledgments

The research work of Sarita Bugalia is supported by the Council of Scientific & Industrial Research (CSIR), India [File No. 09/1131(0025)/2018-EMR-I]. The research work of Jai Prakash Tripathi is supported by Science and Engineering Research Board (SERB), India [File No. ECR/2017/002786] and UGC-BSR Research Start-Up-Grant, India [No. F.30-356/2017(BSR)]. The research work of Hao Wang is partially supported by The Natural Sciences and Engineering Research Council of Canada (NSERC) Individual Discovery Grant RGPIN-2020-03911 and Discovery Accelerator Supplement Award RGPAS-2020-00090. The authors are grateful to the handling editor and reviewers for their helpful comments and suggestions that have improved the quality of the manuscript.

Conflict of interest

All authors declare no conflicts of interest in this paper.

References

1. F. Brauer, C. Castillo-Chavez, Mathematical models in population biology and epidemiology, New York: Springer, **2** (2012).
2. K. Dietz, J. A. Heesterbeek, Daniel Bernoulli's epidemiological model revisited, *Math. Biosci.*, **180** (2002), 1–21.
3. W. O. Kermack, A. G. McKendrick, A contribution to the mathematical theory of epidemics, *Proc. R. Soc. Lond. A Math. Phys. Sci.*, **115** (1927), 700–721.
4. H. W. Hethcote, The mathematics of infectious diseases, *SIAM Rev. Soc. Ind. Appl. Math.*, **42** (2000), 599–653.
5. R. M. Anderson, B. Anderson, R. M. May, Infectious diseases of humans: dynamics and control, Oxford University Press, 1992.

6. S. Ruan, W. Wang, Dynamical behavior of an epidemic model with a nonlinear incidence rate, *J. Differ. Equ.*, **188** (2003), 135–163.
7. J. P. Tripathi, S. Abbas, Global dynamics of autonomous and nonautonomous SI epidemic models with nonlinear incidence rate and feedback controls, *Nonlinear Dyn*, **86** (2016), 337–351.
8. L. J. Gross, Mathematical models in plant biology: An overview, *Applied Mathematical Ecology*, (1989), 385–407.
9. W. M. Liu, H. W. Hethcote, S. A. Levin, Dynamical behavior of epidemiological models with nonlinear incidence rates, *J. Math. Biol.*, **25** (1987), 359–380.
10. Y. Cai, Y. Kang, M. Banerjee, W. Wang, A stochastic SIRS epidemic model with infectious force under intervention strategies, *J. Differ. Equ.*, **259** (2015), 7463–7502.
11. M. Zhou, T. Zhang, Global Analysis of an SEIR Epidemic Model with Infectious Force under Intervention Strategies, *J. Appl. Math. Phys.*, **7** (2019), 1706.
12. J. Cui, Y. Sun, H. Zhu, The impact of media on the control of infectious diseases, *J. Dyn. Differ. Equ.*, **20** (2008), 31–53.
13. J.A. Cui, X. Tao, H. Zhu, An SIS infection model incorporating media coverage, *Rocky Mt. J. Math.*, (2008), 1323–1334.
14. D. Xiao, S. Ruan, Global analysis of an epidemic model with nonmonotone incidence rate, *Math. Biosci.*, **208** (2007), 419–429.
15. Y. Xiao, T. Zhao, S. Tang, Dynamics of an infectious diseases with media/psychology induced non-smooth incidence, *Math. Biosci. Eng.*, **10** (2013), 445.
16. S. Tang, Y. Xiao, L. Yuan, R. A. Cheke, J. Wu, Campus quarantine (Fengxiao) for curbing emergent infectious diseases: Lessons from mitigating A/H1N1 in Xi'an, China, *J. Theor. Biol.*, **295** (2012), 47–58.
17. Y. Xiao, S. Tang, J. Wu, Media impact switching surface during an infectious disease outbreak, *Sci. Rep.*, **5** (2015), 7838.
18. A. B. Gumel, S. Ruan, T. Day, J. Watmough, F. Brauer, P. Van den Driessche, et al., Modelling strategies for controlling SARS outbreaks, *Proc. R. Soc. Lond. B Biol. Sci.*, **271** (2004), 2223–2232.
19. J. Zhang, J. Lou, Z. Ma, J. Wu, A compartmental model for the analysis of SARS transmission patterns and outbreak control measures in China, *Appl. Math. Comput.*, **162** (2005), 909–924.
20. S. Bugalia, V. P. Bajiya, J. P. Tripathi, M. T. Li, G. Q. Sun, Mathematical modeling of COVID-19 transmission: The roles of intervention strategies and lockdown, *Math. Biosci. Eng.*, **17** (2020), 5961–5986.
21. V. P. Bajiya, S. Bugalia, J. P. Tripathi, Mathematical modeling of COVID-19: Impact of non-pharmaceutical interventions in India, *Chaos Interdiscipl. J. Nonlinear Sci.*, **30** (2020), 113143.
22. M. T. Li, G. Q. Sun, J. Zhang, Y. Zhao, X. Pei, L. Li, et al., Analysis of COVID-19 transmission in Shanxi Province with discrete time imported cases, *Math. Biosci. Eng.*, **17** (2020), 3710.
23. C. N. Ngonghala, E. Iboi, S. Eikenberry, M. Scotch, C. R. MacIntyre, M. H. Bonds, et al., Mathematical assessment of the impact of non-pharmaceutical interventions on curtailing the 2019 novel Coronavirus, *Math. Biosci.*, **325** (2020), 108364.
24. S. Batabyal, A. Batabyal, Mathematical computations on epidemiology: A case study of the novel coronavirus (SARS-CoV-2), *Theory Biosci.*, (2021), 1–16.

25. S. Batabyal, COVID-19: Perturbation dynamics resulting chaos to stable with seasonality transmission, *Chaos Solitons Fractals*, **145** (2021), 110772.
26. W. Wang, S. Ruan, Bifurcations in an epidemic model with constant removal rate of the infectives, *J. Math. Anal. Appl.*, **291** (2004), 775–793.
27. W. Wang, Epidemic models with nonlinear infection forces, *Math. Biosci. Eng.*, **3** (2006), 267.
28. C. Shan, H. Zhu, Bifurcations and complex dynamics of an SIR model with the impact of the number of hospital beds, *J. Differ. Equ.*, **257** (2014), 1662–1688.
29. G. H. Li, Y. X. Zhang, Dynamic behaviors of a modified SIR model in epidemic diseases using nonlinear incidence and recovery rates, *PLoS One*, **12** (2017), e0175789.
30. R. Mu, A. Wei, Y. Yang, Global dynamics and sliding motion in A (H7N9) epidemic models with limited resources and Filippov control, *J. Math. Anal. Appl.*, **477** (2019), 1296–1317.
31. H. Zhao, L. Wang, S. M. Oliva, H. Zhu, Modeling and Dynamics Analysis of Zika Transmission with Limited Medical Resources, *Bull. Math. Biol.*, **82** (2020), 1–50.
32. A. Sirijampa, S. Chinviriyasit, W. Chinviriyasit, Hopf bifurcation analysis of a delayed SEIR epidemic model with infectious force in latent and infected period, *Adv. Differ. Equ.*, **1** (2018), 348.
33. E. Beretta, D. Breda, An SEIR epidemic model with constant latency time and infectious period, *Math. Biosci. Eng.*, **8** (2011), 931.
34. Z. Zhang, S. Kundu, J. P. Tripathi, S. Bugalia, Stability and Hopf bifurcation analysis of an SVEIR epidemic model with vaccination and multiple time delays, *Chaos Solitons Fractals*, **131** (2020), 109483.
35. P. Song, Y. Xiao, Global hopf bifurcation of a delayed equation describing the lag effect of media impact on the spread of infectious disease, *J. Math. Biol.*, **76** (2018), 1249–1267.
36. A. K. Misra, A. Sharma, V. Singh, Effect of awareness programs in controlling the prevalence of an epidemic with time delay, *J. Biol. Sys.*, **19** (2011), 389–402.
37. F. Al Basir, S. Adhurya, M. Banerjee, E. Venturino, S. Ray, Modelling the Effect of Incubation and Latent Periods on the Dynamics of Vector-Borne Plant Viral Diseases, *Bull. Math. Biol.*, **82** (2020), 1–22.
38. S. Liao, W. Yang, Cholera model incorporating media coverage with multiple delays, *Math. Methods Appl. Sci.*, **42** (2019), 419–439.
39. K. A. Pawelek, S. Liu, F. Pahlevani, L. Rong, A model of HIV-1 infection with two time delays: mathematical analysis and comparison with patient data, *Math. Biosci.*, **235** (2012), 98–109.
40. D. Greenhalgh, S. Rana, S. Samanta, T. Sardar, S. Bhattacharya, J. Chattopadhyay, Awareness programs control infectious disease–multiple delay induced mathematical model, *Appl. Math. Comput.*, **251** (2015), 539–563.
41. H. Zhao, M. Zhao, Global Hopf bifurcation analysis of an susceptible-infective-removed epidemic model incorporating media coverage with time delay, *J. Biol. Dyn.*, **11** (2017), 8–24.
42. F. Al Basir, S. Ray, E. Venturino, Role of media coverage and delay in controlling infectious diseases: A mathematical model, *Appl. Math. Comput.*, **337** (2018), 372–385.
43. J. Liu, Bifurcation analysis for a delayed SEIR epidemic model with saturated incidence and saturated treatment function, *J. Biol. Dyn.*, **13** (2019), 461–480.

44. G. H. Li, Y. X. Zhang, Dynamic behaviors of a modified SIR model in epidemic diseases using nonlinear incidence and recovery rates, *PLoS One*, **12** (2017), e0175789.
45. D. P. Gao, N. J. Huang, S. M. Kang, C. Zhang, Global stability analysis of an SVEIR epidemic model with general incidence rate, *Bound. Value Probl.*, (2018), 42.
46. G. Huang, Y. Takeuchi, W. Ma, D. Wei, Global stability for delay SIR and SEIR epidemic models with nonlinear incidence rate, *Bull. Math. Biol.*, **72** (2010), 1192–1207.
47. E. Beretta, Y. Kuang, Geometric stability switch criteria in delay differential systems with delay dependent parameters, *SIAM J. Math. Anal.*, **33** (2002), 1144–1165.
48. Q. An, E. Beretta, Y. Kuang, C. Wang, H. Wang, Geometric stability switch criteria in delay differential equations with two delays and delay dependent parameters, *J. Differ. Equ.*, **266** (2019), 7073–7100.
49. Y. Kuang, editor, Delay differential equations: with applications in population dynamics, Academic Press, 1993.
50. X. Yang, Generalized form of Hurwitz-Routh criterion and Hopf bifurcation of higher order, *Appl. Math. Lett.*, **15** (2002), 615–621.
51. C. Castillo-Chavez, B. Song, Dynamical models of tuberculosis and their applications, *Math. Biosci. Eng.*, **1** (2004), 361.
52. C. Castillo-Chavez, Z. Feng, W. Huang, On the computation of R_0 and its role on global stability, *IMA Volumes in Mathematics and Its Applications*, **1** (2002), 229.
53. Y. Y. Min, Y. G. Liu, Barbalat lemma and its application in analysis of system stability, *Journal of Shandong University (engineering science)*, **37** (2007), 51–55.
54. S. Ruan, J. Wei, On the zeros of transcendental functions with applications to stability of delay differential equations with two delays, *Dynamics of Continuous Discrete and Impulsive Systems Series A*, **10** (2003), 863–874.
55. H. L. Freedman, V. S. Rao, The trade-off between mutual interference and time lags in predator-prey systems, *Bull. Math. Biol.*, **45** (1983), 991–1004.
56. L. H. Erbe, H. I. Freedman, V. S. Rao, Three-species food-chain models with mutual interference and time delays, *Math. Biosci.*, **80** (1986), 57–80.
57. B. D. Hassard, N. D. Kazarinoff, Y. H. Wan, Y. W. Wan, Theory and applications of Hopf bifurcation, CUP Archive, **41** (1981).
58. J. J. Benedetto, W. Czaja, Riesz Representation Theorem, In Integration and Modern Analysis, *Birkhäuser Boston*, (2009), 321–357.
59. J. Wu, Symmetric functional differential equations and neural networks with memory, *Trans. Am. Math. Soc.*, **350** (1998), 4799–4838.
60. H. I. Freedman, S. Ruan, M. Tang, Uniform persistence and flows near a closed positively invariant set, *J. Dyn. Differ. Equ.*, **6** (1994), 583–600.
61. Worldometer, coronavirus, available from: `https://www.worldometers.info/coronavirus/`.
62. The print news, available from: `https://theprint.in/world/this-is-how-france\-italy-and-spain-are-easing-their-lockdowns-one-step-at-a-time/413060/`.
63. World Health Organization, COVID-19. Available from: `https://covid19.who.int/`.

64. X. Lin, H. Wang, Stability analysis of delay differential equations with two discrete delays, *Canadian Appl. Math. Quart.*, **20** (2012), 519–533.

65. L. Wang, J. Wang, H. Zhao, Y. Shi, K. Wang, P. Wu, et al., Modelling and assessing the effects of medical resources on transmission of novel coronavirus (COVID-19) in Wuhan, China, *Math. Biosci. Eng.*, **17** (2020), 2936–2949.

Appendices

Appendix A

Proof of Theorem 3.1: From the first equation of system (2.2), we have

$$\frac{dS}{dt} \geq -\mu S - \frac{\gamma I}{f(I)} S,$$

and

$$S(t) \geq S(0) e^{-(\mu + \frac{\gamma I}{f(I)})}.$$

Hence, if $S(0) > 0$, then $S(t) > 0$. In the similar fashion, one can also check the positivity of $E(t), I(t)$, and $R(t)$.

Now, we shall prove the boundedness of all the solutions of system (2.2). For this, we define a function

$$N(t) = S(t) + E(t) + I(t) + R(t).$$

Taking the time derivative of $N(t)$ and using (2.2), we obtain

$$\begin{aligned} \frac{dN}{dt} =& A - \mu S - \mu E - \mu I - \delta I - \mu R, \\ \leq& A - \mu N, \end{aligned}$$

which implies

$$A - (\mu + \delta) N \leq \frac{dN}{dt} \leq A - \mu N,$$

and

$$\begin{aligned} \frac{A}{\mu + \delta} \leq \liminf_{t \to \infty} N(t) \leq \limsup_{t \to \infty} N(t) \leq \frac{A}{\mu}, \\ \frac{A}{\mu + \delta} \leq N(t) \leq \frac{A}{\mu}. \end{aligned}$$

This implies that all the solutions of system (2.2) are bounded. Thus we proved the Theorem 3.1.

Proof of Theorem 3.2: 1. The Jacobian matrix of right hand function in system (2.2) at D_0 is given by

$$J_{D_0} = \begin{bmatrix} -\mu & 0 & -\frac{\beta A}{\mu f(0)} & 0 \\ 0 & -(\mu + q) & \frac{\beta A}{\mu f(0)} & 0 \\ 0 & q & -(\mu + \delta + \frac{\gamma}{g(0)}) & 0 \\ 0 & 0 & \frac{\gamma}{g(0)} & -\mu \end{bmatrix},$$

which has two eigenvalues $-\mu, -\mu$ (which are negative) and the other eigenvalues are the eigenvalues of the following matrix

$$B = \begin{bmatrix} -(\mu+q) & \frac{\beta A}{\mu f(0)} \\ q & -(\mu+\delta+\frac{\gamma}{g(0)}) \end{bmatrix}.$$

The trace and determinant of matrix B are given by $\text{tr}(B) = -(\mu+\delta+\frac{\gamma}{g(0)}+\mu+q) < 0$ and $\det(B) = (\mu+\delta+\frac{\gamma}{g(0)})(\mu+q) - q\frac{\beta A}{\mu f(0)}$. We observe that $\det(B) > 0$ if $R_0 < 1$ and $\det(B) < 0$ if $R_0 > 1$. Therefore, by Routh-Hurwitz criterion [50], it can be concluded that D_0 is locally asymptotically stable when $R_0 < 1$ and unstable when $R_0 > 1$.

2. When $R_0 = 1$, i.e., $\beta = \beta^* = \frac{\mu f(0)(\mu+q)\left(\delta+\mu+\frac{\gamma}{g(0)}\right)}{Aq}$, then

$$J_{(D_0,\beta^*)} = \begin{bmatrix} -\mu & 0 & -\frac{(\mu+q)\left(\delta+\mu+\frac{\gamma}{g(0)}\right)}{q} & 0 \\ 0 & -(\mu+q) & \frac{(\mu+q)\left(\delta+\mu+\frac{\gamma}{g(0)}\right)}{q} & 0 \\ 0 & q & -(\mu+\delta+\frac{\gamma}{g(0)}) & 0 \\ 0 & 0 & \frac{\gamma}{g(0)} & -\mu \end{bmatrix}.$$

One can easily observe that $J_{(D_0,\beta^*)}$ has a simple zero eigenvalue and all other three eigenvalues are $-\mu, -\mu, -(2\mu+q+\delta+\frac{\gamma}{g(0)})$, which are negative. Computing the right eigenvector w and left eigenvector v of J_{D_0} with respect to zero eigenvalue, we have

$$\begin{aligned} w_1 =& -\frac{(\mu+q)(\gamma+g(0)(\delta+\mu))}{\gamma q}, w_2 = \frac{\mu(\gamma+g(0)(\delta+\mu))}{\gamma q}, w_3 = \frac{\mu g(0)}{\gamma}, w_4 = 1, \\ v_1 =& 0, v_2 = \frac{q}{q+\mu}, v_3 = 1, v_4 = 0. \end{aligned}$$

Now from Theorem 4.1 of [51], we need to calculate the bifurcation constants a and b. Denote $S = x_1$, $E = x_2$, $I = x_3$, and $R = x_4$. After some algebraic calculation, we obtain

$$\begin{aligned} a =& \sum_{k,i,j=1}^{4} v_k \omega_i \omega_j \frac{\partial^2 f_k(D_0,\beta^*)}{\partial x_i \partial x_j} \\ =& -\frac{\mu^2(\mu+q)g(0)^2}{Aq\gamma^2}\left(\mu+\gamma+\frac{\gamma}{g(0)}\right)^2 - \frac{2f'(0)(\mu+\delta)}{f(0)}\left(\frac{\mu g(0)}{\gamma}\right)^2 \\ & -\frac{2\mu^2 g(0)}{\gamma}\left(\frac{f'(0)}{f(0)} - \frac{g'(0)}{g(0)}\right) < 0, \\ b =& \sum_{k,i=1}^{4} v_k \omega_i \frac{\partial^2 f_k(D_0,\beta^*)}{\partial x_i \partial \beta} = \frac{Aq\mu g(0)}{\mu\gamma(q+\mu)f(0)} > 0. \end{aligned}$$

Therefore, from Theorem 4.1 of [51], the disease-free equilibrium (D_0) changes its stability from stable to unstable at $R_0 = 1$. Moreover, there exists a positive equilibrium as R_0 crosses value 1, which is locally asymptotically stable. Therefore, system (2.2) undergoes a transcritical bifurcation at $R_0 = 1$.

Proof of Theorem 3.3: To prove the global stability of D_0, we follow the approach given by Castillo-Chavez et al. [52]. We rewrite the system (2.2) as follows

$$\begin{aligned} \frac{dX}{dt} &= F(X,V), \\ \frac{dV}{dt} &= G(X,V), \quad G(X,0)=0, \end{aligned} \tag{.1}$$

where $X = (S, R) \in \mathbb{R}^2$ signifies the number of uninfected individuals and $V = (E, I) \in \mathbb{R}^2$ signifies the number of infected individuals. Disease-free equilibrium (D_0) is globally stable if the following two conditions are fulfilled:

(H1) For $\frac{dX}{dt} = F(X, V)$, X^* is globally asymptotically stable,
(H2) $G(X, V) = MV - \hat{G}(X, V)$, $\hat{G}(X, V) > 0$ for $(X, V) \in \mathfrak{V}$,

where $M = D_V G(X^*, 0)$ is an M-matrix. For the system (2.2), we have

$$F(X,0) = \begin{pmatrix} \Lambda - \mu S \\ 0 \end{pmatrix}. \tag{.2}$$

It is obvious that the equilibrium $X^* = \left(\frac{A}{\mu}, 0\right)$ is globally asymptotically stable of system (.2). Further, for system (2.2), we obtain

$$M = \begin{pmatrix} -(\mu+q) & \frac{\beta A}{\mu f(0)} \\ q & -(\mu+\delta+\frac{\gamma}{g(0)}) \end{pmatrix}, \quad \hat{G}(X,V) = \begin{pmatrix} \frac{\beta I}{f(I)}(\frac{A}{\mu} - S) \\ 0 \end{pmatrix}.$$

It is clear that $\hat{G}(X, V) \geq 0$. Hence, D_0 is globally stable.

Proof of Theorem 3.4: Define the following Lyapunov function:

$$L(S,E,I,R) = |S - S^*| + |E - E^*| + |I - I^*| + |R - R^*|.$$

Clearly, $L(D^*) = 0$ and $L(D) \neq 0$ when $D \neq D^*$. The upper right derivative of $L(S, E, I, R)$ can be calculated as:

$$\begin{aligned} D^+L =& \operatorname{sgn}(S - S^*)\Big[- \Big(\frac{\beta S I}{f(I)} - \frac{\beta S^* I^*}{f(I^*)}\Big) - \mu(S - S^*)\Big] \\ &+ \operatorname{sgn}(E - E^*)\Big[- (\mu+q)(E - E^*) + \Big(\frac{\beta S I}{f(I)} - \frac{\beta S^* I^*}{f(I^*)}\Big)\Big] \\ &+ \operatorname{sgn}(I - I^*)\Big[q(E - E^*) - (\mu+\delta)(I - I^*) - \Big(\frac{\gamma I}{g(I)} - \frac{\gamma I^*}{g(I^*)}\Big)\Big] \\ &+ \operatorname{sgn}(R - R^*)\Big[\Big(\frac{\gamma I}{g(I)} - \frac{\gamma I^*}{g(I^*)}\Big) - \mu(R - R^*)\Big]. \end{aligned}$$

In the above equation, there are 8 different types of situations depending on the size of S and S^*, E and E^*, I and I^*, R and R^*. It would be sufficient to show for $S > S^*, E > E^*, I > I^*, R > R^*$, similarly, one can also do for the other situations. Thus we obtain

$$D^+L \leq -\mu|S - S^*| - \mu|E - E^*| - (\mu+\delta)|I - I^*| - \mu|R - R^*|$$

$$< -\mu|S - S^*| - \mu|E - E^*| - \mu|I - I^*| - \mu|R - R^*|$$
$$< -\mu L.$$

Integrating the above inequality from t_0 to t both sides, we obtain

$$L(t) + \mu \int_{t_0}^{t} L dt \leq L(t_0) < +\infty.$$

Since S, E, I, R are bounded and their derivatives are also bounded, therefore, L is uniformly continuous on $[t_0, +\infty)$. From Barbalat's Lemma [53], $\lim_{t\to+\infty} L(t) = 0$. Hence $D^+L < -\mu L < 0$, which implies D^* is globally stable.

Proof of Theorem 4.1: The characteristic equation of the Jacobian of system (4.1) at D_0 is given by

$$\det(K_0 + K_1 e^{-\lambda\tau_1} + K_2 e^{-\lambda\tau_2} - \lambda I) = 0, \tag{.3}$$

where

$$K_0 = \begin{pmatrix} -\mu & 0 & -\frac{\beta A}{\mu f(0)} \\ 0 & -(\mu+q) & \frac{\beta A}{\mu f(0)} \\ 0 & q & -(\mu+\delta) \end{pmatrix},$$
$$K_1 = \begin{pmatrix} 0 & 0 & 0 \\ 0 & 0 & 0 \\ 0 & 0 & 0 \end{pmatrix},$$
$$K_2 = \begin{pmatrix} 0 & 0 & 0 \\ 0 & 0 & 0 \\ 0 & 0 & -\frac{\gamma}{g(0)} \end{pmatrix},$$

and I is a 3×3 identity matrix. So the characteristic equation (.3) becomes in the following form

$$(\lambda+\mu)\left\{(\lambda + (\mu+\delta) + \frac{\gamma}{g(0)}e^{-\lambda\tau_2})(\lambda+\mu+q) - \frac{\beta A q}{\mu f(0)}\right\} = 0. \tag{.4}$$

One eigenvalue is $-\mu$, which is negative and other eigenvalues are solution of the following equation

$$p(\lambda) = (\lambda + (\mu+\delta) + \frac{\gamma}{g(0)}e^{-\lambda\tau_2})(\lambda+\mu+q) - \frac{\beta A q}{\mu f(0)} = 0 \tag{.5}$$

or

$$\lambda^2 + V_{11}\lambda + V_{12} + (V_{13}\lambda + V_{14})e^{-\lambda\tau_2} = 0,$$

where

$$V_{11} = (2\mu + q + \delta), \quad V_{12} = (\mu+q)(\mu+\delta) - \frac{\beta A q}{\mu f(0)}, \quad V_{13} = \frac{\gamma}{g(0)}, \quad V_{14} = (\mu+q)\frac{\gamma}{g(0)}.$$

Let $\lambda = i\omega, (\omega > 0)$ be a root of Eq. (.5). Putting $\lambda = i\omega$ in Eq. (.5) and separating real and imaginary parts, we have

$$-\omega^2 + V_{12} = -V_{14}\cos(\omega\tau_2) - V_{13}\omega\sin(\omega\tau_2),$$

$$V_{11}\omega = -V_{13}\omega\cos(\omega\tau_2) + V_{14}\sin(\omega\tau_2).$$

Squaring and adding above equations, we obtain

$$\omega^4 + (V_{11}^2 - V_{13}^2 - 2V_{12})\omega^2 + V_{12}^2 - V_{14}^2 = 0. \tag{.6}$$

Let $\omega^2 = v$, then we have

$$v^2 + (V_{11}^2 - V_{13}^2 - 2V_{12})v + V_{12}^2 - V_{14}^2 = 0. \tag{.7}$$

By Descarte's rule of sign, if $V_{11}^2 - V_{13}^2 - 2V_{12} > 0$ and $V_{12}^2 - V_{14}^2 > 0$, then Eq. (.6) has no positive roots. Hence all roots of Eq. (.6) have negative real parts.

If $\tau_2 = 0$, then Eq. (.5) becomes in the following form

$$\lambda^2 + (2\mu + q + \delta + \frac{\gamma}{g(0)})\lambda + (\mu + \delta + \frac{\gamma}{g(0)})(\mu + q) - \frac{\beta A q}{\mu f(0)} = 0,$$
$$\lambda^2 + (2\mu + q + \delta + \frac{\gamma}{g(0)})\lambda + (\mu + \delta + \frac{\gamma}{g(0)})(\mu + q)(1 - R_0) = 0.$$

If $R_0 < 1$ then by Descarte's rule of sign, above equation has all its roots with negative real parts. Hence D_0 is locally asymptotically stable.

From $p(\lambda) = (\lambda + \mu + q)(\lambda + (\mu + \delta) + \frac{\gamma}{g(0)}e^{-\lambda\tau_2}) - \frac{\beta A q}{\mu f(0)}$, since $\lim_{\lambda\to+\infty} p(\lambda) = +\infty$ and

$$\begin{aligned} p(0) &= (\mu + \delta + \frac{\gamma}{g(0)})(\mu + q) - \frac{\beta A q}{\mu f(0)}, \\ &= (\mu + \delta + \frac{\gamma}{g(0)})(\mu + q)(1 - R_0), \\ &< 0, \quad \textit{when} \quad R_0 > 1. \end{aligned}$$

Therefore, $p(\lambda) = 0$ has a positive real root. Hence, D_0 is unstable when $R_0 > 1$.

Proof of Lemma 4.3 and Theorem 4.4: If $\tau_1 > 0, \tau_2 = 0$, then the characteristic Eq. (4.3) becomes

$$\lambda^3 + (P_{11} + P_{16})\lambda^2 + (P_{12} + P_{17})\lambda + (P_{13} + P_{18}) + (P_{14}\lambda + P_{15})e^{-\lambda\tau_1} = 0. \tag{.8}$$

Let $\lambda = i\omega_1, (\omega_1 > 0)$ be a root of Eq. (.8). Putting $\lambda = i\omega_1$ in Eq. (.8) and separating imaginary and real parts, we have

$$\begin{aligned} &P_{15}\cos(\omega_1\tau_1) + P_{14}\omega_1\sin(\omega_1\tau_1) = (P_{11} + P_{16})\omega_1^2 - (P_{13} + P_{18}), \\ &P_{14}\omega_1\cos(\omega_1\tau_1) - P_{15}\sin(\omega_1\tau_1) = \omega_1^3 - (P_{12} + P_{17})\omega_1. \end{aligned} \tag{.9}$$

Squaring and adding above equations, we obtain

$$\omega_1^6 + c_{11}\omega_1^4 + c_{12}\omega_1^2 + c_{13} = 0, \tag{.10}$$

where

$$\begin{aligned} c_{11} &= (P_{11} + P_{16})^2 - 2(P_{12} + P_{17}),\ c_{12} = (P_{12} + P_{17})^2 - 2(P_{11} + P_{16})(P_{13} + P_{18}) - P_{14}^2, \\ c_{13} &= (P_{13} + P_{18})^2 - P_{15}^2. \end{aligned}$$

Let $\omega_1^2 = v_1$, then Eq. (.10) becomes

$$v_1^3 + c_{11}v_1^2 + c_{12}v_1 + c_{13} = 0. \tag{.11}$$

For the sign of the roots of Eq. (.10), by Descartes rule of sign, we have the following cases:

1. If $c_{11} > 0, c_{12} > 0, c_{13} > 0$, then Eq. (.10) has no positive roots. Hence all the roots of Eq. (.10) have negative real parts for $\tau_1 \in (0, +\infty)$.

2. If $c_{13} < 0, c_{11} > 0, c_{12} > 0$ or $c_{13} < 0, c_{11} > 0, c_{12} < 0$ or $c_{13} < 0, c_{11} < 0, c_{12} < 0$, then Eq. (.10) has a unique positive root $\omega_1^{'} = \sqrt{v_1^{'}}$. Eliminating $\sin(\omega_1\tau_1)$ from Eq. (.9), we obtain

$$\tau_{1_j}^{'} = \frac{1}{\omega_1^{'}} \cos^{-1}\left[\frac{P_{14}\omega_1^{'4} + ((P_{11}+P_{16})P_{15} - (P_{12}+P_{17})P_{14})\omega_1^{'2} - P_{15}(P_{13}+P_{18})}{P_{15}^2 + (P_{14}\omega_1^{'2})^2} + 2j\pi\right], \quad j = 0, 1, 2, \ldots. \tag{.12}$$

3. If $c_{11} > 0, c_{12} < 0, c_{13} > 0$ or $c_{11} < 0, c_{12} > 0, c_{13} > 0$ or $c_{11} < 0, c_{12} < 0, c_{13} > 0$, then Eq. (.10) has two positive roots $\omega_1^{\pm} = \sqrt{v_1^{\pm}}$. Eliminating $\sin(\omega_1\tau_1)$ from Eq. (.9), we obtain

$$\tau_{1_k}^{\pm} = \frac{1}{\omega_1^{\pm}} \cos^{-1}\left[\frac{P_{14}\omega_1^{\pm 4} + ((P_{11}+P_{16})P_{15} - (P_{12}+P_{17})P_{14})\omega_1^{\pm 2} - P_{15}(P_{13}+P_{18})}{P_{15}^2 + (P_{14}\omega_1^{\pm 2})^2} + 2k\pi\right], \quad k = 0, 1, 2, \ldots. \tag{.13}$$

4. If $c_{11} < 0, c_{12} > 0, c_{13} < 0$, then Eq. (.10) has three positive roots $\omega_1^{1,2,3} = \sqrt{v_1^{1,2,3}}$. Eliminating $\sin(\omega_1\tau_1)$ from Eq. (.9), we obtain

$$\tau_{1_l}^{1,2,3} = \frac{1}{\omega_1^{1,2,3}} \cos^{-1}\left[\frac{P_{14}\omega_1^{1,2,3\,4} + ((P_{11}+P_{16})P_{15} - (P_{12}+P_{17})P_{14})\omega_1^{1,2,3\,2} - P_{15}(P_{13}+P_{18})}{P_{15}^2 + (P_{14}\omega_1^{1,2,3\,2})^2} + 2l\pi\right], \quad l = 0, 1, 2, \ldots. \tag{.14}$$

Hence, Eq. (.8) has a pair of purely imaginary roots $\pm i\omega_1^{'}$ with $\tau_1 = \tau_{1_j}^{'}, j = 0, 1, 2, \ldots$, a pair of purely imaginary roots $\pm i\omega_1^{\pm}$ with $\tau_1 = \tau_{1_k}^{\pm}, k = 0, 1, 2, \ldots$, and a pair of purely imaginary roots $\pm i\omega_1^{1,2,3}$ with $\tau_1 = \tau_{1_l}^{1,2,3}, l = 0, 1, 2, \ldots$. Let $\left\{\tau_{1_j}\right\}_{j=0}^{+\infty} = \left\{\tau_{1_j}^{'}\right\}_{j=0}^{+\infty}$ such that $\tau_{1_0} < \tau_{1_1} < \tau_{1_2} < \cdots < \tau_{1_j} < \ldots$, $\{\tau_{1_k}\}_{k=0}^{+\infty} = \left\{\tau_{1_k}^{\pm}\right\}_{k=0}^{+\infty}$ such that $\tau_{1_0} < \tau_{1_1} < \tau_{1_2} < \cdots < \tau_{1_k} < \ldots$, where $\tau_{1_0} = \min\left\{\tau_{1_0}^{+}, \tau_{1_0}^{-}\right\}$, and $\{\tau_{1_l}\}_{l=0}^{+\infty} = \left\{\tau_{1_l}^{1,2,3}\right\}_{l=0}^{+\infty}$ such that $\tau_{1_0} < \tau_{1_1} < \tau_{1_2} < \cdots < \tau_{1_l} < \ldots$, where $\tau_{1_0} = \min\left\{\tau_{1_0}^{1}, \tau_{1_0}^{2}, \tau_{1_0}^{3}\right\}$.

Let $\lambda(\tau_1) = \alpha(\tau_1) + i\omega_1(\tau_1)$ be a root of Eq. (.8) near $\tau_1 = \tau_{1_j}$ and $\alpha(\tau_{1_j}) = 0$, $\omega_1(\tau_{1_j}) = \omega_1^{'}$, $j = 0, 1, 2, \ldots$. Further, differentiating Eq. (.8) with respect to τ_1 and substituting $\lambda = i\omega_1^{'}$, $\tau_1 = \tau_{1_j}$, $j = 0, 1, 2, \ldots$, we obtain

$$Re\left(\frac{d\lambda}{d\tau_1}\right)^{-1}_{\lambda = i\omega_1^{'}, \tau_1 = \tau_{1_j}} = \frac{M_{11}M_{13} + M_{12}M_{14}}{M_{13}^2 + M_{14}^2}, \tag{.15}$$

where

$$\begin{aligned}
M_{11} &= P_{15}\omega_1^{'} \sin\left(\tau_{1_j}\omega_1^{'}\right) - P_{14}\omega_1^{'2} \cos\left(\tau_{1_j}\omega_1^{'}\right),\\
M_{12} &= P_{14}\omega_1^{'2} \sin\left(\tau_{1_j}\omega_1^{'}\right) + P_{15}\omega_1^{'} \cos\left(\tau_{1_j}\omega_1^{'}\right),\\
M_{13} &= -P_{14}\tau_{1_j}\omega_1^{'} \sin\left(\tau_{1_j}\omega_1^{'}\right) + P_{14} \cos\left(\tau_{1_j}\omega_1^{'}\right) - P_{15}\tau_{1_j} \cos\left(\tau_{1_j}\omega_1^{'}\right) + P_{12} + P_{17} - 3\omega_1^{'2},\\
M_{14} &= P_{15}\tau_{1_j} \sin\left(\tau_{1_j}\omega_1^{'}\right) - P_{14}\left(\sin\left(\tau_{1_j}\omega_1^{'}\right) + \tau_{1_j}\omega_1^{'} \cos\left(\tau_{1_j}\omega_1^{'}\right)\right) + 2\left(P_{11} + P_{16}\right)\omega_1^{'}.
\end{aligned}$$

Proof of Lemma 4.5 and Theorem 4.6: If $\tau_1 = 0, \tau_2 > 0$, then the characteristic Eq. (4.3) becomes

$$\lambda^3 + P_{11}\lambda^2 + (P_{12} + P_{14})\lambda + (P_{13} + P_{15}) + (P_{16}\lambda^2 + P_{17}\lambda + P_{18})e^{-\lambda\tau_2} = 0. \tag{.16}$$

Let $\lambda = i\omega_2, (\omega_2 > 0)$ be a root of Eq. (.16). Putting $\lambda = i\omega_2$ in Eq. (.16) and separating imaginary and real parts, we have

$$\begin{aligned}(P_{18} - P_{16}\omega_2^2)\cos(\omega_2\tau_2) + P_{17}\omega_2\sin(\omega_2\tau_2) &= P_{11}\omega_2^2 - (P_{13} + P_{15}),\\ P_{17}\omega_2\cos(\omega_2\tau_2) - (P_{18} - P_{16}\omega_2^2)\sin(\omega_2\tau_2) &= -\omega_2^3 + (P_{12} + P_{14})\omega_2.\end{aligned} \tag{.17}$$

Squaring and adding above equations, we obtain

$$\omega_2^6 + d_{11}\omega_2^4 + d_{12}\omega_2^2 + d_{13} = 0, \tag{.18}$$

where

$$\begin{aligned}d_{11} =& P_{11}^2 - 2(P_{12} + P_{14}) - P_{16}^2, \quad d_{12} = (P_{12} + P_{14}) - 2P_{11}(P_{13} + P_{15}) - P_{17}^2 + 2P_{16}P_{18},\\ d_{13} =& (P_{13} + P_{15})^2 - P_{18}^2.\end{aligned}$$

Let $\omega_2^2 = v_2$, then Eq. (.18) becomes

$$v_2^3 + d_{11}v_2^2 + d_{12}v_2 + d_{13} = 0. \tag{.19}$$

1. If $d_{11} > 0, d_{12} > 0, d_{13} > 0$, then Eq. (.18) has no positive roots. Hence all roots of Eq. (.18) have negative real parts when $\tau_2 \in (0, +\infty)$.
2. If $d_{13} < 0, d_{11} > 0, d_{12} > 0$ or $d_{13} < 0, d_{11} > 0, d_{12} < 0$ or $d_{13} < 0, d_{11} < 0, d_{12} < 0$, then Eq. (.18) has a unique positive root $\omega_2' = \sqrt{v_2'}$. Eliminating $\sin(\omega_2\tau_2)$ from Eq. (.17), we obtain

$$\tau_{2_j}' = \frac{1}{\omega_2'}\cos^{-1}\left[\frac{(P_{16}(P_{11} + P_{15}) + P_{11}P_{18} + P_{17}(P_{12} + P_{14}))\omega_2'^2 - (P_{17} + P_{11}P_{16})\omega_2'^4 - (P_{11} + P_{15})P_{18}}{(P_{18} - P_{16}\omega_2'^2)^2 + (P_{17}\omega_2')^2} + 2j\pi\right], \quad j = 0, 1, 2, \ldots. \tag{.20}$$

3. If $d_{11} > 0$, $d_{12} < 0, d_{13} > 0$ or $d_{11} < 0$, $d_{12} > 0, d_{13} > 0$ or $d_{11} < 0$, $d_{12} < 0, d_{13} > 0$, then Eq. (.18) has two positive roots $\omega_2^{\pm} = \sqrt{v_2^{\pm}}$. Eliminating $\sin(\omega_2\tau_2)$ from Eq. (.17), we obtain

$$\tau_{2_k}^{\pm} = \frac{1}{\omega_2^{\pm}}\cos^{-1}\left[\frac{(P_{16}(P_{11} + P_{15}) + P_{11}P_{18} + P_{17}(P_{12} + P_{14}))\omega_2^{\pm 2} - (P_{17} + P_{11}P_{16})\omega_2^{\pm 4} - (P_{11} + P_{15})P_{18}}{(P_{18} - P_{16}\omega_2^{\pm 2})^2 + (P_{17}\omega_2^{\pm})^2} + 2k\pi\right], \quad k = 0, 1, 2, \ldots. \tag{.21}$$

4. If $d_{11} < 0$, $d_{12} > 0, d_{13} < 0$, then Eq. (.18) has two positive roots $\omega_2^{1,2,3} = \sqrt{v_2^{1,2,3}}$. Eliminating $\sin(\omega_2\tau_2)$ from Eq. (.17), we obtain

$$\tau_{2_l}^{1,2,3} = \frac{1}{\omega_2^{1,2,3}}\cos^{-1}\left[\frac{(P_{16}(P_{11} + P_{15}) + P_{11}P_{18} + P_{17}(P_{12} + P_{14}))\omega_2^{1,2,3^2} - (P_{17} + P_{11}P_{16})\omega_2^{1,2,3^4} - (P_{11} + P_{15})P_{18}}{(P_{18} - P_{16}\omega_2^{1,2,3^2})^2 + (P_{17}\omega_2^{1,2,3})^2} + 2l\pi\right], \quad l = 0, 1, 2, \ldots. \tag{.22}$$

Hence, Eq. (.18) has a pair of purely imaginary roots $\pm i\omega_2'$ with $\tau_2 = \tau_{2_j}', j = 0, 1, 2, \ldots$, a pair of purely imaginary roots $\pm i\omega_2^{\pm}$ with $\tau_2 = \tau_{2_k}^{\pm}, k = 0, 1, 2, \ldots$, and a pair of purely imaginary roots $\pm i\omega_2^{1,2,3}$ with $\tau_2 = \tau_{2_l}^{1,2,3}, l = 0, 1, 2, \ldots$. Let $\left\{\tau_{2_j}\right\}_{j=0}^{+\infty} = \left\{\tau_{2_j}'\right\}_{j=0}^{+\infty}$ such that $\tau_{2_0} < \tau_{2_1} < \tau_{2_2} < \cdots < \tau_{2_j} < \ldots$; $\{\tau_{2_k}\}_{k=0}^{+\infty} = \left\{\tau_{2_k}^{\pm}\right\}_{k=0}^{+\infty}$ such that $\tau_{2_0} < \tau_{2_1} < \tau_{2_2} < \cdots < \tau_{2_k} < \ldots$, where $\tau_{2_0} = \min\left\{\tau_{2_0}^{+}, \tau_{2_0}^{-}\right\}$; and $\{\tau_{2_l}\}_{l=0}^{+\infty} = \left\{\tau_{2_l}^{1,2,3}\right\}_{l=0}^{+\infty}$ such that $\tau_{2_0} < \tau_{2_1} < \tau_{2_2} < \cdots < \tau_{2_l} < \ldots$, where $\tau_{2_0} = \min\left\{\tau_{2_0}^{1}, \tau_{2_0}^{2}, \tau_{2_0}^{3}\right\}$.

Let $\lambda(\tau_2) = \alpha(\tau_2) + i\omega_2(\tau_2)$ be a root of Eq. (.18) near $\tau_2 = \tau_{2_j}$ and $\alpha(\tau_{2_j}) = 0$, $\omega_2(\tau_{2_j}) = \omega_2'$, $j = 0, 1, 2, \ldots$. Further, differentiating Eq. (.18) with respect to τ_2 and substituting $\lambda = i\omega_2'$, $\tau_2 = \tau_{2_j}$, $j = 0, 1, 2, \ldots$, we obtain

$$Re\left(\frac{d\lambda}{d\tau_2}\right)^{-1}_{\lambda=i\omega_2', \tau_2=\tau_{2_j}} = \frac{M_{21}M_{23} + M_{22}M_{24}}{M_{23}^2 + M_{24}^2}, \tag{.23}$$

where

$$\begin{aligned}
M_{21} =& P_{16}{\omega_2'}^3\left(-\sin\left(\tau_{2_j}\omega_2'\right)\right) + P_{18}\omega_2'\sin\left(\tau_{2_j}\omega_2'\right) - P_{17}{\omega_2'}^2\cos\left(\tau_{2_j}\omega_2'\right),\\
M_{22} =& P_{17}{\omega_2'}^2\sin\left(\tau_{2_j}\omega_2'\right) + P_{16}{\omega_2'}^3\left(-\cos\left(\tau_{2_j}\omega_2'\right)\right) + P_{18}\omega_2'\cos\left(\tau_{2_j}\omega_2'\right),\\
M_{23} =& 2P_{16}\omega_2'\sin\left(\tau_{2_j}\omega_2'\right) - P_{17}\tau_{2_j}\omega_2'\sin\left(\tau_{2_j}\omega_2'\right) + P_{16}\tau_{2_j}{\omega_2'}^2\cos\left(\tau_{2_j}\omega_2'\right)\\
&+ P_{17}\cos\left(\tau_{2_j}\omega_2'\right) - P_{18}\tau_{2_j}\cos\left(\tau_{2_j}\omega_2'\right) + P_{12} + P_{14} - 3{\omega_2'}^2,\\
M_{24} =& P_{16}\tau_{2_j}{\omega_2'}^2\left(-\sin\left(\tau_{2_j}\omega_2'\right)\right) - P_{17}\sin\left(\tau_{2_j}\omega_2'\right) + P_{18}\tau_{2_j}\sin\left(\tau_{2_j}\omega_2'\right)\\
&+ 2P_{16}\omega_2'\cos\left(\tau_{2_j}\omega_2'\right) - P_{17}\tau_{2_j}\omega_2'\cos\left(\tau_{2_j}\omega_2'\right) + 2P_{11}\omega_2'.
\end{aligned}$$

Proof of Lemma 4.7 and Theorem 4.8: If $\tau_1 = \tau_2 = \tau$, then the characteristic Eq. (4.3) becomes

$$\lambda^3 + P_{11}\lambda^2 + P_{12}\lambda + P_{13} + (P_{16}\lambda^2 + (P_{14} + P_{17})\lambda + P_{15} + P_{18})e^{-\lambda\tau} = 0, \tag{.24}$$

Let $\lambda = i\omega_3, (\omega_3 > 0)$ be a root of Eq. (.24). Putting $\lambda = i\omega_3$ in Eq. (.24) and separating imaginary and real parts, we have

$$\begin{aligned}
(-P_{16}\omega_3^2 + P_{15} + P_{18})\cos(\omega_3\tau) + (P_{14} + P_{17})\omega_3\sin(\omega_3\tau) &= P_{11}\omega_3^2 - P_{13},\\
(P_{14} + P_{17})\omega_3\cos(\omega_3\tau) - (-P_{16}\omega_3^2 + P_{15} + P_{18})\sin(\omega_3\tau) &= \omega_3^3 - P_{12}\omega_3.
\end{aligned} \tag{.25}$$

Squaring and adding above equations, we obtain

$$\omega_3^6 + e_{11}\omega_3^4 + e_{12}\omega_3^2 + e_{13} = 0, \tag{.26}$$

where

$$\begin{aligned}
e_{11} =& P_{11}^2 - 2P_{12} - P_{16}^2, \quad e_{12} = P_{12}^2 - (P_{14} + P_{17})^2 - 2P_{11}P_{13} + 2P_{16}(P_{15} + P_{18}),\\
e_{13} =& P_{13}^2 - (P_{15} + P_{18})^2
\end{aligned}$$

Let $\omega_3^2 = v_3$, then Eq. (.26) becomes

$$v_3^3 + e_{11}v_3^2 + e_{12}v_3 + e_{13} = 0. \tag{.27}$$

1. If $e_{11} > 0, e_{12} > 0, e_{13} > 0$, then Eq. (.26) has no positive roots. Hence all roots of Eq. (.26) have negative real parts when $\tau \in (0, +\infty)$.
2. If $e_{13} < 0, e_{11} > 0, e_{12} > 0$ or $e_{13} < 0, e_{11} > 0, e_{12} < 0$ or $e_{13} < 0, e_{11} < 0, e_{12} < 0$, then Eq. (.26) has a unique positive root $\omega_3' = \sqrt{v_3'}$. Eliminating $\sin(\omega_3\tau)$ from Eq. (.25), we obtain

$$\tau_j' = \frac{1}{\omega_3'}\cos^{-1}\left[\frac{(P_{14} + P_{17} - P_{11}P_{16}){\omega_3'}^4 + (P_{13}P_{16} + P_{11}(P_{15} + P_{18}) - P_{12}(P_{14} + P_{17})){\omega_3'}^2 - P_{13}(P_{15} + P_{18})}{((P_{14} + P_{17})\omega_3')^2 + (-P_{16}{\omega_3'}^2 + P_{15} + P_{18})^2} + 2j\pi\right], \quad j = 0, 1, 2, \ldots. \tag{.28}$$

3. If $e_{11} > 0$, $e_{12} < 0, e_{13} > 0$ or $e_{11} < 0$, $e_{12} > 0, e_{13} > 0$ or $e_{11} < 0$, $e_{12} < 0, e_{13} > 0$, then Eq. (.26) has two positive roots $\omega_3^{\pm} = \sqrt{v_3^{\pm}}$. Eliminating $\sin(\omega_3\tau)$ from Eq. (.25), we obtain

$$\tau_k^{\pm} = \frac{1}{\omega_3^{\pm}}\cos^{-1}\left[\frac{(P_{14}+P_{17}-P_{11}P_{16})\omega_3^{\pm 4}+(P_{13}P_{16}+P_{11}(P_{15}+P_{18})-P_{12}(P_{14}+P_{17}))\omega_3^{\pm 2}-P_{13}(P_{15}+P_{18})}{((P_{14}+P_{17})\omega_3^{\pm 2})^2+(-P_{16}\omega_3^{\pm 2}+P_{15}+P_{18})^2}+2k\pi\right], \quad k=0,1,2,\ldots. \tag{.29}$$

4. If $e_{11} < 0$, $e_{12} > 0, e_{13} < 0$, then Eq. (.26) has two positive roots $\omega_3^{1,2,3} = \sqrt{v_3^{1,2,3}}$. Eliminating $\sin(\omega_3\tau)$ from Eq. (.25), we obtain

$$\tau_l^{1,2,3} = \frac{1}{\omega_3^{1,2,3}}\cos^{-1}\left[\frac{(P_{14}+P_{17}-P_{11}P_{16})\omega_3^{1,2,3\,4}+(P_{13}P_{16}+P_{11}(P_{15}+P_{18})-P_{12}(P_{14}+P_{17}))\omega_3^{1,2,3\,2}-P_{13}(P_{15}+P_{18})}{((P_{14}+P_{17})\omega_3^{1,2,3})^2+(-P_{16}\omega_3^{1,2,3\,2}+P_{15}+P_{18})^2}+2l\pi\right], \quad l=0,1,2,\ldots. \tag{.30}$$

Hence, Eq. (.24) has a pair of purely imaginary roots $\pm i\omega_3'$ with $\tau = \tau_j'$, $j = 0, 1, 2, \ldots$, a pair of purely imaginary roots $\pm i\omega_3^{\pm}$ with $\tau = \tau_k^{\pm}, k = 0, 1, 2, \ldots$, and a pair of purely imaginary roots $\pm i\omega_3^{1,2,3}$ with $\tau = \tau_l^{1,2,3}, l = 0, 1, 2, \ldots$. Let $\left\{\tau_j\right\}_{j=0}^{+\infty} = \left\{\tau_j'\right\}_{j=0}^{+\infty}$ such that $\tau_0 < \tau_1 < \tau_2 < \cdots < \tau_j < \ldots$, $\{\tau_k\}_{k=0}^{+\infty} = \left\{\tau_k^{\pm}\right\}_{k=0}^{+\infty}$ such that $\tau_0 < \tau_1 < \tau_2 < \cdots < \tau_k < \ldots$, where $\tau_0 = \min\left\{\tau_0^+, \tau_0^-\right\}$, and $\{\tau_l\}_{l=0}^{+\infty} = \left\{\tau_l^{1,2,3}\right\}_{l=0}^{+\infty}$ such that $\tau_0 < \tau_1 < \tau_2 < \cdots < \tau_l < \ldots$, where $\tau_0 = \min\left\{\tau_0^1, \tau_0^2, \tau_0^3\right\}$.

Let $\lambda(\tau) = \alpha(\tau) + i\omega_3(\tau)$ be a root of Eq. (.24) near $\tau = \tau_j$ and $\alpha(\tau_j) = 0$, $\omega_3(\tau_j) = \omega_3'$, $j = 0, 1, 2, \ldots$. Further, differentiating Eq. (.24) with respect to τ and substituting $\lambda = i\omega_3'$, $\tau = \tau_j$, $j = 0, 1, 2, \ldots$, we obtain

$$Re\left(\frac{d\lambda}{d\tau}\right)^{-1}_{\lambda=i\omega_3', \tau=\tau_j} = \frac{M_{31}M_{33}+M_{32}M_{34}}{M_{33}^2+M_{34}^2}, \tag{.31}$$

$$\begin{aligned}
M_{31} =& -P_{16}{\omega_3'}^3\sin\left(\tau_j\omega_3'\right)+\omega_3'(P_{15}\sin\left(\tau_j\omega_3'\right)+P_{18}\sin\left(\tau_j\omega_3'\right))\\
&-{\omega_3'}^2(P_{14}\cos\left(\tau_j\omega_3'\right)+P_{17}\cos\left(\tau_j\omega_3'\right)),\\
M_{32} =& {\omega_3'}^2(P_{14}\sin\left(\tau_j\omega_3'\right)+P_{17}\sin\left(\tau_j\omega_3'\right))-P_{16}{\omega_3'}^3\cos\left(\tau_j\omega_3'\right)\\
&+\omega_3'(P_{15}\cos\left(\tau_j\omega_3'\right)+P_{18}\cos\left(\tau_j\omega_3'\right)),\\
M_{33} =& \omega_3'(-P_{14}\tau_j\sin\left(\tau_j\omega_3'\right)+2P_{16}\sin\left(\tau_j\omega_3'\right)-P_{17}\tau_j\sin\left(\tau_j\omega_3'\right))\\
&+{\omega_3'}^2(P_{16}\tau_j\cos\left(\tau_j\omega_3'\right)-3)+P_{14}\cos\left(\tau_j\omega_3'\right)-P_{15}\tau_j\cos\left(\tau_j\omega_3'\right)\\
&+P_{17}\cos\left(\tau_j\omega_3'\right)-P_{18}\tau\cos\left(\tau_j\omega_3'\right)+P_{12},\\
M_{34} =& -P_{16}\tau_j{\omega_3'}^2\sin\left(\tau_j\omega_3'\right)-P_{14}\sin\left(\tau_j\omega_3'\right)+P_{15}\tau_j\sin\left(\tau_j\omega_3'\right)-P_{17}\sin\left(\tau_j\omega_3'\right)\\
&+P_{18}\tau_j\sin\left(\tau_j\omega_3'\right)+\omega_3'(-P_{14}\tau_j\cos\left(\tau_j\omega_3'\right)+2P_{16}\cos\left(\tau_j\omega_3'\right)-P_{17}\tau_j\cos\left(\tau_j\omega_3'\right)+2P_{11}).
\end{aligned}$$

Proof of Lemma 4.9 and Theorem 4.10: If $\tau_1 > 0, \tau_2 \in (0, \tau_{2_j})$. In this case, we take τ_1 as a bifurcation parameter and τ_2 is in stable interval. Let $\lambda = i\omega_4, (\omega_4 > 0)$ be a root of Eq. (4.3). Putting $\lambda = i\omega_4$ in Eq. (4.3) and separating imaginary and real parts, we have

$$\begin{aligned}
P_{15}\cos(\omega_4\tau_1)+P_{14}\omega_4\sin(\omega_4\tau_1) =& P_{11}\omega_4^2-P_{13}-(P_{18}-P_{16}\omega_4^2)\cos(\omega_4\tau_2)-P_{17}\omega_4\sin(\omega_4\tau_2),\\
P_{14}\omega_4\cos(\omega_4\tau_1)-P_{15}\sin(\omega_4\tau_1) =& -P_{12}\omega_4+\omega_4^3-P_{17}\omega_4\cos(\omega_4\tau_2)+(P_{18}-P_{16}\omega_4^2)\sin(\omega_4\tau_2).
\end{aligned} \tag{.32}$$

From above equation, we obtain the following equation with respect to ω_4

$$h_{11}(\omega_4) + h_{12}(\omega_4)\cos(\omega_4\tau_2) + h_{13}(\omega_4)\sin(\omega_4\tau_2) = 0, \tag{.33}$$

with

$$\begin{aligned}
h_{11}(\omega_4) =&\omega_4^6 + (P_{11}^2 - 2P_{12} + P_{16}^2)\omega_4^4 + (P_{12}^2 + P_{17} - 2P_{11}P_{13} - 2P_{16}P_{18} - P_{14}^2)\omega_4^2 \\
&+ P_{13}^2 - P_{15}^2 + P_{18}^2, \\
h_{12}(\omega_4) =& -2\omega_4^4(P_{17} - P_{11}P_{16}) + 2(P_{12}P_{17} + P_{13}P_{16} - P_{11}P_{18})\omega_4^2 + 2P_{13}P_{18}, \\
h_{13}(\omega_4) =& -2\omega_4^5 P_{16} + 2\omega_4(P_{13}P_{17} - P_{18}P_{12}) - 2\omega_4^3(P_{11}P_{17} - P_{16}P_{12} - P_{18}).
\end{aligned}$$

Assume that **H1:** Eq. (.33) has a positive root ω_4^*. Eliminating $\sin(\omega_4\tau_1)$ from Eq. (.32), we obtain

$$\tau_{1_j}^* = \frac{1}{\omega_4^*}\cos^{-1}\left[\frac{P_{14}\omega_4^{*4} + (P_{11}P_{15} - P_{12}P_{14})\omega_4^{*2} - P_{13}P_{15} - (P_{15}P_{18} + (P_{17}P_{14} - P_{15}P_{16})\omega_4^{*2})\cos(\tau_2\omega_4^*) + ((P_{18}P_{14} - P_{15}P_{17})\omega_4^* - P_{14}P_{16}\omega_4^{*3})\sin(\tau_2\omega_4^*)}{P_{15}^2 + (P_{14}\omega_4^*)^2} + 2j\pi\right], \tag{.34}$$

$j = 0, 1, 2, \ldots$. Now differentiating Eq. (4.3) with respect to τ_1 and substituting $\lambda = i\omega_4^*$, $\tau_1 = \tau_{1_j}^*$, $j = 0, 1, 2, \ldots$, we obtain

$$Re\left(\frac{d\lambda}{d\tau_1}\right)^{-1}_{\lambda=i\omega_4^*,\tau_1=\tau_{1_j}^*} = \frac{M_{41}M_{43} + M_{42}M_{44}}{M_{43}^2 + M_{44}^2}, \tag{.35}$$

where

$$\begin{aligned}
M_{41} =&P_{15}\omega_4^*\sin\left(\tau_{1_j}^*\omega_4^*\right) - P_{11}\omega_4^{*2}\cos\left(\tau_{1_j}^*\omega_4^*\right), \\
M_{42} =&P_{11}\omega_4^{*2}\sin\left(\tau_{1_j}^*\omega_4^*\right) + P_{15}\omega_4^*\cos\left(\tau_{1_j}^*\omega_4^*\right), \\
M_{43} =&\omega_4^*(-2P_{16}\sin(\tau_2\omega_4^*) - P_{11}\tau_{1_j}^*\sin\left(\tau_{1_j}^*\omega_4^*\right) + P_{17}\tau_2\sin(\tau_2\omega_4^*)) \\
&- \omega_4^{*2}(P_{16}\tau_2\cos(\tau_2\omega_4^*) - 3) + P_{11}\cos\left(\tau_{1_j}^*\omega_4^*\right) - P_{17}\cos(\tau_2\omega_4^*) \\
&- P_{15}\tau_{1_j}^*\cos\left(\tau_{1_j}^*\omega_4^*\right) + P_{18}\tau_2\cos(\tau_2\omega_4^*) + P_{12}, \\
M_{44} =& -P_{11}\sin\left(\tau_{1_j}^*\omega_4^*\right) + P_{17}\sin(\tau_2\omega_4^*) + P_{15}\tau_{1_j}^*\sin\left(\tau_{1_j}^*\omega_4^*\right) - P_{18}\tau_2\sin(\tau_2\omega_4^*) \\
&\omega_4^*(-2P_{16}\cos(\tau_2\omega_4^*) - P_{11}\tau_1\cos\left(\tau_{1_j}^*\omega_4^*\right) + P_{17}\tau_2\cos(\tau_2\omega_4^*) + 2P_{11}) \\
&+ P_{16}\tau_2\omega_4^{*2}\sin(\tau_2\omega_4^*).
\end{aligned}$$

Appendix B

Let $p_1 = S - S^*, p_2 = E - E^*, p_3 = I - I^*$ and $\tau_1 = \zeta + \tau_1^*$, where $\zeta \in \mathbb{R}$. Normalize the delay τ_1 by the time-scaling $t \to t/\tau_1$. Then, the reduced system (4.1) becomes in the following functional differential form:

$$\dot{p}(t) = L_\zeta(p_t) + F(\zeta, p_t), \tag{.36}$$

where $L_\zeta : C \to \mathbb{R}^3$ and $F : \mathbb{R} \times C \to \mathbb{R}^3$ are defined as

$$L_\zeta\varphi = (\zeta + \tau_1^*)\left(\Delta_{1\max}\varphi(0) + \Delta_{2\max}\varphi\left(-\frac{\tau_2^*}{\tau_1^*}\right) + \Delta_{3\max}\varphi(-1)\right),$$

and

$$F(\zeta,\varphi)=\begin{pmatrix}\alpha_{11}\varphi_1(0)\varphi_3(0)+\alpha_{12}\varphi_1(0)\varphi_3(-1)+\alpha_{13}\varphi_3(0)\varphi_3(-1)\\ \alpha_{21}\varphi_1(0)\varphi_3(0)+\alpha_{22}\varphi_1(0)\varphi_3(-1)+\alpha_{23}\varphi_3(0)\varphi_3(-1)\\ \alpha_{31}\varphi_3^2(\frac{\tau_2^*}{\tau_1^*})\end{pmatrix},$$

with

$$\Delta_{1\max}=\begin{pmatrix}J_{11}&0&J_{12}\\J_{13}&J_{14}&J_{15}\\0&J_{16}&J_{17}\end{pmatrix},\quad \Delta_{3\max}=\begin{pmatrix}0&0&J_{18}\\0&0&J_{19}\\0&0&0\end{pmatrix},\quad \Delta_{2\max}=\begin{pmatrix}0&0&0\\0&0&0\\0&0&J_{20}\end{pmatrix},$$

and

$$\alpha_{11}=-\frac{\beta}{f(I^*)}=-\alpha_{21},\quad \alpha_{12}=\frac{\beta I^* f'(I^*)}{f(I^*)^2}=-\alpha_{22},\quad \alpha_{13}=\frac{\beta S^* f'(I^*)}{f(I^*)^2}=-\alpha_{23},$$
$$\alpha_{31}=\frac{\gamma I^*}{g(I^*)}\left[\frac{g'(I^*)^2}{g(I^*)}-\frac{g'(I^*)}{g(I^*)^2}-\frac{g''(I^*)}{2g(I^*)}\right].$$

By the Riesz representation theorem [58], there exists a function $\vartheta(\theta,\zeta)$, whose components are of bounded variation for $\theta\in[-1,0]$ such that

$$L_\zeta\varphi=\int_{-1}^{0}d\vartheta(\theta,\zeta)\varphi(\theta).$$

We can choose

$$\vartheta(\theta,\zeta)=\begin{cases}(\tau_1^*+\zeta)(\Delta_{1\max}+\Delta_{2\max}+\Delta_{3\max}), & \theta=0,\\ (\tau_1^*+\zeta)(\Delta_{2\max}+\Delta_{3\max}), & \theta\in\left[-\frac{\tau_2^*}{\tau_1^*},0\right),\\ (\tau_1^*+\zeta)(\Delta_{3\max}), & \theta\in\left(-1,-\frac{\tau_2^*}{\tau_1^*}\right),\\ 0, & \theta=-1,\end{cases}$$

with $\delta(\theta)=\begin{cases}0, & \theta\neq 0,\\ 1, & \theta=1.\end{cases}$

For $\varphi\in C([-1,0],\mathbb{R}^3)$, define

$$A(\zeta)\varphi=\begin{cases}\frac{d\varphi(\theta)}{d\theta}, & -1\le\theta<0,\\ \int_{-1}^{0}d\vartheta(\theta,\zeta)\varphi(\theta), & \theta=0,\end{cases}$$

$$R(\zeta)\varphi=\begin{cases}0, & -1\le\theta<0,\\ F(\zeta,\theta), & \theta=0.\end{cases}$$

Then, the system (.36) is equivalent to the following system

$$\dot p(t)=A(\zeta)p(t)+R(\zeta)p(t).\tag{.37}$$

For $\kappa\in C'([0,1],(\mathbb{R}^3)^*)$, the adjoint operator A^* of $A(0)$ is defined by

$$A^*(\kappa)=\begin{cases}-\frac{d\kappa(s)}{ds}, & 0<s\le 1,\\ \int_{-1}^{0}d\vartheta^T(s,0)\kappa(-s), & s=0.\end{cases}$$

For $\varphi \in C([-1,0],\mathbb{R}^3)$ and $\kappa \in C'([0,1],(\mathbb{R}^3)^*)$, we define the following bilinear inner form:

$$\langle \kappa(s),\varphi(s)\rangle = \bar{\kappa}(0)\varphi(0) - \int_{\theta=-1}^{0}\int_{\nu=0}^{\theta}\bar{\kappa}(\nu-\theta)d\vartheta(\theta)\varphi(\nu)d\nu, \tag{.38}$$

where $\vartheta(\theta)=\vartheta(\theta,0)$.

From subsection 4.3, it can be seen that $\pm i\tau_1^*\omega_4^*$ are the eigenvalues of $A(0)$, therefore, $\pm i\tau_1^*\omega_4^*$ are also the eigenvalues of $A^*(0)$. Let $p(\theta)=(1,p_2,p_3)^T e^{i\tau_1^*\omega_4^*\theta}$ and $p^*(s)=D(1,p_2^*,p_3^*)^T e^{i\tau_1^*\omega_4^* s}$ be the eigenvectors of $A(0)$ and $A^*(0)$ corresponding to the eigenvalues $+i\tau_1^*\omega_4^*$ and $-i\tau_1^*\omega_4^*$, respectively. Hence, we obtain

$$\begin{aligned}
p_2 =& \frac{\omega_4^{*2}-(J_{11}+J_{17})i\omega_4^*+J_{11}J_{17}+J_{20}(J_{11}-i\omega_4^*)e^{-i\tau_2^*\omega_4^*}}{J_{16}(J_{12}+J_{18}e^{-i\tau_1^*\omega_4^*})}, \quad p_3=\frac{i\omega_4^*-J_{11}}{J_{12}+J_{18}e^{-i\tau_1^*\omega_4^*}}\\
p_2^* =& \frac{-i\omega_4^*-J_{11}}{J_{13}}, \quad p_3^*=\frac{J_{11}(J_{13}-J_{15})-J_{15}i\omega_4^*+(J_{13}J_{18}-J_{19}(J_{11}+i\omega_4^*))e^{i\tau_1^*\omega_4^*}}{J_{13}(-i\omega_4^*-J_{17}-J_{20}e^{i\tau_2^*\omega_4^*})}
\end{aligned}$$

In order to show that $\langle p^*,\bar{p}\rangle=0$ and $\langle p^*,p\rangle=1$, we need to compute the value of $\bar{D}$. In view of Eq. (.38), we may choose

$$\bar{D}=\left[1+p_2\bar{p}_2^*+p_3\bar{p}_3^*+\tau_1^*e^{-i\tau_1^*\omega_4^*}(J_{18}p_3+J_{19}p_3\bar{p}_3^*)+\tau_2^*e^{-i\tau_2^*\omega_4^*}J_{20}p_2\bar{p}_2^*\right]^{-1}.$$

Using the same notation as in Hassard et al. [57], we compute the coordinates to describe the center manifold C_0 at $\zeta=0$. Let p_t be the solution of Eq. (.36), when $\zeta=0$. Define

$$\begin{aligned}
z(t) &= \langle p^*,p_t\rangle,\\
W(t,\theta) &= p_t(\theta)-2Re\left\{z(t)p(\theta)\right\}.
\end{aligned} \tag{.39}$$

On the center manifold C_0, we have

$$W(t,\theta)=W(z(t),\bar{z}(t),\theta),$$

where

$$\begin{aligned}
W(z(t),\bar{z}(t),\theta) =& W(z,\bar{z}),\\
=& W_{20}(\theta)\frac{z^2}{2}+W_{11}(\theta)z\bar{z}+W_{02}(\theta)\frac{\bar{z}^2}{2}+W_{30}(\theta)\frac{z^3}{2}+\ldots,
\end{aligned}$$

and z and $\bar{z}$ are local coordinates for center manifold C_0 in the direction of p^* and $\bar{p}^*$. Note that W is also real if p_t is real, we consider only real solutions. For solutions $p_t\in C_0$ of Eq. (.36), since $\zeta=0$,

$$\begin{aligned}
\dot{z}(t) =& i\tau_1^*\omega_4^*z+\bar{p}^*(0)F(0,W(z,\bar{z},\theta))+2Re\left\{z(t)p(\theta)\right\},\\
=& i\tau_1^*\omega_4^*z+g(z,\bar{z}),
\end{aligned}$$

where

$$g(z,\bar{z})=g_{20}\frac{z^2}{2}+g_{11}z\bar{z}+g_{02}\frac{\bar{z}^2}{2}+g_{21}\frac{z^2\bar{z}}{2}+\ldots, \tag{.40}$$

then it follows from Eq. (.36), that

$$\begin{aligned}
p_t =& W(t,\theta)+2Re\left\{z(t)p(\theta)\right\},\\
=& W_{20}(\theta)\frac{z^2}{2}+W_{11}(\theta)z\bar{z}+W_{02}(\theta)\frac{\bar{z}^2}{2}+(1,p_2)e^{i\tau_1^*\omega_4^*\theta}z+(1,\bar{p}_2)e^{-i\tau_1^*\omega_4^*\theta}\bar{z}+\ldots.
\end{aligned}$$

Hence, we have

$$g(z,\bar{z}) = \bar{p}^*(0)F(0,p_t).$$

After some algebraic calculation and comparing the coefficients with (.40), we obtain

$$\begin{aligned}
g_{20} =&2\bar{D}\tau_1^*[(\alpha_{11}p_3+\alpha_{12}p_3+\alpha_{13}p_3^2)+p_2^*(\alpha_{21}p_3+\alpha_{22}p_3+\alpha_{23}p_3^2)+p_3^*(\alpha_{31}p_3^2)],\\
g_{11} =&\bar{D}\tau_1^*[(\alpha_{11}\bar{p}_3+\alpha_{11}p_3+\alpha_{12}p_3+\alpha_{12}\bar{p}_3+2\alpha_{13}p_3\bar{p}_3)+p_2^*(\alpha_{21}\bar{p}_3+\alpha_{21}p_3\\
&+\alpha_{22}\bar{p}_3+\alpha_{22}p_3+2\alpha_{23}p_3\bar{p}_3)+p_3^*(2\alpha_{31}p_3\bar{p}_3)],\\
g_{02} =&2\bar{D}\tau_1^*[(\alpha_{11}\bar{p}_3+\alpha_{12}\bar{p}_3+\alpha_{13}\bar{p}_3^2)+p_2^*(\alpha_{21}\bar{p}_3+\alpha_{22}\bar{p}_3+\alpha_{23}\bar{p}_3^2)+p_3^*(\alpha_{31}\bar{p}_3^2)],\\
g_{21} =&\bar{D}\tau_1^*[(\alpha_{11}\bar{p}_3W_{20}^{(1)}(0)+2\alpha_{11}p_3W_{11}^{(1)}(0)+2\alpha_{11}W_{11}^{(3)}(0)+\alpha_{11}W_{20}^{(3)}(0)\\
&+\alpha_{12}W_{20}^{(1)}(0)\bar{p}_3+2\alpha_{12}p_3W_{11}^{(1)}(0)+2\alpha_{12}W_{11}^{(3)}(-1)+\alpha_{12}W_{20}^{(3)}(-1)\\
&+\alpha_{13}\bar{p}_3W_{20}^{(3)}(0)+2\alpha_{13}p_3W_{11}^{(3)}(0)+2p_3W_{11}^{(3)}(-1)+W_{20}^{(3)}(-1))\\
&+p_2^*(\alpha_{21}\bar{p}_3W_{20}^{(1)}(0)+2\alpha_{21}p_3W_{11}^{(1)}(0)+2\alpha_{21}W_{11}^{(3)}(0)+\alpha_{21}W_{20}^{(3)}(0)\\
&+\alpha_{22}W_{20}^{(1)}(0)\bar{p}_3+2\alpha_{22}p_3W_{11}^{(1)}(0)+2\alpha_{22}W_{11}^{(3)}(-1)+\alpha_{22}W_{20}^{(3)}(-1)\\
&+\alpha_{23}\bar{p}_3W_{20}^{(3)}(0)+2\alpha_{23}p_3W_{11}^{(3)}(0)+2p_3W_{11}^{(3)}(-1)+W_{20}^{(3)}(-1))\\
&+p_3^*(2\alpha_{31}W_{20}^{(3)}\left(-\frac{\tau_2^*}{\tau_1^*}\right)\bar{p}_3+4\alpha_{31}W_{11}^{(3)}\left(-\frac{\tau_2^*}{\tau_1^*}\right))].
\end{aligned}$$

with

$$\begin{aligned}
W_{20}(\theta) =&\frac{ig_{20}p(0)}{\tau_1^*\omega_4^*}e^{i\tau_1^*\omega_4^*\theta}+\frac{i\bar{g}_{02}\bar{p}(0)}{3\tau_1^*\omega_4^*}e^{-i\tau_1^*\omega_4^*\theta}+E_1e^{2i\tau_1^*\omega_4^*\theta},\\
W_{11}(\theta) =&-\frac{ig_{11}p(0)}{\tau_1^*\omega_4^*}e^{i\tau_1^*\omega_4^*\theta}+\frac{i\bar{g}_{11}\bar{p}(0)}{\tau_1^*\omega_4^*}e^{-i\tau_1^*\omega_4^*\theta}+E_2.
\end{aligned}$$

E_1 and E_2 can be determined by the following equations

$$E_1 = 2\begin{pmatrix} J_{11}^* & 0 & -J_{12}+J_{18}^* \\ -J_{13} & J_{14}^* & -J_{15}+J_{19}^* \\ 0 & -J_{16} & -J_{17}+J_{20}^* \end{pmatrix}^{-1}\times\begin{pmatrix} E_{11}' \\ E_{12}' \\ E_{13}' \end{pmatrix},$$

$$E_2 = -\begin{pmatrix} J_{11} & 0 & J_{12}+J_{18} \\ J_{13} & J_{14} & J_{15}+J_{19} \\ 0 & J_{16} & J_{17}+J_{20} \end{pmatrix}^{-1}\times\begin{pmatrix} E_{14}' \\ E_{15}' \\ E_{16}' \end{pmatrix},$$

where

$$\begin{aligned}
J_{11}^* =&2i\omega_4^*-J_{11},\ J_{18}^*=-J_{18}e^{-2i\tau_1^*\omega_4^*},\ J_{14}^*=2i\omega_4^*-J_{14},\\
J_{19}^* =&-J_{19}e^{-2i\tau_1^*\omega_4^*},\ J_{20}^*=2i\omega_4^*-J_{20}e^{-2i\tau_2^*\omega_4^*},\\
E_{11}' =&\alpha_{11}p_3+\alpha_{12}p_3+\alpha_{13}p_3^2,\ E_{12}'=\alpha_{21}p_3+\alpha_{22}p_3+\alpha_{23}p_3^2,\ E_{13}'=\alpha_{31}p_3^2,\\
E_{14}' =&\alpha_{11}\bar{p}_3+\alpha_{11}p_3+\alpha_{12}p_3+\alpha_{12}\bar{p}_3+2\alpha_{13}p_3\bar{p}_3,\ E_{16}'=2\alpha_{31}p_3\bar{p}_3,\\
E_{15}' =&\alpha_{21}\bar{p}_3+\alpha_{21}p_3+\alpha_{22}\bar{p}_3+\alpha_{22}p_3+2\alpha_{23}p_3\bar{p}_3.
\end{aligned}$$

Hence, we can determine the following values

$$
\begin{aligned}
c_1(0) &= \frac{i}{2\tau_1^*\omega_4^*}\left(g_{20}g_{11} - 2|g_{11}|^2 - \frac{|g_{02}|^2}{3}\right) + \frac{g_{21}}{2},\\
\beta_2 &= 2Re\left\{c_1(0)\right\},\\
\mu_2 &= -\frac{Re\left\{c_1(0)\right\}}{Re\left\{\lambda'(\tau_1^*)\right\}},\\
T_2 &= -\frac{Im\left\{c_1(0)\right\} + \mu_2 Im\left\{\lambda'(\tau_1^*)\right\}}{\tau_1^*\omega_4^*}.
\end{aligned}
$$

The above expressions regulate the behavior of bifurcating periodic solution at the critical value τ_1^*. Specifically, μ_2 regulates the direction of Hopf bifurcation: if $\mu_2 > 0$ ($\mu_2 < 0$) then the Hopf bifurcation is supercritical (subcritical) and bifurcating periodic solution exists for $\tau_1 > \tau_1^*$ ($\tau_1 < \tau_1^*$). β_2 regulates the stability of the bifurcating periodic solution: the bifurcating periodic solution is stable (unstable) if $\beta_2 < 0$ ($\beta_2 > 0$). T_2 regulates the period of bifurcating periodic solution: if $T_2 > 0$, the period increases, otherwise decreases.

Appendix C

Proof of Theorem 5.1: To prove this theorem, we use Theorem 4.3 of [60]. We note that disease-free equilibrium (D_0) is unstable whenever $R_0 > 1$ for both systems (2.2) and (2.3). To show that (2.2) and (2.3) satisfy all the conditions of Theorem 4.3, when $R_0 > 1$, we choose $X = \mathbb{R}^4$ and $E = \mathfrak{V}$. The maximal invariant set M on the boundary $\partial\mathfrak{V}$ is the singleton D_0 and is isolated. Thus the hypothesis of Theorem 4.3 of [60] holds for both systems (2.2) and (2.3). We obtained that our systems have a unique endemic equilibrium whenever $R_0 > 1$. Hence the necessary and sufficient condition for uniform persistence in Theorem 4.3 of [60] is equivalent to D_0 being unstable.

AIMS Press